

Neuroprotective Effects of Polysialic Acid and SIGLEC-11 in Activated Phagocytic Cells

Dissertation

Zur

Erlangung des Doktorgrades (Dr. rer. nat.)

der

Mathematisch-Naturwissenschaftlichen Fakultät

der

Rheinischen-Friedrich-Wilhelms-Universität Bonn

vorgelegt von

Anahita Shahraz

Aus
Babol, Iran

Bonn 2015

Angefertigt mit Genehmigung der Mathematisch-Naturwissenschaftlichen
Fakultät der Rheinischen Friedrich-Wilhelms-Universität Bonn.

1. Gutachter: Prof. Dr. Harald Neumann

2. Gutachter: Prof. Dr. Sven Burgdorf

Tag der Promotion: 01.03.2016

Erscheinungsjahr: 2016

Index

Table of content

I Abbreviations

II Abstract

1 Introduction	1
1.1 Microglia	1
1.1.1 Microglia and Macrophages in CNS.....	1
1.1.2 Origin of Microglia and Replenishment	2
1.2 Alzheimer’s Disease	3
1.3 Polysialic Acid	8
1.3.1 Sialic Acid Binding Immunoglobulin-like Lectin Receptors	9
1.3.2 ITIM / ITAM Signaling	10
1.3.3 Modulation of A β Neurotoxicity by Sia and SIGLECs	12
1.4 Aim of the Study	14
2 Materials and Methods	15
2.1 Cells and Cultures	15
2.1.1 Generation of Primitive Neural Stem Cells (pNSCs) from iPS Cells	15
2.1.2 Generation of Human Neurons from pNSCs	16
2.1.3 iPSdM Cell Line	17
2.1.4 THP1 Cell Line.....	18
2.1.5 HEK293FT Cell Line	20

Index

2.1.6 Co-culture of Neurons with iPScDM or THP-1 Macrophages	20
2.1.7 Debris Production	21
2.2 Cellular Assays.....	21
2.2.1 Fibrillar A β ₁₋₄₂ and Debris Phagocytosis Assays.....	21
2.2.2 Detection of Superoxide Production.....	22
2.2.3 Neurite Branch Length Analysis.....	23
2.3 Molecular Assays	24
2.3.1 RT-PCR	24
2.3.2 qRT-PCR	26
2.4 Lentivirus Generation	27
2.5 Immunological Techniques	28
2.5.1 Immunocytochemistry (ICC).....	28
2.5.2 Enzyme-Linked Immunosorbent Assay (ELISA).....	30
2.5.3 Fluorescence-Activated Cell Sorting (FACS)	31
2.5.4 MTT Assay.....	32
2.6 Other Materials	33
2.6.1 Technical Equipment	33
2.6.2 Consumables.....	34
2.6.3 Chemicals and Reagents.....	35
2.6.4 Kits.....	36
2.7 Statistical Analysis.....	36

3 Results.....	37
3.1 SIGLEC-11 Receptor and PolySia avDP20 as It's Ligand	37
3.1.1 SIGLEC-11 Expression on iPSdM Cells and THP1 Macrophages	37
3.1.2 OligoSias Do Not Prevent Superoxide Production	39
3.1.3 PolySia avDP20 and PolySia avDP 60 Prevent Superoxide Production	39
3.1.4 PolySia avDP20 Directly Binds to SIGLEC-11 Receptor	41
3.2 PolySia avDP20 Modulates Macrophage Function via SIGLEC-11 Receptor	43
3.2.1 PolySia avDP20 Reduces Fibrillary A β_{1-42} and Debris Uptake in Macrophages.....	43
3.2.2 PolySia avDP20 Reduces Superoxide Production Triggered by Fibrillary A β_{1-42} and Debris Uptake in iPSdM and Macrophages	47
3.2.3 PolySia avDP20 Acts as Effectively as an Antioxidant	50
3.2.4 Knockdown of SIGLEC-11 Diminishes PolySia avDP20 Anti-Superoxide Effect	53
3.3 PolySia avDP20 Modulates iPSdM/Macrophage Function in Co-culture with Neurons.....	54
3.3.1 Primitive Neural Stem Cells (pNSCs)	54
3.3.2 pNSCs Differentiation towards Mature Neurons.....	56
3.3.3 PolySia avDP20 Has no Effect on Metabolic Activity of Neurons	59

Index

3.3.4 PolySia avDP20 Is Neuroprotective in iPSdM/Macrophage-Neuron Co-culture Systems against A β ₁₋₄₂ Mediated Toxicity	61
3.3.5 PolySia avDP20 Is Neuroprotective in iPSdM/Macrophage-Neuron Co-culture Systems against LPS Mediated Toxicity	65
4 Discussion.....	69
4.1 PolySia avDP20 Is the Potential Ligand for SIGLEC-11.....	69
4.1.1 SIGLEC-11 Expression.....	70
4.1.2 OligoSia and PolySia as a Ligand	70
4.1.3 PolySia avDP20 Binds to SIGLEC-11	72
4.2 PolySia avDP20 Changes iPSdM Cell and THP-1 Macrophage Function.....	72
4.2.1 PolySia avDP20 Reduces Phagocytosis Function	73
4.2.2 PolySia avDP20 Reduces ROS Production	75
4.2.3 PolySia avDP20 Inhibits ROS Production as Effectively as Antioxidants	76
4.3 PolySia avDP20 Has Neuroprotective Function.....	77
4.3.1 Human Neuron Culture from iPS Cells.....	77
4.3.2 PolySia avDP20 Is Neurotrophic.....	78
4.3.3 PolySia avDP20 Effect in A β Stimulated iPSdM/macrophage-neuron Co-culture Systems	79
4.3.4 PolySia avDP20 Effect in LPS Stimulated iPSdM/macrophage-neuron Co-culture Systems	81
4.4 Summary.....	83

Index

References	84
Acknowledgements	100
Declaration	101
Curriculum Vitae	102

Abbreviation

I Abbreviations

AA	ascorbic acid
A β	amyloid- β
ABCA7	ATP-Binding Cassette, Sub-Family A, Member 7
α -CTF	C-terminal fragment
AD	alzheimer's disease
ADAM	a disintegrin and metalloprotease family enzyme
AGM	aorta-gonad-mesonephros
AICD	APP intracellular domain
ALP	alkaline phosphatase
ANOVA	analysis of variance
APH-1	anterior pharynx-defective 1
APOE	apolipoprotein E
APP	amyloid precursor protein
Arg	arginine
Asp	aspartic acid
avDP20	average degree of polymerization 20
BACE1	β -site APP cleaving enzyme 1
BAL1	brain-specific angiogenesis inhibitor1
BBB	blood brain barrier
β -CTF	C-terminal fragment
BDNF	brain derived neurotrophic factor
BIN1	bridging integrator 1
BM	bone marrow
BSA	bovine serum albumin
C2-set	constant domain
CaCl ₂	calcium chloride
cAMP	cyclic adenosine monophosphate
CD33	siglec-3
cDNA	complementary DNA
ChAT	choline acetyltransferase
CLU	clusterin gene
CNS	central nervous system
CpG	C phosphate G
CR1	complement receptor type 1
CX3CL1	chemokine (C-X3-C motif) ligand 1
CX3CR1	CX3C chemokine receptor 1
Cy	cyanine dye
DAP-12	DNAX activation protein of 12 kDa
DAPI	4',6-diamidino-2-phenylindole
DC	dendritic cells

Abbreviation

ddH ₂ O	double-distilled water
DHE	dihydroethidium
DMEM/F12	dulbecco's modified eagle medium: nutrient mixture F-12
DMSO	dimethyl sulfoxide
DTT	dithiothreitol
EDTA	ethylenediaminetetraacetic acid
EOAD	early onset alzheimer's disease
EPHA1	ephrin type-A receptor 1
F4/80	EGF-like module-containing mucin-like hormone receptor-like 1
FACS	fluorescence-activated cell sorter
FAD	familial alzheimer's disease
FBS	fetal bovine serum
GAD	glutaraldehyde
GAPDH	glyceraldehyde-3-phosphate dehydrogenase
GDNF	glial cell-line derived neurotrophic factor
GD1a	disialoganglioside
GD1b	disialoganglioside
GFAP	glial fibrillary acidic proteins
GFP	green fluorescent protein
GM1	monosialotetrahexosylganglioside
GSK-3 β	glycogen synthase kinase 3 beta
GT1b	trisialoganglioside
GWAS	Genome-wide association studies
HCl	hydrochloric acid
HEK	human embryonic kidney
HEPES	4-(2-hydroxyethyl)-1-piperazineethanesulfonic acid
hLIF	human leukemia inhibiting factor
HO-1	hemeoxygenase-1
HSC	hematopoietic stem cells
Iba-1	ionized calcium binding adaptor molecule I
IDE	insulin degrading enzyme
Ig	immunoglobulin
IgG	Immunoglobulin G
IL-34	interleukin-34
IL-1 β	interleukin-1 β
iPS	induced pluripotent stem cell
ITAM	immunoreceptor tyrosine-based activation motif
ITIM	immunoreceptor tyrosine-based inhibition motif
KCl	potassium chloride
KDN	2-keto-3-deoxy-D-glycero-D-galacto-nonulosonic acid
LOAD	late onset alzheimer's disease
LPS	lipopolysaccharide
LTA	lipoteichoic acid

Abbreviation

Lys	lysine
MDP	muramyl dipeptide
MEF	mouse embryonic fibroblast
MFG-E8	milk fat globule EGF factor 8
MgCl ₂	magnesium chloride
MS4A6A	membrane-spanning 4-domains subfamily A member 6A
MTT	3-(4,5-Dimethylthiazol-2-Yl)-2,5-Diphenyltetrazolium Bromide
NaOH	sodium hydroxide
NaCl	sodium chloride
NCAM	neural cell adhesion molecule
Neu5Ac	n-acetylneuraminic acid
Neu5Gc	n-glycolylneuraminic acid
NeuN	neuronal nuclei
NFT	neurofibrillary tangles
nGS	normal goat serum
NK	natural killer
NLR	nod-like receptor
NOS2	Nitric Oxide Synthase 2
OligoSia	oligosialic acid
Opti-MEM	eagle´ minimum essential media
P3	amyloid β - peptide _{17-40/42}
Pax6	paired box protein 6
PBS	phosphate buffered saline
PCR	polymerase chain reaction
PE	R-Phycoerythrin
PFA	paraformaldehyde
PICALM	phosphatidylinositol binding clathrin assembly protein
PLL	poly-l-lysine
PLO	poly-l-ornithine
PNS	peripheral nervous system
pNSC	primitive neural stem cells
PolySia	polysialic acid
PS	phosphatidylserine
PSA-NCAM	polysialylated-neural cell adhesion molecule
RAGE	receptor for advanced glycation end products
ROS	reactive oxygen species
RT	reverse transcription
sAPP α	soluble N-terminal APP α fragment
sAPP β	soluble N-terminal APP fragment
SEM	standard error of mean
SHP	SH2 domain-containing tyrosine phosphatase
Sia	sialic acid

Abbreviation

Siglec	sialic acid binding immunoglobulin-like lectin
SHP1	Src homology region 2 domain-containing phosphatase-1
SHP2	tyrosine-protein phosphatase non-receptor type 11
SIRP β 1	signal regulatory protein- β 1
Sox1	sex determining region Y-box 1
Sox2	sex determining region Y-box 2
Src	sarcoma
Syk	Spleen tyrosine kinase
TGF- β	transforming growth factor beta
TH	tyrosine hydroxylase
TLR	toll-like receptor
TNF- α	tumor necrosis factor alpha
TREM2	triggering receptor expressed on myeloid cells 2
TYROBP	TYRO protein tyrosine kinase binding protein
V-set	variable domain
YS	yolk sac
Zo1	zona occludens protein1

Abstract

II Abstract

Phagocytes show an over-activated complement-phagosome-NADPH oxidase (NOX) signaling pathway in Alzheimer's disease. Polysialic and oligosialic acids (polySia and oligoSia) are glycans composed of sialic acid monomers, which are attached to the outermost ends of lipids and proteins on the surface of healthy brain cells. These structures are recognized by sialic acid-binding immunoglobulin-like lectin (SIGLEC) receptors of microglia and macrophages, which contain immunoreceptor tyrosine-based inhibitory motifs (ITIM)-signaling and counteract the complement-phagosome-NOX signaling pathway.

Here, we show that low molecular weight polysialic acid with average degree of polymerization 20 (polySia avDP20) binds to recombinant SIGLEC-11-Fc-fusion protein. *In vitro*, the induced pluripotent stem cell derived microglia (iPSdM) like cell line and the THP-1 human macrophage cell line were used as model systems of SIGLEC-11 expressing cells. PolySia avDP20 treatment slightly reduced phagocytosis of amyloid- β_{1-42} fibrils and neural debris. In addition, polySia avDP20 completely prevented production of reactive oxygen species (ROS) by iPSdM cells and THP-1 macrophage cells when stimulated with amyloid- β_{1-42} fibrils or neural debris. Reduction of ROS was as strong as known superoxide scavenger 6-hydroxy-2,5,7,8-tetramethylchroman-2-carboxylic acid (Trolox) and enzyme superoxide dismutase-1 (SOD1). By using *in vitro* neuron-iPSdM and neuron-macrophage co-culture systems, A β and LPS treatment resulted in iPSdM and macrophage neurotoxicity with loss of neurites that was abrogated by treatment with polySia avDP20.

In total, data show that polySia avDP20 binds to human SIGLEC-11 and acts as an anti-inflammatory signaling molecule on SIGLEC-11-expressing iPSdM cells and THP-1 macrophages.

Introduction

1 Introduction

In this current era, the world's elderly population is confronted with the biggest problematic neurodegenerative disorder, "Alzheimer's disease (AD)". From a neurologic point of view, AD is a brain disorder with three major hallmarks: formation of amyloid- β ($A\beta$) plaques, formation of neurofibrillary tangles, and activation of microglial cells; which all together results in loss of neuronal connections and memory impairment. Every factor that could have an effect on these three main hallmarks may be considered as a potential therapeutic agent.

1.1 Microglia

1.1.1 Microglia and Macrophages in CNS

Microglial cells are the resident macrophages of the brain, which constitute about 10-15% of the entire brain cell population. In the healthy brain, microglial cells are in surveillance mode and constantly explore their microenvironments. This task helps them recognize changes such as apoptotic material. They always interact with neurons to remove synaptic structure for remodelling the presynaptic components or to remove newborn neurons during early development [1]. In addition, microglial cells represent the first line of defence against invading pathogens or other types of brain tissue injury. To fulfill this task, they may directly remove the particles by phagocytosis or indirectly through inflammatory responses such as cytokine or reactive oxygen species (ROS) release [2].

Other types of resident immune cells of the brain are **brain macrophages** such as perivascular macrophages, meningeal macrophages and choroid plexus macrophages, which can be detected with the same specific markers as microglial cells (Iba1, CX3CR1, F4/80); however, they have a different ontogeny [3].

In pathological conditions or neurodegenerative diseases, in which the blood brain barrier (BBB) is compromised, blood monocytes and leukocytes recognize

Introduction

chemoattractant molecules and enter to the brain to form a new population named **exogenous macrophages** [4], [5].

1.1.2 Origin of Microglia and Replenishment

Del Rio-Hortega (1932) described for the first time microglia as the "third element", besides neurons and neuroglia (astrocytes and oligodendrocyte), in the central nervous system (CNS). Hortega was also the first person who postulated that microglial cells have a mesodermal origin [6]. Nowadays, it is believed that unlike neurons and macroglia (astrocytes and oligodendrocyte), which are derived from neuroectoderm, microglial progenitors have a mesodermal (myeloid) origin [7].

In mice, primitive hematopoiesis occurs between E7 to E9, and leads to the appearance of **microglial progenitors** [8]. During this time, erythromyeloid progenitors appear in the extra-embryonic yolk sac (YS) at E7. Later on, they migrate to the brain via the circulatory system around E9 and populate the brain mesenchyme [9]. Definitive hematopoiesis occurs at E10.5, when hematopoietic stem cells (HSCs) appear in aorta-gonad-mesonephros (AGM) region. These cells subsequently produce myeloid cells that are the **brain macrophage** and **exogenous macrophage** progenitors [3]. Later on, myeloid cells derived from HSCs populate fetal liver (E12.5) and bone marrow (after birth) as major hematopoietic organs [10].

The next debate concerned the replicative capacity of microglia and whether they are replicated *in situ* or are replenished by circulating precursor cells. Because of their mesodermal origin, the contribution of circulating monocytes or myeloid progenitor cells to the steady-state population of microglia in healthy CNS was under debate. Early studies, which mainly focus on transplantation of labeled bone marrow cells to irradiated recipients, yield to the conclusion that precursors originate from bone marrow and can cross BBB, where they differentiate into microglial cells [11], [12]. However, irradiation caused the BBB to become permeabilized and, as a result, the circulating labeled bone marrow cells could easily enter CNS [13]. Recent findings from parabiosis experiments

Introduction

show that under an intact BBB, recruitment of labeled bone marrow circulating cells to the brain of host animals is negligible [14]. Parabiosis experiments also show that under pathological conditions (which lead to a permeable BBB), transient recruitment of circulating cells to CNS occurs. However, these cells will never have a permanent contribution to CNS microglial pool [15].

In summary, microglial cells originate from primitive progenitors in the YS and migrate to the CNS during early embryogenesis. Their population is maintained by local precursors that colonize the brain before birth independent of circulating monocytes. Data from bone marrow transplantations have shown that during CNS inflammation or disease conditions there will be recruitment and differentiation of blood monocytes to microglial like cells [16].

1.2 Alzheimer's Disease

AD is the most common form of neurodegenerative disorder in the elderly population, with prevalence of around 25% in those over 90 years old [17]. AD has a well-known progression, which starts in brain regions responsible for learning and memory, mainly pyramidal cell loss in CA1 region of hippocampus [18]. The most pathologically accepted concept is the amyloid cascade hypothesis. According to this hypothesis, the pathological steps which lead to AD consist of (i) appearance of senile plaques, (ii) formation of neurofibrillary tangles (NFT), and (iii) microglial cell inflammatory response (Heppner et al. 2015). In reality, there is no border between the three steps; however, these steps are described separately to simplify the explanation.

First step: The most important components of senile plaques are A β peptides, which are produced through sequential cleavage of the amyloid precursor protein (APP) (Fig 1-1). APP cleavage can occur either in a non-amyloidogenic pathway or an amyloidogenic pathway. In the non-amyloidogenic (physiological) pathway, APP is first cleaved in the middle by an α -secretase (a disintegrin and metalloprotease family enzyme, ADAM), producing a soluble N-terminal APP α fragment (sAPP α) and a

Introduction

transmembrane C-terminal fragment (α -CTF). α -CTF is then further cleaved by a γ -secretase (multi-subunit protease complex) to generate a short peptide P3 and APP intracellular domain (AICD; Fig 1-1 A; [19], [20]).

In the amyloidogenic (pathological) pathway, which leads to $A\beta$ peptide formation, APP is first cleaved by a β -secretase (β -site APP cleaving enzyme 1, BACE1) at the N-terminus of the future $A\beta$ peptide sequence. This cleavage produces a soluble N-terminal APP β fragment (sAPP β) and a transmembrane C-terminal fragment (β -CTF). β -CTF is further cleaved by a γ -secretase to generate $A\beta$ and AICD (Fig 1-1 B; Moore et al. 2015; Zhang et al. 2011).

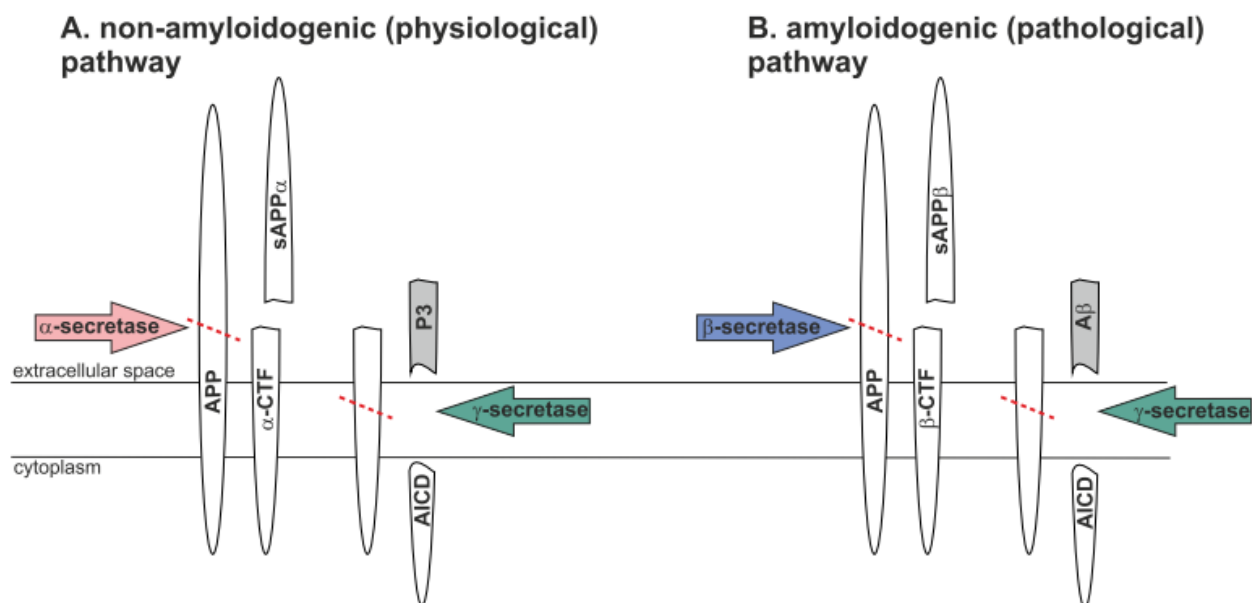


Figure 1-1: $A\beta_{1-42}$ production. In the physiological condition, APP is first cleaved by an α -secretase and is divided into two fragments: sAPP α and α -CTF. The α -CTF piece is further cleaved by a γ -secretase and is cut up into the smaller peptides P3 and AICD (**A**). In the pathological condition, APP is cleaved by a β -secretase; afterwards, the β -CTF is split by a γ -secretase to form the $A\beta$ peptide and AICD (**B**).

A γ -secretase is a multi-subunit protease complex, which consists of presenilin, nicastrin, anterior pharynx-defective 1 (APH-1) and presenilin enhancer 2 [20].

Introduction

Depending on the cleavage site of the γ -secretase, various lengths of A β (A β_{43} , A β_{42} , A β_{40} , A β_{38} , and A β_{37}) are produced [22]. The most produced forms of A β are A β_{1-40} and A β_{1-42} peptides [23]. However, A β_{1-42} is more neurotoxic since it is hydrophobic and can incite fibril polymerization, leading to stable clusters. These clusters are able to produce even larger aggregates [24], [25].

AD cases can mainly be divided to two groups: early onset AD (EOAD; also known as familial AD or FAD) and late onset AD (LOAD). EOAD occurs in people between the ages of 30 to 60. Mutations in genes coding APP, presenilin-1 or presenilin-2 (subunits of γ -secretase) increase A β_{1-42} production [25] and lead to FAD. LOAD occurs usually above the age of 65. Recent studies showed that genetic factors have a big effect on LOAD progression. The most widely-known gene is APOE, which has 3 alleles. The APOE ϵ 4 allele highly increases the risk of LOAD [26]. Genome-wide association studies (GWAS) have led to the detection of several AD risk genes (CLU, MS4A6A, ABCA7, EPHA1, PICALM, TREM2, BIN1, CR1, and CD33) that may increase the risk of AD development [27], [28]. Some of these genes, such as TREM2, CD33, and CR1, are expressed in microglia. This shows that the role of microglia should be considered in the study of LOAD.

Second step: neurofibrillary tangles consist of clusters of microtubule-associated protein tau. Under physiological conditions, tau protein plays a role in stabilizing microtubules in a specific direction, especially in axons through mutual actions of kinases and phosphatases [29]. However, under pathological conditions like AD, tau proteins undergo modifications, predominantly hyper-phosphorylation, and lose their biological function. As a result, they cannot bind to microtubules and form aggregates inside neurons [30]. There are different points of view about the role of tau in AD. Some studies suggest that A β works upstream of tau and accelerates NFT formation [31]. On the other side, other studies mention that tau pathology is independent of A β or at least is needed for A β pathology [32].

Introduction

Third step: In 1987, McGeer has shown that in contrast to the normal brain, where microglia are distributed uniformly throughout the gray and white matter, AD brains have microglia clustered in and around A β deposits [33].

Microglial cells show a double-edged role in AD pathogenesis. On one hand, *in vitro* studies show that microglia have a **neurotoxic** role. Activation of microglial cells by A β caused an increase in extracellular glutamate concentration, which contributes to neuronal dysfunction and death [34], [35]. In addition, A β can induce the production of pro-inflammatory cytokines (TNF- α , IL-1 β) by microglial cells, which can directly impair neurons [36], [37]. In addition, A β can initiate the secretion of superoxide anions or ROS by a Syk kinase-dependent pathway in primary mouse microglia and THP-1 monocytes [38]. A β can also lead to peroxynitrite secretion that can induce neuronal exposure of the eat-me signal phosphatidylserine (PS) for microglial cells [39], [40]. Subsequently, microglial cells remove damaged neurons by phagocytosis.

On the other hand, microglia can be **neuroprotective** via clearance of A β peptides and release of neurotrophic factors. Phagocytosis function by itself plays a pivotal role. On one side, phagocytosis can occur without neurotoxicity. Microglial cells, which were activated by Toll-like receptor-9 ligand (CpG), could increase uptake of A β and release of hemoxygenase-1 (HO-1), an antioxidant enzyme, without producing neurotoxic molecules [41]. There are some molecules such as Fractalkine (CX3CL1) and interleukin (IL)-34, which are supposed to be secreted by neurons to modulate microglial function in a neuroprotective way. For example, IL-34 promotes microglial proliferation, clearance of soluble oligomeric A β via insulin degrading enzyme (IDE) (A β degrading enzyme), and induces secretion of HO-1 by microglial cells [42] (Figure1-2). On the other side, phagocytosis can be associated with inflammation. For example, the uptake of microbes leads to the production of pro-inflammatory cytokines or ROS release that are toxic for neurons [43].

Introduction

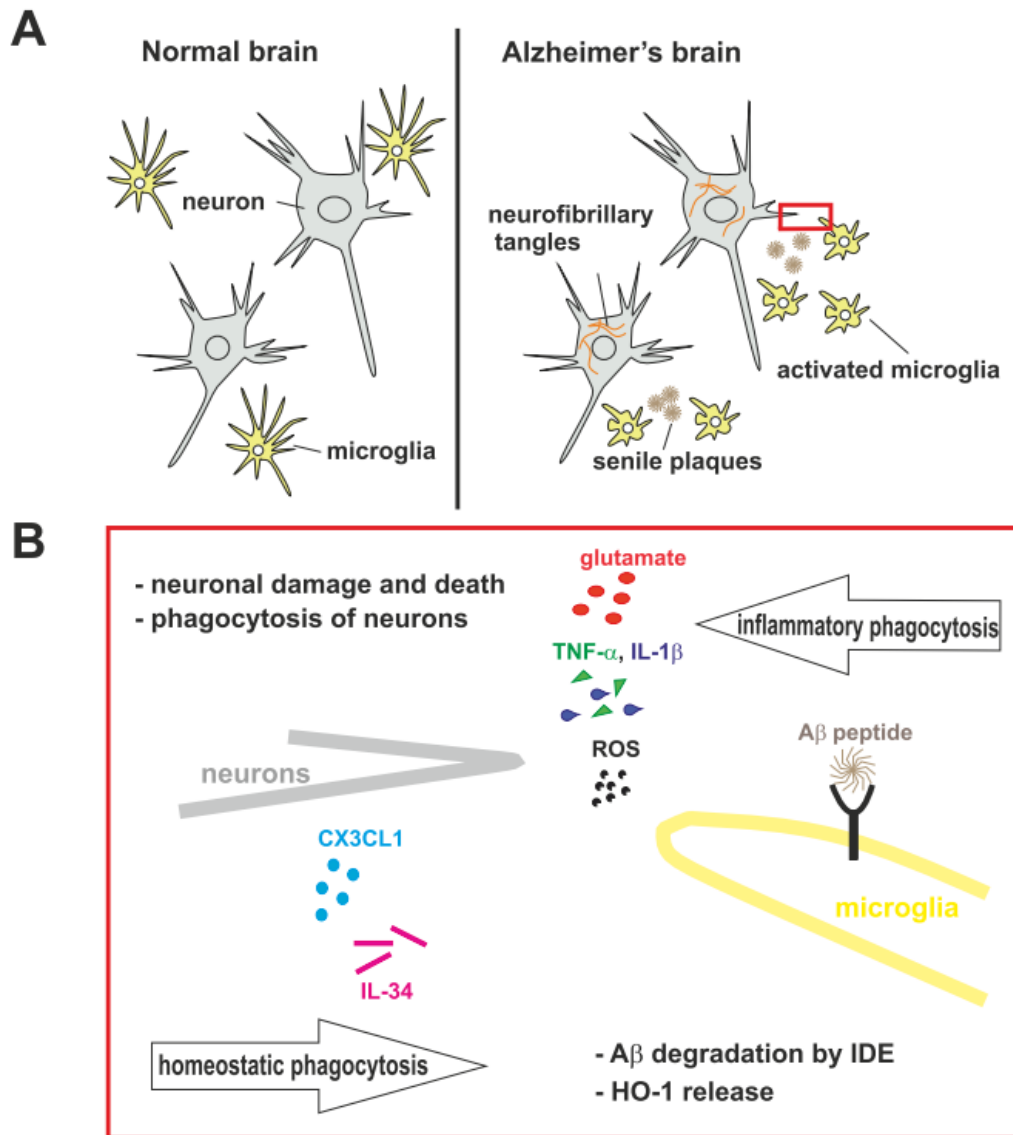


Figure 1-2: Microglial cells plays a double-edged role in AD. The most evident features of the AD brain compared to healthy brain are the appearance of senile plaques, NFT formation, and activated phenotype of microglia (**A**). Microglial cell activation can be inflammatory and neurotoxic. Attachment of A β to its receptor on microglia can trigger release of glutamate, TNF- α , IL- β and ROS, which are toxic to neurons (panel **B** right to left). On the other side, neurons can produce CX3CL1 and IL-34 and provoke homeostatic phagocytosis and neurotrophic function of microglia. This activation leads to microglial proliferation and release IDE enzyme or HO-1 enzyme (panel **B** left to right).

Introduction

Every component, which can either reduce the inflammatory response of microglia in the presence of A β or increase A β uptake without inflammation could be a therapeutic candidate for AD.

1.3 Polysialic Acid

Sialic acids (Sias) are derivatives of the 9-carbone carboxylated sugar, neuraminic acid [44]. N-acetylneuraminic acid (Neu5Ac), N-glycolylneuraminic acid (Neu5Gc), and 2-keto-3-deoxy-D-glycero-D-galacto-nonulosonic acid (KDN) are the metabolic precursors for all other Sias [45] (Fig 1-3). Sias can often form extended homopolymers of oligosialic acids (oligoSias) and polysialic acids (polySias) which are diverse according to four factors: (i) backbone components (Neu5Ac, Neu5Gc and KDN), (ii) modifications (acetylation, methylation, sulphation, lactylation, lactonization), (iii) position of sialic acid residue linkages (α 2 \rightarrow 4, α 2 \rightarrow 5, α 2 \rightarrow 8 and α 2 \rightarrow 9) and (iv) degree of polymerization (2-400) [46].

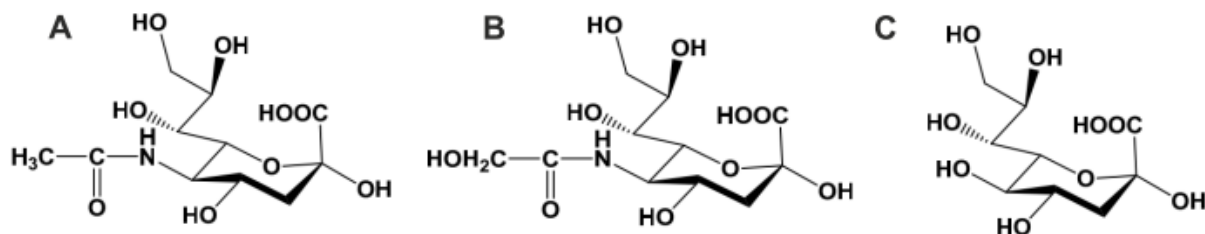


Figure 1-3: The three main sialic acid structures derived from neuraminic acid. N-acetylneuraminic acid (Neu5Ac), which is the most common member of Sia in human (**A**). N-glycolylneuraminic acid (Neu5Gc, **B**) and 2-keto-3-deoxy-D-glycero-D-galacto-nonulosonic acid (KDN, **C**) (modified from Yamamoto 2010).

Usually at the cell surface, Sias provide an acidic cap to the outermost ends of lipids and proteins of the glycocalyx [48]. This Sia layer causes specific biophysical properties such as negative charge, hydrophilicity, binding to specific factors such as complement factor H, and masking of cell surface receptors [45], [49]. Among the multiple functions

Introduction

of Sias, one of the most important roles is the ligand recognition process. This recognition is mediated by specific receptors named SIGLEC receptors [50].

1.3.1 Sialic Acid Binding Immunoglobulin-like Lectin Receptors

Sialic acid binding immunoglobulin-like lectins (SIGLEC) consist of a family of cell surface receptors expressed on immune cells (such as macrophages, dendritic cells (DC), monocytes, neutrophils and microglial cells) that can recognize Sia residues and mediate mostly inhibitory but also activatory signaling [51]. SIGLECs are divided into two major subgroups: first, the evolutionary conserved subfamily which consists of SIGLEC-1 (sialoadhesin or CD169), SIGLEC-2 (CD22), SIGLEC-4 (myelin-associated glycoprotein, MAG) and SIGLEC-15, which are conserved across all mammalian species and share 30% sequence homology [52]. The second subgroup is the SIGLEC3/CD33-related subfamily, which shows 50-90% sequence similarity to CD33 in their extracellular part. However, they show poor species homology and different numbers between species because of evolutionary events [53]. For example, the human SIGLEC3-related group contains 11 members (SIGLEC-3, -5, -6, -7, -8, -9, -10, -11, -12, -14, -16), and mouse contain 5 members (CD33, siglec-e, -f, -g, -h)[54].

All SIGLEC receptors are composed of four parts: (i) Extracellular N-terminal V-set immunoglobulin (Ig) domain, which is responsible for Sia recognition, (ii) variable number of C2-set Ig domains, (iii) one transmembrane part, and (iv) the cytoplasmic tail (Fig 1-4) [51], [52]. According to the transmembrane and cytoplasmic tail, SIGLECs can be divided into three groups: The first group of SIGLECs, like SIGLEC-1 and -4, do not have any inhibitory motif in their intracellular tail. The second group (SIGLEC-2, -3, -5, -6, -7, -8, -9, -10, -11 and -12) consist of at least one immunoreceptor tyrosine-based inhibition motif (ITIM) which allows them to act as inhibitory receptors (Fig. 1-4). The third group (SIGLEC-14, -15, -16) of SIGLECs carries a positively charged residue in the transmembrane region. This positive charge enables them to recruit a disulfide-linked homodimer of DNAX-associated protein of 12 kDa (DAP-12), an adaptor protein

Introduction

that contains an immunoreceptor tyrosine-based activatory motif (ITAM), which permits these SIGLECs to function as activatory receptors (Fig 1-4) [53].

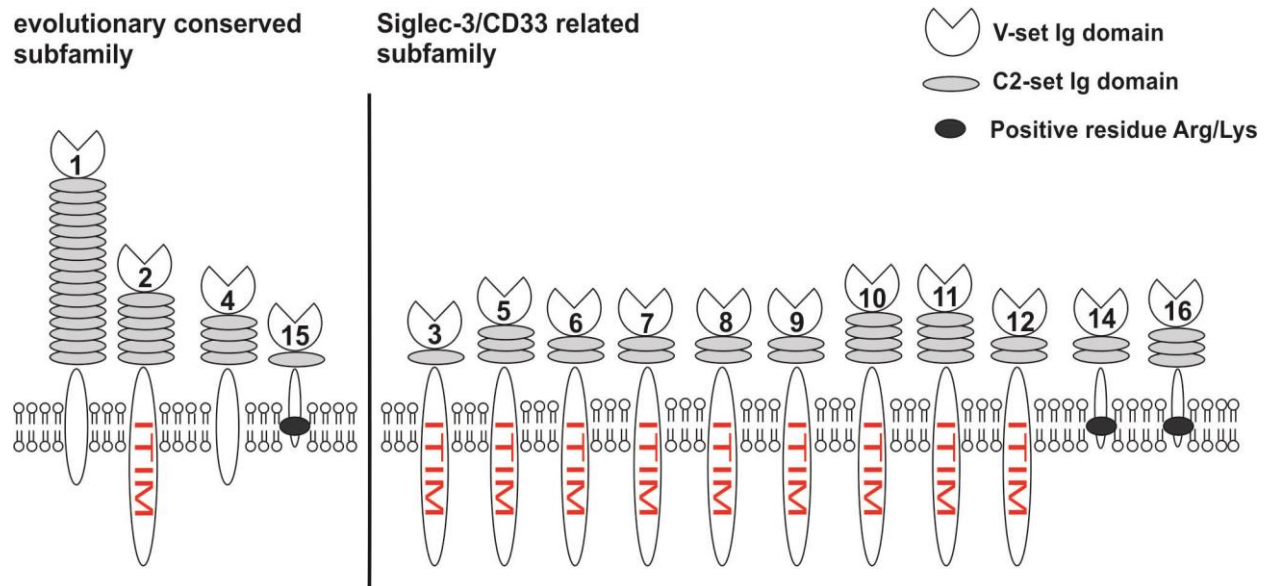


Figure 1-4: Human SIGLECs. SIGLECs are type I transmembrane proteins. Each SIGLEC contains one N-terminal V-set Ig domain to recognize the ligand. They have variable C2-set Ig domains to extend from the cell surface. In the intracellular part, according to the motif they carry, their function can be inhibitory (contain ITIM domain) or activatory (contain positive residues, which enable them to recruit ITAM containing adaptor protein). Modified according to Pillai et al., 2012.

1.3.2 ITIM / ITAM Signaling

Upon ligand binding to SIGLECs, depending on the type of intracellular motif, dephosphorylation or phosphorylation processes will cause an inhibitory or activatory response by cells.

There are two pairs of ITIM/ITAM-carrying receptors in SIGLEC3/CD33-related subfamily (SIGLEC-5 vs SIGLEC-14 and SIGLEC-11 vs SIGLEC-16). Pair receptors are developed to provide a balance in SIGLEC response toward ligand binding [53]. SIGLEC-11 and SIGLEC-16 share about 99% amino acid identity with each other in the extracellular domains [55]. Human brain microglia have a specific expression of

Introduction

SIGLEC-11, which recognizes Neu5Ac $\alpha 2 \rightarrow 8$ as its ligand [56]. Neu5Ac $\alpha 2 \rightarrow 8$ can be recognized by SIGLEC16 as well.

SIGLEC-11 is neutrally charged in the transmembrane part and contains an ITIM motif in the intracellular part, which enables it to act as an inhibitory receptor [51]. Following ligand attachment to the receptor, members of the Src kinase family become activated and phosphorylate the ITIM motif tyrosine residues. Phosphorylated tyrosines provide the docking sites for SH2 domain-containing tyrosine phosphates (SHP1 and SHP2), which upon activation counteract functions of ITAM signaling pathways (Fig 1-5) [57].

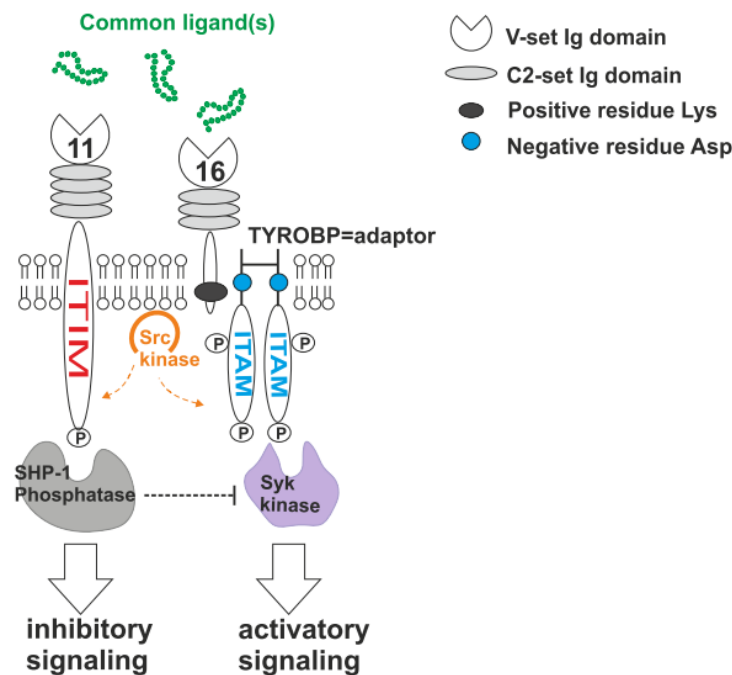


Figure 1-5: SIGLEC-11 vs SIGLEC-16 pair. Upon ligand attachment to SIGLEC-11, the tyrosine within the ITIM domain will be phosphorylated by Src kinase and will provide the docking site for SHP-1 phosphatase. SHP-1 phosphorylation leads to the de-phosphorylation of downstream proteins, and downregulation of activatory signaling pathways. Alternatively, upon ligand binding to SIGLEC-16, it will recruit the adaptor protein TYROBP by interaction between positively charged lysine and negatively charged aspartic acid. TYROBP adaptor contains ITAM domains. ITAM domains phosphorylation will provide sites for Syk kinase and starts the activatory signal transduction.

Introduction

SIGLEC-16 does not have any intracellular motif; however, it contains a positively charged lysine in the transmembrane part, which enables this receptor to recruit the ITAM-containing adaptor molecule DAP-12 (TYROBP) [51]. Upon ligand binding, the ITAM motif of the adaptor molecule will be phosphorylated by the Src kinase family and will provide the docking site for Syk kinase. This kinase will, upon phosphorylation, trigger several downstream signaling pathways, leading to phagocytosis or release of ROS (Fig 1-5) [58].

1.3.3 Modulation of A β Neurotoxicity by Sia and SIGLECs

The human brain is a rich source of glycolipids. Gangliosides (GM1, GD1a, GD1b, GT1b) are members of glycolipids, which comprise ~ 0.6% of total brain lipid, and carry ~ 75% of brain's Sia [48]. Gangliosides, especially GM1, have been shown to be sufficient for A β binding and aggregation; they are also the main suspect in immune masking of A β plaques [59], [60]. A β binding to gangliosides, especially GM1, results in an altered secondary structure towards β -sheets folding [61]. GM1 gangliosides can bind to A β isoforms with the following affinities: A β ₁₋₄₂ > A β ₄₀₋₁ > A β ₁₋₄₀ > A β ₁₋₃₈ [62],[64]. On the other hand, sialylation provide the recognition signal for microglial cells which carry SIGLEC-11 or SIGLEC-3 on their surface. Both of these SIGLEC receptors have an ITIM motif, which upon activation start immunosuppressive signals [60], [65]. The inhibitory signals can inhibit the function of other microglial pattern recognition receptors, such as TREM2 and SIRP β 1, which are amyloid plaque-associated microglial phagocytic receptors and signal via ITAM [66], [67]. Upon ITIM activation, phagocytosis is reduced, but simultaneously the A β induced cytokine release and ROS production are attenuated.

Recent data show that SIGLEC receptors on microglia can recognize Sias on the neuronal glycocalyx. Siglec-e, which is a member of the mouse CD33-related SIGLEC family, can reduce phagocytosis and ROS release in microglial cells mediated by neural debris if overexpressed. In addition, in a mouse neuron-microglia co-culture system, siglec-e on microglial cells showed neuroprotective features by binding to Sias of intact

Introduction

neuronal glycoalyx [68]. Moreover, activation of SIGLEC-11 in mouse microglia, which ectopically expresses flag-tagged human SIGLEC-11 by crosslinking with flag-specific antibodies, reduces gene transcription of pro-inflammatory mediators such as IL- β , NOS-2. In the mouse neuron-microglia co-culture system, microglial SIGLEC-11 could interact with Sias on the neuronal glycoalyx and reduce microglial cell neurotoxicity [69].

Introduction

1.4 Aim of the Study

In AD, neuronal glycoalyx is changed and A β plaques are present. Both of these situations can lead to inflammatory responses of microglial cells, which are harmful for neurons. Previously, it has been shown that alteration in polySia of neuronal glycoalyx can modulate microglia functions through SIGLEC receptors present on microglial cells. Still, it is not clear which length of polySia as a ligand can interact with microglial SIGLEC-11 receptor and how this interaction can change microglial cell behavior. Therefore, in this study, we attempted to fulfill three different aims.

The first aim of the thesis at hand was to investigate whether polySia could act as a ligand for SIGLEC-11 receptor. To fulfill this, different lengths of polySia were used and the response of A β_{1-42} activated microglia (iPSdM cells) toward them was studied.

The second aim of the thesis was to explore how this specific ligand can change phagocytosis and superoxide production of iPSdM/macrophages toward A β_{1-42} and neural debris stimulation .

The third aim of the thesis was to test whether the SIGLEC-11 ligand – polysia is capable of preventing the iPSdM/macrophages toxic effect mediated by A β_{1-42} or Lipopolysaccharide (LPS) in neuron-iPSdM or neuron-macrophage co-culture systems.

2 Materials and Methods

2.1 Cells and Cultures

2.1.1 Generation of Primitive Neural Stem Cells (pNSCs) from iPS Cells

Human induced pluripotent stem (iPS) cells generated from MP-1 (AG Brüstle, University of Bonn, Germany) were used for pluripotent neural stem cell (pNSC) induction by a modified protocol, which was originally described to obtain primitive neural precursors from human embryonic stem cells [70]. iPS cells were cultured on mouse embryonic fibroblast (MEF) feeder cells in iPS-knockout/serum replacement medium (table 2-1) to form small colonies for 2 days in an incubator with 5% CO₂, 37°C. Next, the medium was changed to neural stem cell medium (table 2-2) which contains leukaemia inhibiting factor (LIF) and three small molecules CHIR99021 (inhibitor of GSK-3 β) and SB431542 (inhibitor of TGF- β and activin receptors), and Compound E (inhibitor of γ -secretase) for 10 days. The medium was changed every day. Cells were split by accutase and replated on Poly-L-ornithine (PLO) + Fibronectin (Fn) coated dishes in neural stem cell medium supplemented with LIF, CHIR99021 and SB431542 to keep them in pluripotent state in an incubator with 5% CO₂, 37°C.

Table 2-1 iPS knockout/serum replacement medium

Component	Quantity	Company
Dulbecco's Modified Eagle Media (DMEM) + factor12 (1:1) + L-glutamine + 15 mM HEPES	200 ml	Gibco, Life Technologies
KnockOut serum replacement	50 ml	Gibco, Life Technologies
Non-Essential Amino Acids	2.5 ml	Gibco, Life Technologies
L-Glutamine	1.2 ml	Gibco, Life Technologies
β -mercaptoethanol	5 μ l	Millipore
Recombinant human FGF basic	75 μ l	R & D system

Materials and Methods

Table 2-2 neural stem cell medium

Component	Quantity	Company
Dulbecco's Modified Eagle Media (DMEM) + factor12 (1:1) + L-glutamine + 15 mM HEPES	250 ml	Gibco, Life Technologies
Neurobasal medium	250 ml	Gibco, Life Technologies
N2 supplement	5 ml	Gibco, Life Technologies
B27 supplement	10 ml	Gibco, Life Technologies
GlutaMAX supplement	5 ml	Gibco, Life Technologies
Human Leukemia inhibitory factor	0.5 ml	Millipore
CHIR99021	0.05 ml	Axon medchem
SB431542	0.05 ml	Axon medchem
Compound E	0.05 ml	Axon medchem

2.1.2 Generation of Human Neurons from pNSCs

To induce differentiation towards neurons, pNSCs were dissociated by accutase. Then, pNSCs were cultured on PLO + Laminin (Ln) coated 4-chamber slides in neural stem cell medium till cells attached and started to form small colonies in an incubator with 5% CO₂, 37°C. Afterwards, medium was changed to neuronal differentiation medium (table 2-3) for 2 weeks. Medium containing the neurotrophic factors was changed every second day.

Materials and Methods

Table 2-3 neuronal differentiation medium

Component	Quantity	Company
Dulbecco's Modified Eagle Media (DMEM) + factor12 (1:1) + L-glutamine + 15 mM HEPES	500 ml	Gibco, Life Technologies
N2 supplement	5 ml	Gibco, Life Technologies
B27 supplement	10 ml	Gibco, Life Technologies
Cyclic adenosine monophosphate	0.15 ml	Sigma-Aldrich
Ascorbic acid	0.5 ml	Tocris
Glial derived neurotrophic factor	0.5 ml	Prospect
Brain derived neurotrophic factor	0.5 ml	Prospect

2.1.3 iPSdM Cell Line

Induced pluripotent stem cell-derived microglia (iPSdM) cells, a microglia-like cell line, were generated from human induced pluripotent stem cells. These cells show microglial cell surface markers such as CD11b, CD11c, CD16/32, CD36, CD40, CD45, CD49d, CD86, CD206 and CX3CR1. They also show functional abilities like microglial cells such as phagocytosis, release of ROS, release of pro-inflammatory cytokines and migration toward chemokines [71].

iPSdM cells grow in adherent culture. After thawing in pre-warmed N2 culture medium (table 2-4), the cell suspension was centrifuged to get rid of DMSO (1300 rpm, 3 minutes). Then, the pellet was resuspended in N2 culture medium and kept in 10 cm² diameter culture dish, in an incubator with 5% CO₂, 37°C. When cultured cells reached 90% confluency, cells were detached by trypsinization, centrifuged (1300 rpm, 3 minutes), and resuspended in a new 10 cm² diameter culture dish.

Materials and Methods

Table 2-4 N2 culture medium

Component	Quantity	Company
Dulbecco's Modified Eagle Media (DMEM) + factor12 (1:1) + L-glutamine + 15 mM HEPES	500 ml	Gibco, Life Technologies
N2 supplement	5 ml	Gibco, Life Technologies
L-glutamine	1.2 ml	Gibco, Life Technologies
Penicillin-Streptomycin	5 ml	Gibco, Life Technologies

2.1.4 THP1 Cell Line

The human monocytic cell line THP-1 derived from an acute monocytic leukaemia patient was used to obtain macrophages. These cells were kindly provided by Prof. Veit Hornung (University of Bonn, Germany). After thawing in pre-warmed monocyte culture medium (table 2-5), the cell suspension was centrifuged to get rid of DMSO (1300 rpm, 3 minutes). Since THP-1 monocytes are cultured in suspension, the pellet was resuspended in monocyte culture medium and kept in 25 cm² flask in an incubator with 5% CO₂, 37°C. When cultured cells reached about 1x10⁶ cells/ml, the cell suspension was collected, centrifuged (1300 rpm, 3 minutes), and resuspended in 75 cm² flasks.

Table 2-5 THP-1 monocyte culture medium

Component	Quantity	Company
Roswell Park Memorial Institute medium (RPMI) + L-glutamine	450 ml	Gibco, Life Technologies
Fetal Calf Serum	50 ml	Gibco, Life Technologies
Penicillin-Streptomycin	5 ml	Gibco, Life Technologies
L-glutamine	5 ml	Gibco, Life Technologies
Sodium pyruvate	5 ml	Gibco, Life Technologies

Materials and Methods

One week after thawing, THP-1 monocytes were transferred to differentiation medium (table 2-6). To induce differentiation, cells were plated at appropriate density in differentiation medium and were incubated with 0.5 μ M Phorbol-12-Myristate-13-Acetate (PMA) for 3 hours. Then, the attached monocytes were washed 2 times with medium and cultured for 48 hours more in differentiation medium. The medium was changed to stimulation medium (table 2-7) which contains no serum for stimulation of the cells.

Table 2-6 THP-1 differentiation medium

Component	Quantity	Company
Roswell Park Memorial Institute medium (RPMI) + L-glutamine	450 ml	Gibco, Life Technologies
Chicken serum	5 ml	Gibco, Life Technologies
N2 supplement	5 ml	Gibco, Life Technologies
Penicillin-Streptomycin	5 ml	Gibco, Life Technologies
L-glutamine	5 ml	Gibco, Life Technologies
Sodium pyruvate	5 ml	Gibco, Life Technologies

Table 2-7 THP-1 stimulation medium

Component	Quantity	Company
Roswell Park Memorial Institute medium (RPMI) + L-glutamine	450 ml	Gibco, Life Technologies
N2 supplement	5 ml	Gibco, Life Technologies
Penicillin-Streptomycin	5 ml	Gibco, Life Technologies
L-glutamine	5 ml	Gibco, Life Technologies
Sodium pyruvate	5 ml	Gibco, Life Technologies

Materials and Methods

2.1.5 HEK293FT Cell Line

Human Embryonic Kidney (HEK) 293 cells are a specific cell line originally derived from human embryonic kidney cells from an aborted human embryo. After thawing in pre-warmed MEF medium (table 2-8), the cell suspension were centrifuged to get rid of DMSO (1300 rpm, 3 minutes). Next, the pellet was resuspended in MEF medium and kept in 15 cm² diameter culture dish, in an incubator with 5% CO₂, 37°C. When cultured cells reached 90% confluency, cells were detached by trypsinization and seeded onto Poly-L-lysine (PLL) coated dishes for transduction.

Table 2-8 MEF medium

Component	Quantity	Company
Dulbecco's Modified Eagle Media (DMEM) + L-glutamine + 4500 mg/l D-glucose	450 ml	Gibco, Life Technologies
L-glutamine	5 ml	Gibco, Life Technologies
Non-Essential Amino Acids	5 ml	Gibco, Life Technologies
Sodium pyruvate	5 ml	Gibco, Life Technologies
Fetal Calf Serum	50 ml	Gibco, Life Technologies

2.1.6 Co-culture of Neurons with iPsdM or THP-1 Macrophages

To prepare iPsdM/macrophages for co-culture experiments, in LPS stimulated groups, 80% confluent dishes of either iPsdM cells or THP-1 macrophages were pre-treated for 24 hours with 1 µg/ml LPS. Next, iPsdM/macrophages were washed once with 1x PBS, scraped, and counted. The appropriate number of iPsdM/macrophages were added to neurons with/without 1.5 µM polySia avDP20 with a 1 : 5 iPsdM/macrophages : neuron ratio in neuronal differentiation medium for 48 hours.

In fibrillar A β ₁₋₄₂ stimulated groups, unbiotinylated A β ₁₋₄₂ was incubated 72 hours before the experiment in 37°C to stimulate fibrillar formation. iPsdM/macrophages and 1 µM fibrillar A β ₁₋₄₂ were added to the neurons with/without 1.5 µM polySia avDP20 in a 1 : 5

Materials and Methods

iPSdM/macrophages : neuron ratio in neuronal differentiation medium for 48 hours. To test the antioxidant effect of 6-hydroxy-2,5,7,8-tetramethylchroman-2-carboxylic acid (Trolox), 40 μ M Trolox was together with 1 μ M fibrillar A β ₁₋₄₂ and iPSdM/macrophages to the neurons and incubated in neuronal differentiation medium for 48 hours.

2.1.7 Debris Production

Neural stem cells were seeded. When 90% confluency was reached, cells were incubated with 40 nM okadaic acid for 24 hours. Medium containing cell debris was collected and centrifuged (1500 rpm, 4 minutes) to aggregate the remaining cell membranes and washed once with 1x PBS. Then, debris was incubated with DNase to break down DNA and subsequently washed 2 times with 1x PBS. For phagocytosis experiments, debris was stained with “Dil Derivatives for Long-Term Cellular Labelling” Molecular Probes (1 μ g/ml) according to supplier’s manual. The obtained debris was washed, weighed, aliquoted, and stored in -20°C.

2.2 Cellular Assays

2.2.1 Fibrillar A β ₁₋₄₂ and Debris Phagocytosis Assays

To get fibril forms, biotinylated A β ₁₋₄₂ diluted in PBS (1 mg/ml) was incubated for 72 hours at 37°C as previously described [72]. iPSdM cells were seeded at a density of 40,000 cells per well in a chamber slide 24 hours before the experiment. THP-1 monocytes were seeded and differentiated at a density of 100,000 cells per well in a chamber slide to obtain macrophages 48 hours before the experiment. iPSdM/macrophages were pre-incubated for 1 hour with different concentrations of polySia avDP20 (0.15, 0.5 and 1.5 μ M), followed by 1.5 hour incubation with 2 μ M fibrillary biotinylated A β ₁₋₄₂. Then, the cells were fixed, blocked, and incubated with rabbit anti-Iba1 antibody (iPSdM, table 2-17) or rat anti-CD11b antibody (macrophages, table 2-17) overnight at 4°C. Afterwards, cell were washed and incubated with a secondary Alexa 488-conjugated antibody directed against rabbit IgG and streptavidin-

Materials and Methods

Cy3 (iPSdM, table 2-17) or a secondary Alexa 488-conjugated antibody directed against rat IgG and streptavidin-Cy3 (macrophages, table 2-17) for 2 hours at room temperature. The staining protocol is mentioned in table 2-16 in detail. For analysis, images were obtained with a confocal laser scanning microscope and the fluorescent labeled $A\beta_{1-42}$ was visualized inside the iPSdM and macrophages by 3D reconstruction. Percentage of the cells ingested fluorescently labeled $A\beta_{1-42}$ was analyzed in 5 randomly selected areas per condition per experiment by using ImageJ software.

Similar to $A\beta$ phagocytosis experiments, 40,000 iPSdM and 100,000 macrophages were seeded per well in a chamber slide. iPSdM and macrophages were pre-incubated for 1 hour with different concentrations of polySia avDP20 (0.15, 0.5 and 1.5 μ M), followed by 1.5 hour incubation with 5 μ g/ μ l stained debris. Then, the cells were fixed, blocked, and incubated with first and secondary antibodies as mentioned for $A\beta$ phagocytosis. For analysis, images were obtained with a confocal laser scanning microscope. Percentage of the cells with fluorescently labeled debris was analyzed in 5 randomly selected areas per condition per experiment by using ImageJ software.

2.2.2 Detection of Superoxide Production

To measure the superoxide production by iPSdM, cells were seeded at a density of 40,000 cells per well in 4-chamber slides. 24 hours later, cells were treated with 10 μ M fibrillary $A\beta_{1-42}$ or 5 μ g/ μ l debris for 15 minutes with or without 1 hour polySia avDP20 (different concentrations) pre-incubation.

To measure the superoxide production by THP-1 macrophages, monocytes were seeded at a density of 100,000 cells per well in 4-chamber slides and differentiated to macrophages as mentioned before. 48 hours later, macrophages were treated with 10 μ M fibrillary $A\beta_{1-42}$ or 5 μ g/ μ l debris for 15 minutes with or without 1 hour polySia avDP20 (different concentrations) pre-incubation.

To test the antioxidant effect of SOD1 or Trolox as positive controls, iPSdM/macrophages were pre-incubated for 1 hour either with 60 U/ml SOD1 or 40 μ M Trolox, then fibrillary $A\beta_{1-42}$ or debris was added to them for 15 minutes. Afterwards,

Materials and Methods

cells were incubated for 15 minutes with 30 μ M DHE solution (diluted in Krebs-HEPES-buffer, table 2-9) at 37°C. Finally, cells were washed twice with Krebs-HEPES-buffer and fixed with 4% PFA/Glutaraldehyde (GAD) and mounted with Mowiol 4-88. Three pictures were taken of each condition per experiment by confocal laser scanning microscopy. Analyzing of the pictures has done by Image J software.

Table 2-9 Krebs-HEPES-buffer

Component	concentration	Company
HEPES	8.3 mM	Carl Roth GmbH
NaCl	130 mM	Sigma-Aldrich
KCl	5.6 mM	Sigma-Aldrich
CaCl ₂	2 mM	Sigma-Aldrich
MgCl ₂	0.24 mM	Sigma-Aldrich
Glucose	11 mM	Carl Roth GmbH

2.2.3 Neurite Branch Length Analysis

To analyze neurite branch length, co-cultures were prepared as mentioned in section 2.1.6. After 48 hours of iPScM:neuron co-culture incubation, cells were fixed, blocked, and immunostained with rabbit-anti-Iba1 and mouse-anti- β -tubulinIII antibodies (table 2-17) overnight at 4°C followed by secondary Cy3-conjugated goat antibody directed against rabbit IgG and Alexa488-conjugated antibody directed against mouse IgG (table 2-17) for 2 hours at room temperature. After 48 hours of THP-1 macrophage:neuron co-culture incubation, cells were fixed, blocked, and immunostained with monoclonal rat anti-CD11b and rabbit-anti-neurofilament antibodies (table 2-17) overnight at 4°C followed by secondary Cy3-conjugated goat antibody directed against rat IgG and Alexa 488-conjugated antibody directed against rabbit IgG (table 2-17) for 2 hours at room temperature. Five images per condition per experiment were randomly collected by confocal laser scanning microscopy and total lengths of neuronal branches from β -tubulinIII or neurofilament stained neurites was determined by the NIH ImageJ/NeuronJ software.

Materials and Methods

2.3 Molecular Assays

2.3.1 RT-PCR

THP-1 monocytes that were kept in THP1 differentiation medium or macrophages after 48 hours differentiation in this medium were lysed with 1 ml QIAzol. Afterwards, RNA was isolated using a modified phenol-chloroform based method according to table 2-10.

Table 2-10 RNA isolation

	Step	Quantity	Condition	Time
	Add QIAzol to cells	1 ml	Room temperature	5 min
	Incubation with chloroform	200 µl	Room temperature	3 min
	Centrifugation		13000 rpm, 4° C	15 min
	Collect the upper colorless phase			
	Incubation with isopropanol	(1:1) vol	Room temperature	5 min
	Centrifugation		13000rpm, 4°C	20 min
	Collect the sediment			
x3	Add 70% ethanol	300 µl		
	Centrifugation		13000rpm, 4°C	5 min
	Collect the sediment, dry, and resuspend in 12µl RNase free water			

To obtain cDNA, the total RNA which was obtained by protocol described in table 2-10 was used. Reverse transcription (RT) was performed by SuperScript III reverse transcriptase and random hexamer primers as claimed by table 2-11.

Materials and Methods

Table 2-11 Reverse Transcription			
Prepare RT mix (I)	Components	Amount	Company
	RNA	11 µl	
	Hexanucleotide (mM)	1 µl	Roche
	dNTP	1 µl	Paqlab
Start RT program	Temperature	Time	
	65°C	5 min	
	4°C	1 min	
	4°C	pause	
Add RT mix (II)	Components	Amount	Company
	5x first-strand buffer	4 µl	Invitrogen, life technologies
	DTT (100mM)	2 µl	Invitrogen, life technologies
	Superscript® III	1 µl	Invitrogen, life technologies
Continue RT program	Temperature	Time	
	25°C	5 min	
	55°C	1 h	
	70°C	15 min	
	4°C	pause	

RT-PCR reaction has been done by Taq DNA polymerase with primers mentioned in table 2-12.

Table 2-12 Primers		
Gene	Forward Primer (5' → 3')	Reverse Primer (5' → 3')
<i>SIGLEC11</i>	CACTGGAAGCTGGAGCATGG	ATTCATGCTGGTGACCCTGG
<i>GAPDH</i>	CTGCACCACCAACTGCTTAG	TTCAGCTCAGGGATGACCTT

Amplification program has been done by a Biometra Thermocycler machine as described in table 2-13.

Materials and Methods

Table 2-13 RT-PCR Program

Prepare PCR mix	Components	Amount	Company
	PCR reaction buffer 10x	5 µl	Roche
	dNTP	2 µl	Paqlab
	Forward Primer	2 µl	Invitrogen
	Reverse Primer	2 µl	Invitrogen
	Taq polymerase	0.2 µl	Roche
	cDNA	~ 500 ng	
	DEPC Treated Water	up to 50 µl	invitrogen
PCR program	Temperature	Time	
	94 °C	3 min	
x35	94 °C	1 min	
	60 °C	1 min	
	72 °C	1 min	
	72 °C	10 min	
	4 °C	pause	

2.3.2 qRT-PCR

To compare SIGLEC-11 transcription levels, qRT-PCR was performed with 200 ng cDNA, SYBR GreenEP™ qPCR SuperMix and 400 nM primers (table 2-12) in a final reaction volume of 25 µl. Amplification was done as mentioned in table 2-14 by a Mastercycler egradient S®. Results were analyzed by the manufacturer's software, amplification specificity was checked by melting curve analysis, and relative quantifications were done by $\Delta\Delta C_t$ method.

Materials and Methods

Table 2-14 qRT-PCR Program

Step		Temperature	Time	Cycle
1- Initial denaturation		95°C	10 min	
2- Amplification	Denaturation	95°C		x40
	Annealing	60°C		
	Elongation	72°C		
5- Inactivation		95°C	10 min	
6- Melting curve		59°C - 95°C	20 min	
7- Final denaturation		95°C	15 s	
8- Pause		4°C	pause	

2.4 Lentivirus Generation

For lentiviral knockdown of *SIGLEC11*, a 2nd generation packaging system was used. The lentiviral knockdown plasmid (shRNASig11: TRCN0000062842) in a human pLKO.1 lentiviral shRNA target gene set backbone or a pLenti 6.2/V5_DEST Gateway Vector without target gene were used as control vector. HEK293FT cells pre-seeded on PLL coated 15 cm² dishes were transduced by *SIGLEC11* knockdown plasmid or control plasmid mixed with packaging plasmids (psPAX2 and pMD2.G) as described in table 2-15.

Table 2-15 Lentivirus generation

Step	Components	Amount	Time	Company
1- Plasmid mix for 20 ml Advanced DMEM medium plus 25µM chloroquine	H ₂ O	1300 µl		
	Plasmid	40 µg		Open Biosystem
	Packging plasmid (psPAX2)	20 µg	5 min	Addgene
	Envelop plasmid (pMD2.G)	20 µg		Addgene
Complex formation	CaCl ₂ (2.5 M)	133 µl	15 min	
2- Add the whole plasmid mix to the dish	2xHBS	1300 µl	5 h	
3- Change the medium to normal MEF	20 ml		48 h	
4- harvest the virus				

Materials and Methods

For precipitation of viral particles, the virus-containing medium was collected and filtered (0.4 mm filter). Afterwards, the medium was mixed and incubated for 1.5 hour on ice with 8.5% polyethylenglycol, 0.3 M NaCl and PBS. Next, the solution was centrifuged at 4500 rpm for 30 minutes. At the end, the viral particle-containing pellet was resuspended in 1x PBS and added to THP-1 monocytes. After 48 hours, the transduced cells were selected by 1 µg/ml puromycin. The efficiency of knockdown was checked by FACS analysis. THP-1 cells transduced by either *SIGLEC11* plasmid or control plasmid after differentiation to macrophages were used for further analysis.

2.5 Immunological Techniques

2.5.1 Immunocytochemistry (ICC)

For cell culture immunostaining, cells were washed once with 1x PBS. Afterwards, all the stainings were done according to the protocol as mention in table 2-16. Antibodies used in satinings are mentioned in table 2-17. Images were taken by confocal laser scanning microscopy or Fluorescence microscopy.

Table 2-16 ICC Protocol

Step	Components	Time	Temperature
Fixation	4% PFA	15 min	Room temperature
Washing (3times)	1x PBS		
Blocking	10% BSA 5% nGS 0.1% Triton 100x	1 h	Room temperature
Primary antibody	in PBS	overnight	4°C
Washing (3times)	1x PBS		
Secondary antibody	in PBS	2 h	Room temperature
Washing (3times)	1x PBS		
Mounting	Mowiol		

Materials and Methods

Table 2-17 Antibodies

Antibody	Type	Host	Specificity	Working conc.	Company
Anti-NeuN monoclonal	1 st	mouse	mouse/human	10 µg/ml	Millipore
β-tubulin III monoclonal	1 st	mouse	rat/human	1 µg/ml	Sigma-Aldrich
β-tubulin III polyclonal	1 st	chicken	mouse/human	1 µg/ml	Millipore
CD11b (Integrin alpha-M) monoclonal	1 st	rat	mouse/human	1 µg/ml	BD Biosciences
ChAT polyclonal	1 st	goat	mouse/human	2 µg/ml	Millipore
GABA polyclonal	1 st	rabbit	rat/human	1 µg/ml	Sigma-Aldrich
GFAP polyclonal	1 st	rabbit	cow/human	1 µg/ml	Dako
Iba-1 polyclonal	1 st	rabbit	mouse/human	1 µg/ml	Wako
Ki67 monoclonal	1 st	mouse	human	10 µg/ml	Dako
MAP2 polyclonal	1 st	rabbit	mouse/human	1 µg/ml	Millipore
Nestin monoclonal	1 st	mouse	human	10 µg/ml	R&D system
Neurofilament 200 polyclonal	1 st	rabbit	mouse/human	1 µg/ml	Sigma-Aldrich
Olig2 polyclonal	1 st	rabbit	mouse/human	1 µg/ml	Millipore
Pax 6 polyclonal	1 st	rabbit	mouse/human	10 µg/ml	Covance
Siglec-11 monoclonal	1 st	mouse	human	2 µg/ml	Abmart
Sox1 polyclonal	1 st	rabbit	mouse/human	10 µg/ml	Millipore
Sox2 monoclonal	1 st	mouse	mouse/human	10 µg/ml	R&D system
Tyrosine Hydroxylase monoclonal	1 st	rabbit	mouse/human	1 µg/ml	Sigma-Aldrich
Zo1 polyclonal	1 st	rabbit	mouse/human	2 µg/ml	Invitrogen

Materials and Methods

Alexa 488-conjugated	2 nd	chicken	2 µg/ml	life technologies
Alexa 488-conjugated	2 nd	goat	2 µg/ml	Invitrogen
Alexa 488-conjugated	2 nd	rabbit	2 µg/ml	Invitrogen
Alexa 488-conjugated	2 nd	rat	2 µg/ml	Invitrogen
Cy3-conjugated	2 nd	mouse	2 µg/ml	Dianova
Cy3-conjugated	2 nd	rabbit	2 µg/ml	Dianova
Cy3-conjugated	2 nd	rat	2 µg/ml	Dianova
PE-conjugated	2 nd	mouse	2 µg/ml	Jackson Immuno Research

2.5.2 Enzyme-Linked Immunosorbent Assay (ELISA)

For ELISA, biotinylated polySia avDP20 had to be produced (table 2-18). PolySia avDP20 was coupled with a biotin molecule at the N-terminus of the polySia avDP20 chain. Biotinylated-dextran with same molecular weight was used as a control.

Table2-18 Biotinylation Protocol

Step	Components	Time	Comments	Company
Oxidation	Sodium Periodate (NaIO ₄) 0.02 M diluted in oxidation buffer	30 min in dark at 4 °C		Sigma-Aldrich
Washing	HiTrap Desalting, 5 x 5 ml		5 times (25ml 1x PBS)	GE Healthcare Life Sciences
Hydrazination	EZ-Link™ Hydrazide-Biotin 12.9 mg/ml dilute in DMSO	2 h at Room teperature		Thermo Scientific
Washing	wash the column		5 times (25ml 1x PBS)	
Purification	biotinylated polySia avDP20		load to the column wash through with 5ml 1xPBS	

Oxidation buffer: 0.1 M Natrium acetate (C₂H₃NaO₂)

Different concentrations of biotinylated-polySia avDP20 (0.01, 0.05, 0.25, 1.25, 6.25 µg/ml) or biotinylated-dextran (0.01, 0.05, 0.25, 1.25, 6.25 µg/ml) were used to test the binding affinity to the recombinant human SIGLEC-11 Fc-fusion (rhSIGLEC-11/Fc) protein coated plate according to table 2-19.

Materials and Methods

Table 2-19 ELISA Protocol

Step	Components	Concentration	Time	Temperature	Company
Coat plate	Protein A	10 µg/ml	overnight	4°C	Thermo Scientific
Washing	1x PBS + 0.05 % tween20		x 3		
Blocking	3% BSA		1 h	Room teperature	
Coat receptor	SIGLEC11-Fc	5 µg	2 h	Room teperature	R&D system
Washing	1x PBS + 0.05 % tween20		x 3		
Blocking	3% BSA		1 h	Room teperature	
Add ligand	biotinylated - polySia avDP20 or biotinylated - dextran	different conc.	2 h	Room teperature	
Washing	1x PBS + 0.05 % tween20		x 3		
First reaction	HRP	1:5000	1 h	Room teperature	Pharmingen
Washing	1x PBS + 0.05 % tween20		x 3		
Second reaction	TMB	100 µl	15 min	Room teperature	Sigma-Aldrich
Stop reaction	HCL	1N			
Read the plate with ELISA plate reader (PerkinElmer) at 450 nm					

2.5.3 Fluorescence-Activated Cell Sorting (FACS)

The same number of iPsdM and THP-1 macrophages were collected to study surface expression of SIGLEC-11. Afterwards, samples were prepared as stated in table 2-20. SIGLEC-11 expression was measured by a BD FACSCalibur and data was analyzed by the FlowJo 8.7 Software.

Table 2-20 FACS Protocol

Step	Components	Time	Temperature
Washing	1x PBS		
First antibody isotype control PBS control	in PBS	1 h	4°C
Washing	1x PBS	x2	
Secondary antibody	PE-conjugated Ab	30 min	4°C
Washing	1x PBS	x2	

Materials and Methods

2.5.4 MTT Assay

Cell viability was determined by the MTT (3-(4,5-Dimethylthiazol-2-yl)-2,5-diphenyltetrazolium bromide) assay. IPSdM cells were treated for 20 hours with different concentrations of distinct sialic acid chain lengths. Afterwards, yellow MTT was added to the cells and incubated for more 4 hours. At the end of this time, the purple MTT formazan was produced by living cells. The reaction was stopped by addition of isopropanol with HCl (0.04 N). Isopropanol dissolves formazan to give a homogeneous blue solution suitable for absorbance measurement, which was determined by a spectrophotometer at a wavelength of 570 nm.

Materials and Methods

2.6 Other Materials

2.6.1 Technical Equipment

Equipment	Article	Company
Autoclave	Systec D150	Systec GmbH
Automatic Pipettes	1, 10, 100, 1000 µl	Thermo Scientific
Centrifuge	Megafuge 1.0R	Heraeus Holding GmbH
Centrifuge	MCF 2360	LMS
Electrophoresis	Power Supply EPS 301	Amersham Bioscience
Electrophoresis	40-0911	Paqlab Biotechnologies
Flow Cytometer	BD FACSCaliber	BD Bioscience
Freezer (-20°C)	Premium	Liebherr
Freezer (-20°C)	Profiline GG5260	Liebherr
Freezer (-80°C)	Herafreeze	Heraeus Holding GmbH
Fridge (4°C)	Medline LKUv 1612	Liebherr
Gel Imaging System	ChemiDoc	Bio-Rad
Incubator	Hera Cell 150	Heraeus Holding GmbH
Laminar flow hood	Hera Safe	Kendo Laboratory products GmbH
Microscope	Confocal Olympus IX81	Olympus
Microscope	Axioskop HBO 50	Carl Zeiss AG
Microscope	Apotom	Carl Zeiss AG
Microwave Oven	Severin 800	SEVERIN Elektrogeräte
N2 Tank	MVE 611	German-cryo
Peristaltic Pump	Pump drive PD 5001	Heidolph
PH-meter	CG840	Schott
Pipetteboy	Cell Mate II	Thermo Fische Scientific Inc.
Scale	Acculab	Sartorius
Shaker	KS-15 control	Edmund Buhler GmbH
Spectrophotometer	Envision Multiplate Reader	Perkin Elmer
Spectrophotometer	NanoDrop 1000	Thermo Scientific
Thermocycler	T3	Biometra
Thermoshaker	Thermomixer compact	Eppendorf AG
Ultracentrifuge	Sorvall Discovery 90 SE	HITACHI
Ultracentrifuge	Sorvall RC 6+	Thermo Scientific
Ultracentrifuge	Sorvall 5B Plus	Thermo Scientific
Vaccum controller	VaccuHandControl	Vaccumbrand
Vaccum pump	Vaccu-lan network for lab	Vaccumbrand
Vortex	2X ²	Velp Scientifica
Waterbath	WB/OB7-45	Memmert GmbH & CoKG

Materials and Methods

2.6.2 Consumables

Product	Specification	Company
Cell Culture Pipette	5, 10, 25 ml	Sarstedt
Cell Scraper	17 mm	Sarstedt
Chamber Slides	Lab-Tek 4-chambers	Nalge Nunc
Culture dish	35, 100, 150 mm	Sarstedt
Culture dish	6-well plate	Greiner Bio One
Culture flasks	25, 75 cm ²	Sarstedt
Erlenmeyer flask	250 ml	Schott-Duran
Filter	0.22 µm	Sarstedt
Filter	0.45 µm	Corning Inc.
Glass bottle	100, 500, 1000 ml	Schott-Duran
Gloves	Micro-touch	Ansell
IHC Glass cover slips	24 x 60 mm	Engelbrecht
Lables	Tough-Spots 3/8"	DiversifiedBiotech
Neubauer counting-chamber	0.100 mm	Paul Marienfeld GmbH
Parafilm	M	Sigma-Aldrich
Pasteur pipettes	glass	Brand
Pasteur pipettes	plastic	Ratiolab
Pipette tips	10, 100, 1000 µl	Starlab GmbH
QPCR Optical Adhesive Film	QPCR seal	Paqlab Biotechnologies
QPCR plates	Semi-Skirted 96 wells	Paqlab Biotechnologies
Scalpel	Feather disposable scalpel	Thermo Fisher Scientific
Syringe	1, 50 ml	BD Bioscience
Tubes	0.2 ml; 8-strip	Biozym Scientific GmbH
Tubes	0.5, 1.5, 2 ml	Biozym Scientific GmbH
Tubes	1.8 ml cryotubes	Nalge Nunc
Tubes	5ml (flow cytometry)	Sarstedt
Tubes	15, 50 ml	Sarstedt

Materials and Methods

2.6.3 Chemicals and Reagents

Product	Company
4',6-diamidino-2-phenylindole (DAPI)	Sigma-Aldrich
Accutase	PAA
Agarose	Biozym Scientific GmbH
biotinylated Amyloid- β 1-42	Bachem
Amyloid- β 1-42	Bruker
Bovine Serum Albumin (BSA)	Sigma-Aldrich
Deoxynucleotide triphosphates (dNTP) 10 mM	Paqlab Biotechnologies
Dihydroethidium (DHE)	Thermo Fisher Scientific
Dil Derivatives for Long-Term Cellular Labelling (Dil)	Thermo Fisher Scientific
Dimethyl sulfoxide (DMSO)	Roche
Dithiothreiton DTT 10 mM	Invitrogen
DNA ladder 100 bp	Roche
Ethanol 99%	Carl Roth GmbH
Ethidium bromide	Carl Roth GmbH
Ethylenediaminetetraacetic acid (EDTA)	Carl Roth GmbH
Glycerol 99%	Sigma-Aldrich
Hexanucleotide mix 10x	Roche
Iso-propanol 99%	Sigma-Aldrich
Lipopolysaccharide (LPS)	InvivoGen
Media Advanced DMEM	Gibco
Media DMEMF-12, HEPES	Gibco
Media DMEM high glucose	Gibco
Media Opti-MEM	Gibco
Media Neurobasal®	Gibco
Media RPMI	Gibco
Mounting reagent Mowiol 4-88	Sigma-Aldrich
Normal goat serum	Sigma-Aldrich
Paraformaldehyde (PFA)	Merk & Co., Inc.
Phosphate Buffer Saline (PBS)	Gibco
Phorbol-12-Myristate-13-Acetate (PMA)	Sigma-Aldrich
Poly-L-lysine (PLL)	Sigma-Aldrich
Poly-L-ornithine (PLO)	Sigma-Aldrich
QIAzol®	Qiagen
Superoxide dismutase from bovine erythrocytes (SOD1)	Serva
Tris	Carl Roth GmbH
Triton X-100	Sigma-Aldrich
6-hydroxy-2,5,7,8-tetramethylchroman-2-carboxylic acid (Trolox)	Cayman
Trypan blue 0.4%	Gibco
Trypsin 0.25%	Gibco
Tween	Sigma-Aldrich
β -mercaptoethanol 99%	Carl Roth GmbH

Materials and Methods

2.6.4 Kits

Product	Company
Colorimetric (MTT) kit for cell survival and proliferation	Millipore
KAPA™ Mouse Genotyping Hot Start Kit	Peqlab
REDExtract-N-Amp™ Tissue PCR Kit	Sigma-Aldrich
RNeasy Mini Kit	Qiagen

2.7 Statistical Analysis

Data are presented as mean \pm SEM (standard error of mean) of at least three independent experiments. Data were analyzed by SPSS 20 software followed by either t-test for two samples or One-Way ANOVA followed by Bonferroni post hoc tests. Results are considered significant if *, $P < 0.05$; **, $P < 0.01$; ***, $P < 0.001$.

Results

3 Results

3.1 SIGLEC-11 Receptor and PolySia avDP20 as It's Ligand

3.1.1 SIGLEC-11 Expression on iPSdM Cells and THP1 Macrophages

SIGLEC-11 is expressed on human brain microglial cells [56]. Accordingly, to test the suitability of cell-lines, *SIGLEC-11* gene expression was analyzed in iPScM cells and THP-1 monocytes/macrophages via RT-PCR as mentioned in section 2.3.1. The human monocytic cell line THP-1, derived from an acute monocytic leukaemia patient, was differentiated by PMA to macrophages as a model system for human tissue macrophages (more details in section 2.1.4). iPScM cell line is an induced pluripotent stem cell derived microglial like cells, which used as a model system for human microglial cells (more details in section 2.1.3). The RT-PCR outcome showed clear expression of *SIGLEC-11* in all cells lines (Fig 3-1 A). Further comparison of mRNA levels between THP-1 monocytes and macrophages was performed by qRT-PCR as stated in section 2.3.2. Data showed that *SIGLEC-11* mRNA expression increased from 1 +/- 0.36 fold change in monocytes to 4.8 +/- 0.99 fold change in macrophages ($p=0.026$; Fig 3-1 B).

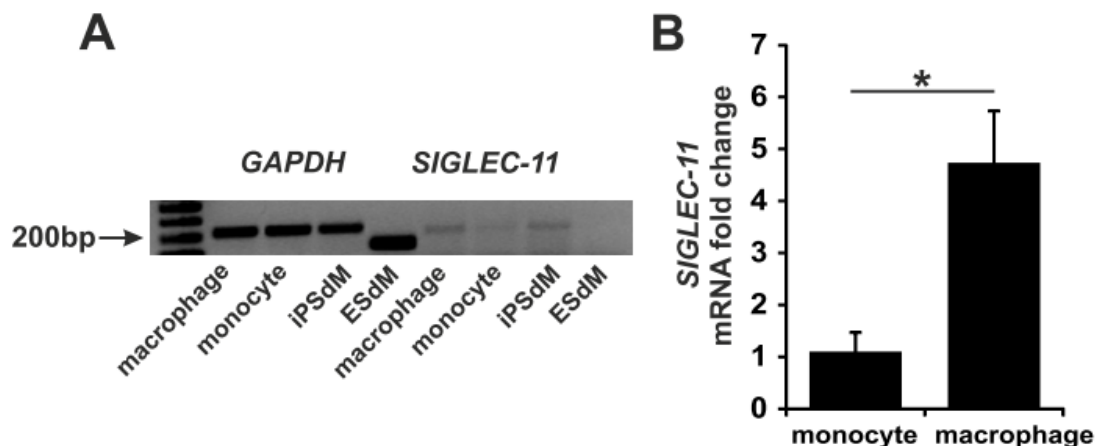


Figure 3-1: *SIGLEC-11* gene expression. *SIGLEC-11* gene expression in iPScM cells, THP1 monocytes and macrophages. Representative images out of at least three independent

Results

experiments; GAPDH is the internal control and mouse embryonic stem cell derived microglial cells (ESdM) cDNA is the negative control (A). *SIGLEC-11* gene expression comparison in THP-1 monocytes and THP-1 macrophages (B). Data are presented as mean \pm SEM of at least three independent experiments and were analyzed using t-test for independent samples. *, $p < 0.05$.

Afterward, SIGLEC-11 protein expression in iPSdM cells and THP-1 macrophages was evaluated as mentioned in section 2.5.3. Results showed that in a normal culture situation, around 30% of iPSdM cells and 35% of THP-1 macrophages express SIGLEC-11 (Fig 3-2).

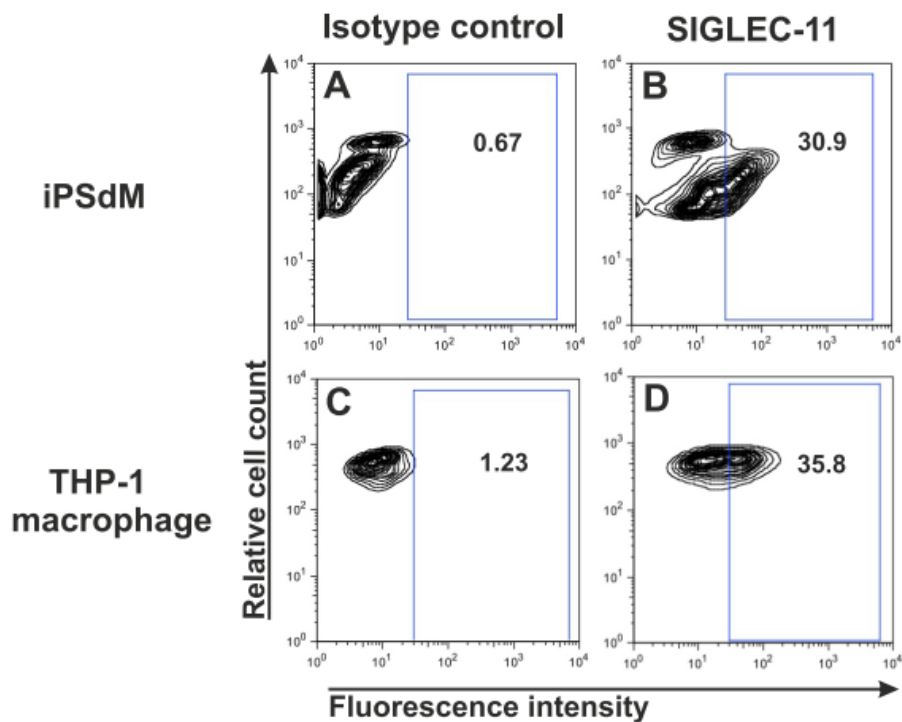


Figure 3-2: SIGLEC-11 protein expression. Expression of SIGLEC-11 protein on the cell surface of iPSdM cells with isotype control (A) and a SIGLEC-11 specific monoclonal antibody (B). Expression of SIGLEC-11 protein on the cell surface of THP-1 macrophages with isotype control (C) and a SIGLEC-11 specific monoclonal antibody (D). Representative images out of at least three independent experiments.

Results

3.1.2 OligoSias Do Not Prevent Superoxide Production

One feature of microglial cells is their ability to produce ROS upon A β stimulation, which is directly toxic for neurons [73][74]. To investigate ROS production upon fibrillar A β_{1-42} stimulation, iPsdMs were pre-incubated for 1 hour with monoSia and oligoSias (triSia and hexaSia) and were then stimulated for 15 minutes with fibrillar A β_{1-42} . The ROS production was measured by DHE staining (described in section 2.2.2). A β_{1-42} stimulation significantly increased ROS production (1.4 +/- 0.1 fold) compared to the control group (1 +/- 0.06; p=0.004; Fig 3-3). Pre-incubation with monoSia and oligoSias (triSia and hexaSia) could not prevent the A β_{1-42} effect (mono: 1.10 +/- 0.06 fold, tri: 1.22 +/- 0.1 fold, hexa: 1.25 +/- 0.07 fold; Fig 3-3).

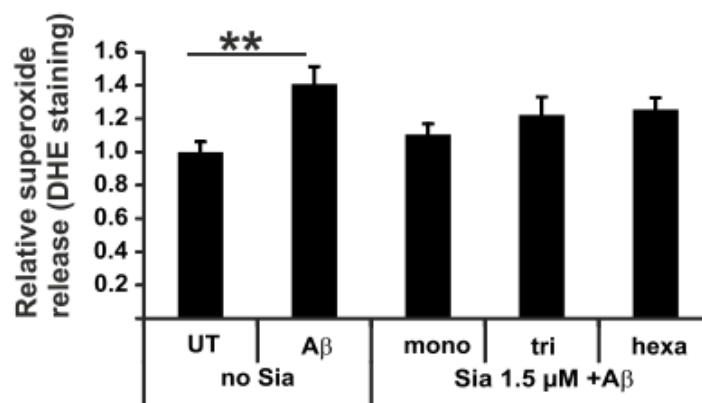


Figure 3-3: OligoSias cannot prevent superoxide production. A β_{1-42} treatment leads to significant superoxide production while monoSia, triSia, and hexaSia pre-incubation did not prevent this effect. Data are presented as mean +/- SEM of at least three independent experiments and were analyzed using one-way ANOVA (Bonferroni). **, p<0.01.

3.1.3 PolySia avDP20 and PolySia avDP 60 Prevent Superoxide Production

To examine if longer sizes of polySias were able to hamper the fibrillar A β_{1-42} effect or not, the synthesized polySias that had been produced in our laboratory, by Dr. Jens Kopats, were used. These polySias were homopolymers of α 2 \rightarrow 8 linked Sias with average degree of polymerizations of 20, 60, and 180 (polySia avDP20, avDP60, and

Results

avDP180). Pre-incubation with both polySia avDP20 and polySia avDP60 were able to reduce the superoxide production (Fig 3-4). To determine the optimal concentrations, different concentrations of polySia avDP20, avDP60, and avDP180 (0.15 μ M, 0.5 μ M, 1.5 μ M) were used. As demonstrated in Fig 3-4, polySia avDP20 incubation prevented fibrillar A β_{1-42} induced superoxide production at the concentrations of 0.5 μ M and 1.5 μ M (1.08 +/- 0.07 fold; p=0.038 and 0.98 +/- 0.04 fold; p<0.001, respectively) and polySia avDP60 at the concentration of 0.5 μ M (0.96 +/- 0.05 fold; p<0.001) in comparison to fibrillar A β_{1-42} (1.4 +/- 0.1; Fig 3-4). Despite the strong effects of polySia avDP20 and avDP60, different concentrations of high molecular weight polySia (polySia avDP180) pre-incubation did not reduce the superoxide production (Fig 3-4).

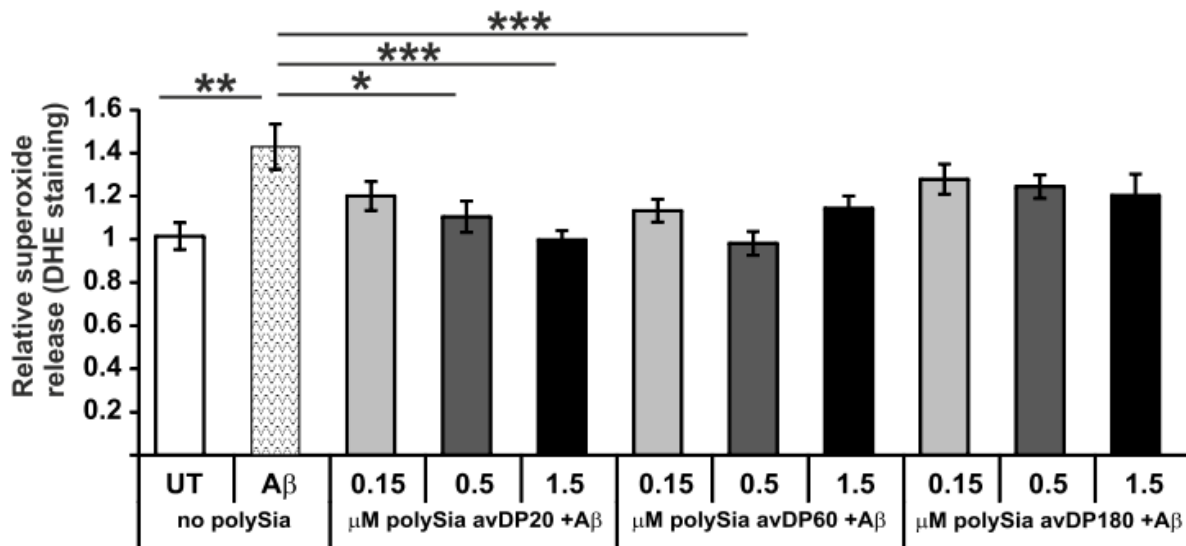


Figure 3-4: PolySias avDP20 and avDP60 are able to significantly reduce superoxide production. DHE intensity measurements showed that 0.5 μ M and 1.5 μ M of polySia avDP20 and 0.5 μ M of polySia avDP60 pre-incubation significantly prevented fibrillar A β_{1-42} induced superoxide production. PolySia avDP180 pre-incubation did not reduce the superoxide production induced by fibrillar A β_{1-42} . Data are presented as mean +/- SEM of at least three independent experiments and were analyzed using one-way ANOVA (Bonferroni). *, p<0.05; **, p<0.01; ***, p<0.001.

Results

DHE results showed that both polySia avDP20 and avDP60 prevent superoxide production upon fibrillar A β_{1-42} stimulation. To receive information about changes in metabolic activity of the cells, iPSdM were incubated with different concentrations of polySia avDP20, avDP60, and avDP180 (0.15 μ M, 0.5 μ M, 1.5 μ M) for 24 hours and an MTT assay was performed as mentioned in section 2.5.4. PolySia avDP60 and avDP180 at 1.5 μ M reduced the metabolic activity of iPSdM cells from 1 +/- 0.04 to 0.66 +/- 0.04 fold (p=0.037), and 0.71 +/- 0.02 fold (p=0.008), respectively (Fig 3-5). The concentration of 1.5 μ M polySia avDP20 was chosen for further experiments. Modified from [75].

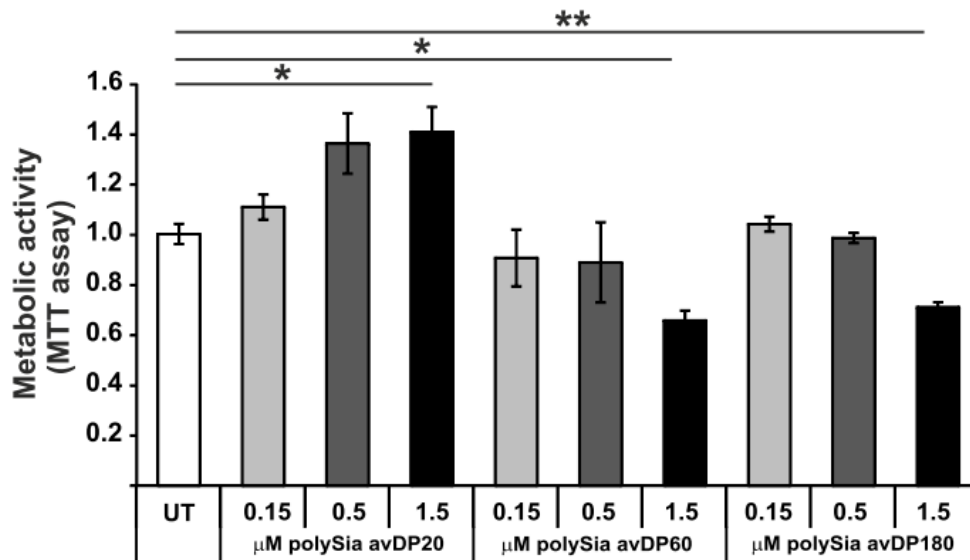


Figure 3-5: PolySias avDP60 and avDP180 are able to significantly reduce iPSdM cells metabolic activity. Metabolic activity measurements of iPSdM cells showed that 1.5 μ M of polySia avDP60 and avDP180 reduced the metabolic activity of iPSdM cells. Data are presented as mean +/- SEM of at least three independent experiments and were analyzed using one-way ANOVA (Bonferroni). *, p<0.05; **, p<0.01.

3.1.4 PolySia avDP20 Directly Binds to SIGLEC-11 Receptor

To investigate direct binding of the SIGLEC-11 receptor to polySia avDP20, a rhSIGLEC-11/Fc plate was used. Different concentrations of biotinylated polySia

Results

avDP20 (molecular weight between 4 and 8 kDa), which was produced according to the table 2-18, were added to the plate. Biotinylated dextran as a linear polysaccharide with a similar molecular weight (~ 5 kDa) was used as the control. ELISA was done as mentioned in table 2-19. Results showed that polySia avDP20 bound to the rhSIGLEC-11/Fc fusion protein in a concentration dependent manner, while no binding of dextran was observed. The relative binding to SIGLEC-11 shows the measured values of the OD450 from the ELISA. In detail, 0.01 $\mu\text{g/ml}$, 0.05 $\mu\text{g/ml}$, 0.25 $\mu\text{g/ml}$, 1.25 $\mu\text{g/ml}$, and 6.25 $\mu\text{g/ml}$ polySia avDP20 displayed binding to rhSIGLEC-11/Fc as 0.31 \pm 0.01 fold, 1.03 \pm 0.01 fold, 3.14 \pm 0.04 fold, and over saturated respectively. In comparison, 0.01 $\mu\text{g/ml}$, 0.05 $\mu\text{g/ml}$, 0.25 $\mu\text{g/ml}$, 1.25 $\mu\text{g/ml}$, and 6.25 $\mu\text{g/ml}$ biotinylated dextran showed binding to rhSIGLEC-11/Fc as 0.12 \pm 0.01 fold, 0.11 \pm 0.006 fold, 0.11 \pm 0.005 fold, and 0.10 \pm 0.005 fold respectively (Fig 3-6).

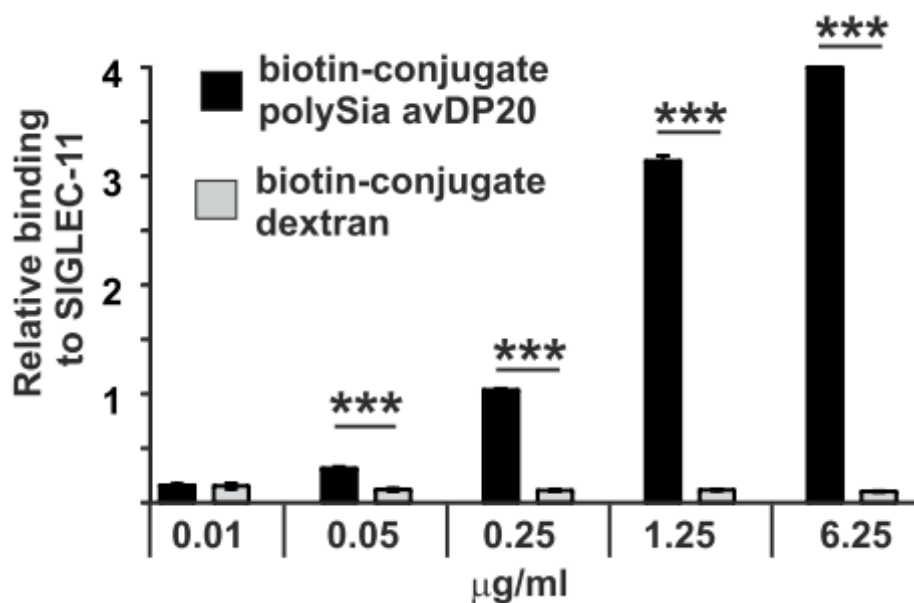


Figure 3-6: Direct binding of biotinylated polySia avDP20 to SIGLEC-11. ELISA measurements show the direct interaction between polySia avDP20 and SIGLEC-11/Fc fusion protein, while the binding of biotinylated dextran was negligible. Data are presented as mean \pm SEM of at least three independent experiments and were analyzed using one-way ANOVA (Bonferroni). ***, $p < 0.001$.

Results

3.2 PolySia avDP20 Modulates Macrophage Function via SIGLEC-11 Receptor

Macrophages and microglial cells have different functions in the brain, but they have two main tasks which can be harmful if misregulated. One of these tasks is phagocytosis and engulfment of apoptotic material, debris or A β peptides. The other task is release of superoxide which can be directly toxic for neurons (Block et al. 2007; Bordt & Polster 2014).

3.2.1 PolySia avDP20 Reduces Fibrillary A β_{1-42} and Debris Uptake in Macrophages

Formation of A β plaques is one of the hallmarks of AD. It was shown that ITAM-bearing receptors might be included in the removal of A β [77][66]. SIGLEC-11 is an ITIM-bearing receptor, which upon activation can counter regulate activation of ITAM receptors [58]. Here, we attempted to determine if polySia avDP20 is able to influence the function of iPSdM and macrophages through SIGLEC-11.

IPSdM cell and THP-1 macrophage preparation and experimental procedures were done as mentioned in section 2.2.1. Ingestion of fibrillary A β_{1-42} into the iPSdMs and macrophages was observed by confocal microscopy and 3D-reconstruction (Fig 3-7 A and B). IPSdM cells were incubated with three different concentrations of polySia avDP20 (0.15 μ M, 0.5 μ M, and 1.5 μ M). Among them, 0.5 μ M ($p=0.039$) and 1.5 μ M ($p=0.015$) of polySia avDP20 were able to significantly reduce fibrillary A β_{1-42} phagocytosis (Fig 3-7 C). In detail, pre-incubation with 0.15 μ M, 0.5 μ M, and 1.5 μ M polySia avDP20 reduced relative uptake of A β_{1-42} from 1 ± 0.12 to 0.76 ± 0.06 fold, 0.74 ± 0.06 fold, and 0.71 ± 0.06 fold, respectively (Fig 3-7 C). Similarly, THP-1 macrophages were also incubated with three different concentrations of polySia avDP20 (0.15 μ M, 0.5 μ M, and 1.5 μ M). Only 1.5 μ M ($p=0.003$) polySia avDP20 was able to significantly reduce the relative fibrillary A β_{1-42} phagocytosis. In detail, pre-incubation with 0.15 μ M, 0.5 μ M and 1.5 μ M polySia avDP20 reduced uptake of A β_{1-42} from 1 ± 0.08 to 0.94 ± 0.07 fold, 0.82 ± 0.02 fold, and 0.61 ± 0.06 fold, respectively (Fig 3-7 D).

Results

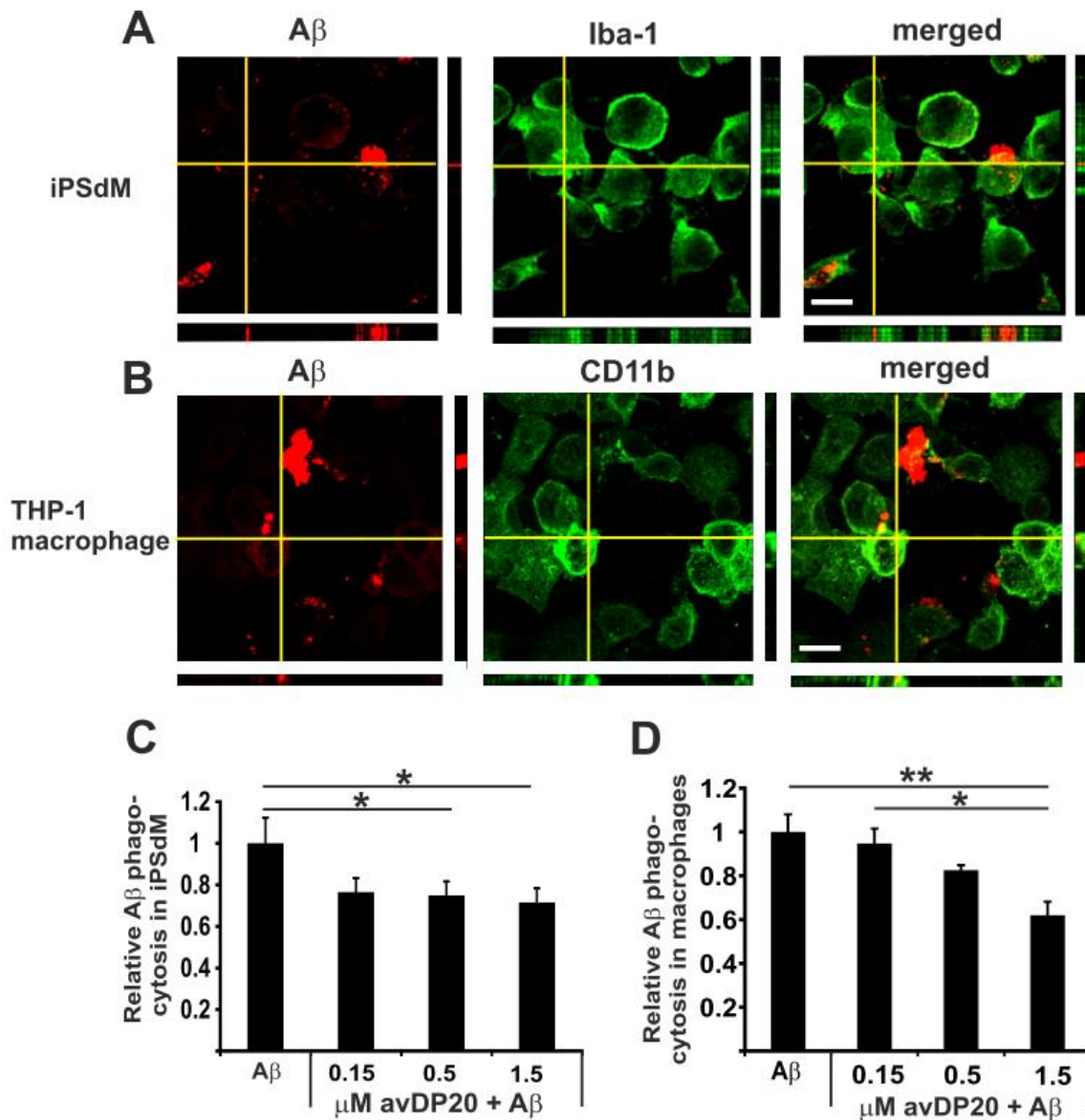


Figure 3-7: PolySia avDP20 reduced phagocytosis of fibrillary A β_{1-42} in iPScDM and THP-1 macrophages. Representative Z-stack confocal images and 3D reconstruction of A β (red) and iPScDM labeled Iba1 (green, **A**) or macrophages labeled CD11b (green, **B**) immunostaining shows A β internalization. Scale bar: 20 μ m. In iPScDM cells, 0.5 μ M and 1.5 μ M polySia avDP20 pre-incubation reduced A β uptake (**C**). In THP-1 macrophages, 1.5 μ M polySia avDP20 decreased A β uptake by these cells (**D**). Data are presented as mean \pm SEM of at least three independent experiments and were analyzed using one-way ANOVA (Bonferroni). *, $p < 0.05$; **, $p < 0.01$.

Results

Overexpression of siglec-e, which is an ITIM-bearing receptor in mouse, reduced neural debris engulfment into a microglial cell-line [68]. To explore the role of polySia avDP20 in debris uptake via SIGLEC-11 receptor, iPSdM cells and THP-1 macrophages were prepared as mentioned in section 2.2.1. Uptake of neural debris into the iPSdM cells and macrophages was observed by confocal microscopy and 3D-reconstruction (Fig 3-8 A and B). iPSdM cells were treated with three different concentrations of polySia avDP20. Only 1.5 μM ($p=0.004$) polySia avDP20 was able to significantly reduce phagocytosis of debris (Fig 3-8 C). In detail, pre-incubation with 0.15 μM , 0.5 μM , and 1.5 μM polySia avDP20 reduced relative uptake of debris from 1 ± 0.07 in untreated group to 1.04 ± 0.06 fold, 0.78 ± 0.06 fold, and 0.68 ± 0.05 fold, respectively. THP-1 macrophage responses to polySia avDP20 treatments were similar. Again, only 1.5 μM ($p=0.007$) polySia avDP20 was able to significantly reduce labeled debris phagocytosis (Fig 3-8 D). In detail, pre-incubation with 0.15 μM , 0.5 μM , and 1.5 μM polySia avDP20 reduced relative uptake of debris by macrophages from 1 ± 0.06 to 0.95 ± 0.03 fold, 0.84 ± 0.03 fold, and 0.7 ± 0.07 fold, respectively (Fig 3-8 D).

Results

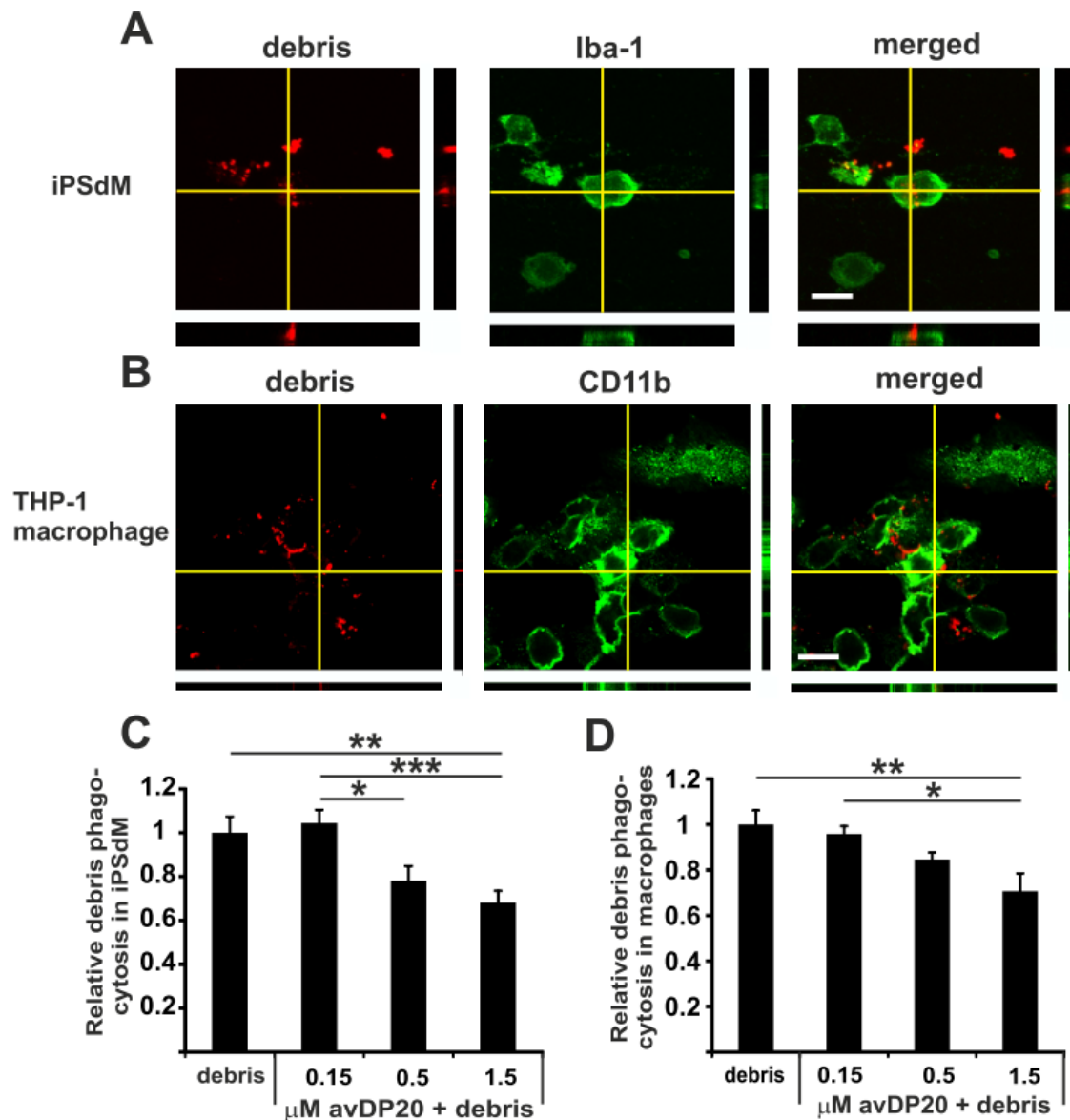


Figure 3-8: PolySia avDP20 reduced phagocytosis of labeled debris in iPScM and macrophages. Representative Z-stack confocal images and 3D reconstruction of debris (red) and iPScM labeled Iba1 (green, **A**) or macrophages labeled CD11b (green, **B**) immunostaining shows debris internalization. Scale bar: 20 μm . In iPScM cells, 1.5 μM polySia avDP20 pre-incubation reduced debris uptake (**C**). In THP-1 macrophages, 1.5 μM polySia avDP20 decreased debris ingestion by these cells (**D**). Data are presented as mean \pm SEM of at least three independent experiments and were analyzed using one-way ANOVA (Bonferroni). *, $p < 0.05$; **, $p < 0.01$; ***, $p < 0.001$.

Results

3.2.2 PolySia avDP20 Reduces Superoxide Production Triggered by Fibrillary A β ₁₋₄₂ and Debris Uptake in iPSdM and Macrophages

A β attachment to the cell surface of microglia results in activation of the tyrosine kinase Syk, which starts the assembly of a multi-subunit enzyme NADPH oxidase [78]. These microglial cells then release superoxides via the NADPH oxidase [79]. Accordingly, in this study the superoxide release from iPSdM cells or THP-1 macrophages after fibrillary A β ₁₋₄₂ stimulation was measured. In addition, the effect of polySia avDP20 was investigated.

iPSdM cells and THP-1 macrophages were prepared for experiments as mentioned in section 2.2.2. Signal intensity quantification of DHE-labeled superoxide measurements showed that in iPSdM cells, fibrillary A β ₁₋₄₂ significantly increased the superoxide production compared to untreated cells ($p=0.001$; Fig 3-9 A). However, pre-incubation with 0.5 μ M ($p=0.02$) and 1.5 μ M ($p=0.001$) polySia avDP20 significantly prevented superoxide production (Fig 3-9 A). In detail, A β incubation increased the release of superoxides from 1 ± 0.06 in untreated cells to 1.4 ± 0.1 fold in A β treated cells. Pre-incubation with 0.15 μ M, 0.5 μ M, and 1.5 μ M PolySia avDP20 reduced the A β -caused superoxide release from 1.4 ± 0.1 to 1.18 ± 0.06 fold, 1.08 ± 0.07 fold, and 0.98 ± 0.04 fold, respectively (Fig 3-9 A).

Likewise, in THP-1 macrophages fibrillary A β ₁₋₄₂ significantly increased the superoxide production compared to untreated cells ($p=0.004$; Fig 3-9 B). Pre-incubation with 0.5 μ M ($p=0.048$) and 1.5 μ M ($p=0.031$) polySia avDP20 significantly prevented the superoxide production (Fig 3-9 B). In detail, A β incubation increased the superoxide release from 1 ± 0.05 in untreated cells to 1.43 ± 0.1 fold in A β treated cells. In detail, 0.15 μ M, 0.5 μ M, and 1.5 μ M polySia avDP20 treatment reduced the A β induced superoxide release from 1.43 ± 0.1 to 1.17 ± 0.04 fold, 1.10 ± 0.07 fold, and 1.08 ± 0.03 fold, respectively (Fig 3-9 B).

Results

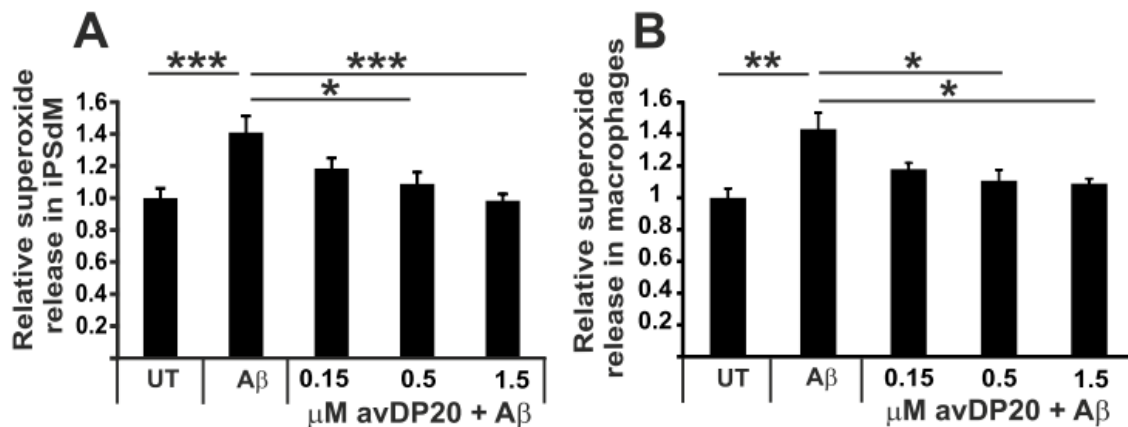


Figure 3-9: PolySia avDP20 prevented the superoxide release induced by fibrillary A β_{1-42} in iPSdM and macrophages. Measurements superoxide release by DHE staining showed that A β_{1-42} incubation significantly increased superoxide release in iPSdM (A) and macrophages (B). PolySia avDP20 pre-incubation prevented this increase both in iPSdM cells (A) and macrophages (B). Data are presented as mean \pm SEM of at least three independent experiments and were analyzed using one-way ANOVA (Bonferroni). *, $p < 0.05$; **, $p < 0.01$; ***, $p < 0.001$.

Cellular debris can be recognized by ITAM-bearing receptors which leads then to superoxide release [80]. In an *in vitro* model, it has been shown that knockdown of siglec-e increased the superoxide release upon neural debris stimulation [68]. To test the stimulatory effect of cellular debris in the human *in vitro* system, superoxide release from iPSdM cells or THP-1 macrophages was measured after debris treatment. In addition, the effect of polySia avDP20 was investigated.

iPSdM cells and THP-1 macrophages were prepared and experiments were done as mentioned in section 2.2.2. Signal intensity quantification of DHE-labeled superoxide measurements showed a significant increase in relative superoxide production in iPSdM cells after debris incubation compared to untreated cells ($p < 0.001$; Fig 3-10 A). Pre-incubation with 0.5 μ M ($p = 0.047$) and 1.5 μ M ($p < 0.001$) polySia avDP20 significantly prevented the relative superoxide production (Fig 3-10 A). In detail, debris incubation increased the superoxide release from 1 ± 0.05 in untreated cells to 1.45 ± 0.07 fold in

Results

debris treated cells. PolySia avDP20 pre-incubation with 0.15 μM , 0.5 μM , and 1.5 μM reduced debris mediated superoxide release from 1.4 ± 0.07 to 1.21 ± 0.08 fold, 1.18 ± 0.05 fold and 0.92 ± 0.04 fold, respectively (Fig 3-10 A).

In THP-1 macrophages, debris treatment significantly increased the superoxide production compared to untreated cells as well ($p=0.01$; Fig 3-10 B). Pre-incubation with 1.5 μM polySia avDP20 significantly prevented the superoxide production ($p=0.01$; Fig 3-10 B). In detail, debris incubation increased relative superoxide release from 1 ± 0.09 in untreated cells to 1.61 ± 0.1 fold in debris treated cells. 0.15 μM , 0.5 μM , and 1.5 μM polySia avDP20 reduced debris stimulated superoxide release from 1.61 ± 0.1 to 1.37 ± 0.08 fold, 1.35 ± 0.08 fold, and 0.99 ± 0.1 fold, respectively (Fig 3-10 B).

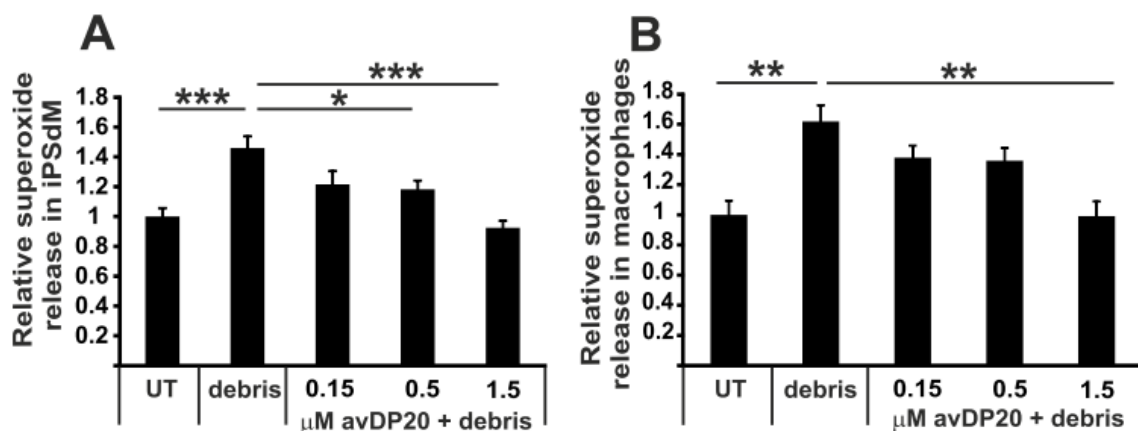


Figure 3-10: PolySia avDP20 prevented the superoxide release in debris stimulated iPSdM and macrophages. Measurements superoxide release by DHE staining showed that neural debris incubation significantly increased superoxide release in iPSdM (A) and macrophages (B). PolySia avDP20 pre-incubation hampered this raise in both iPSdM cells (A) and macrophages (B). Data are presented as mean \pm SEM of at least three independent experiments and were analyzed using one-way ANOVA (Bonferroni). *, $p < 0.05$; **, $p < 0.01$; ***, $p < 0.001$.

Results

3.2.3 PolySia avDP20 Acts as Effectively as an Antioxidant

A biological antioxidant is a substance that, at low concentration, prevents the oxidation of the substrate [81]. Already polySia avDP20 pre-incubation at 1.5 μ M prevented superoxide release upon fibrillary A β ₁₋₄₂ and debris stimulation. Trolox and SOD1, which are well-known antioxidants, were chosen to compare the scavenging effect of antioxidants with polySia avDP20 to reduce oxidative stress.

IPSdM cells and THP-1 macrophages were prepared and pre-incubated with 1.5 μ M polySia avDP20, 60 U/ml SOD1 or 40 μ M Trolox. Then, fibrillar A β ₁₋₄₂ or debris were added and the experiments were done as mentioned in section 2.2.2. Signal intensity quantification of DHE-labeled superoxide measurements showed in iPSdM cells the elevation in superoxide production upon fibrillary A β ₁₋₄₂ incubation (1.29 ± 0.05 fold) were reduced by both SOD1 (1.08 ± 0.05 fold; $p=0.061$; Fig 3-11 A) and Trolox (1.08 ± 0.06 fold; $p=0.074$; Fig 3-11 A) pre-incubation. Comparably, this reducing effect was similar to polySia avDP20 pre-incubation (0.97 ± 0.05 fold; $p<0.001$; Fig 3-11 A).

In THP-1 macrophages, the increased superoxide production upon fibrillary A β ₁₋₄₂ incubation (1.42 ± 0.05 fold) was significantly prevented by both SOD1 (0.92 ± 0.1 fold; $p=0.005$; Fig 3-11 B) and Trolox (0.91 ± 0.1 fold; $p=0.004$; Fig 3-11 B) pre-incubation. Equivalently, this hampering effect was identical to polySia avDP20 pre-incubation (0.99 ± 0.02 fold; $p=0.02$; Fig 3-11 B).

Results

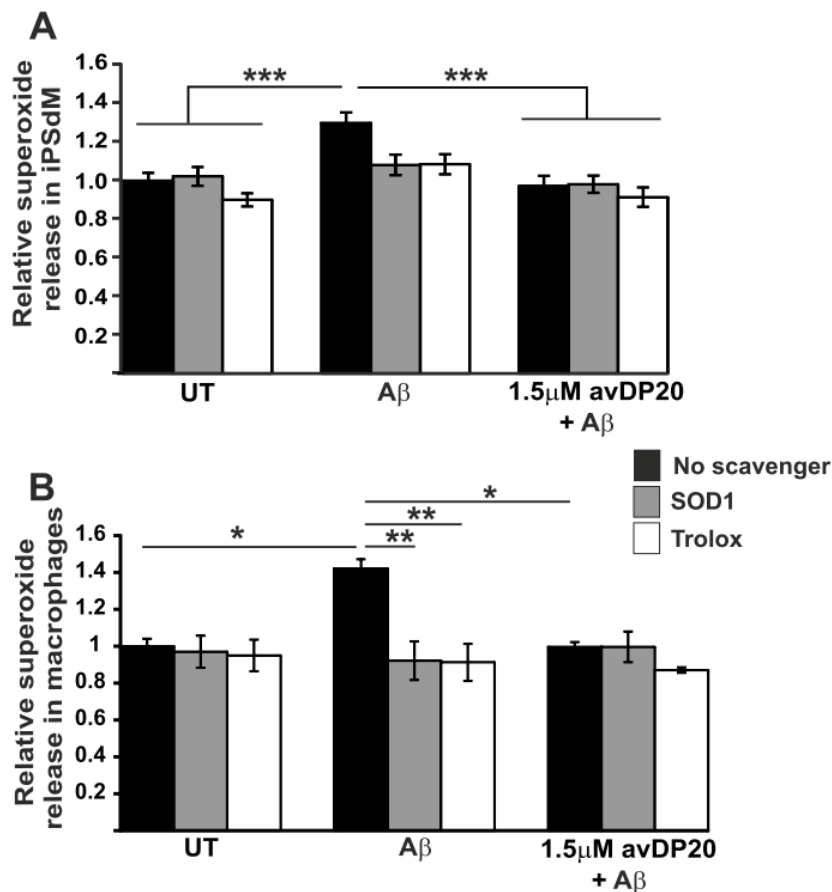


Figure 3-11: PolySia avDP20 inhibitory effect upon A β ₁₋₄₂ stimulation is as strong as common antioxidants SOD1 and Trolox. Relative intensity of the superoxide-sensitive fluorescent dye measurements showed that SOD1 and Trolox pre-incubation reduced superoxide release upon fibrillary A β ₁₋₄₂ stimulation both in iPSdM cells (**A**) and THP-1 macrophages (**B**). The level of reduction was similar to polySia avDP20 pre-incubation. Data are presented as mean \pm SEM of at least three independent experiments and were analyzed using one-way ANOVA (Bonferroni). *, $p < 0.05$; **, $p < 0.01$; ***, $p < 0.001$.

To study the effect of neural debris, iPSdM cells and THP-1 macrophages were prepared for experiments as mentioned in section 2.2.2. In iPSdM, the elevation in superoxide production upon debris incubation (1.24 ± 0.05 fold) was significantly prevented by both SOD1 (0.85 ± 0.05 fold; $p < 0.001$; Fig 3-12 A) and Trolox (0.96 ± 0.04 fold; $p = 0.01$; Fig 3-12 A) pre-incubation. The reducing effects of scavengers were as strong as polySia avDP20 pre-incubation (0.97 ± 0.04 fold; $p = 0.017$; Fig 3-12 A).

Results

Same experiments in THP-1 macrophages showed that the elevation in superoxide production upon cell debris incubation (1.4 ± 0.1 fold) significantly decreased by either SOD1 (0.86 ± 0.03 fold; $p < 0.001$; Fig 3-12 B) or Trolox (0.93 ± 0.02 fold; $p < 0.001$; Fig 3-12 B) pre-incubation. PolySia avDP20 pre-incubation reduced superoxide release to the same level as scavengers (0.94 ± 0.03 fold; $p < 0.001$; Fig 3-12 B).

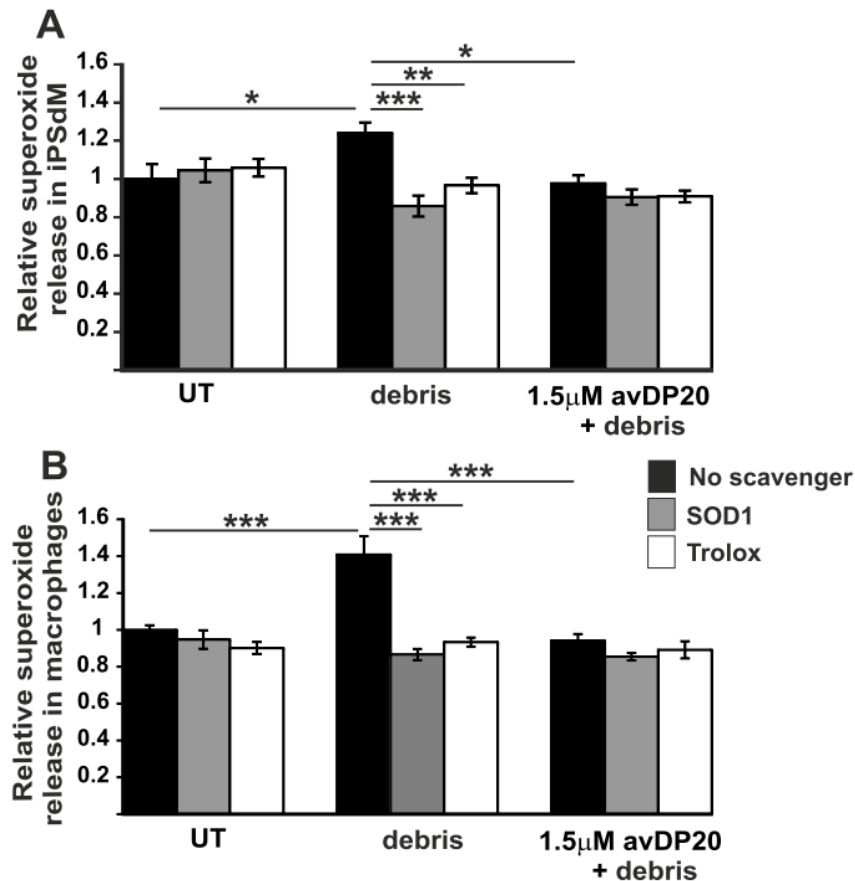


Figure 3-12: PolySia avDP20 inhibitory effect upon cell debris stimulation is similar to common antioxidants SOD1 and Trolox. Relative intensity of the superoxide-sensitive fluorescent dye measurements showed that SOD1 and Trolox pre-incubation reduced stimulatory production of superoxide upon cell debris addition both in iPScM cells (A) and THP-1 macrophages (B). The level of reduction is similar to polySia avDP20 pre-incubation. Data are presented as mean \pm SEM of at least three independent experiments and were analyzed using one-way ANOVA (Bonferroni). *, $p < 0.05$; **, $p < 0.01$; ***, $p < 0.001$.

Results

3.2.4 Knockdown of SIGLEC-11 Diminishes PolySia avDP20 Anti-Superoxide Effect

The potential receptor of polySia avDP20 on iPSdM is SIGLEC-11. To confirm that polySia avDP20 has its inhibitory effects through SIGLEC-11 receptor, a knockdown experiment was performed. SIGLEC-11 knockdown cells were prepared as mentioned in section 2.4. Afterwards, DHE experiments were performed as mentioned in section 2.2.2. In iPSdM cells which contained the control plasmid, A β ₁₋₄₂ stimulation increased superoxide release (1.19 +/- 0.01 fold; p=0.012; Fig 3-13) and polySia avDP20 pre-incubation prevented this stimulation (0.93 +/- 0.03 fold; p<0.000; Fig 3-13). However, SIGLEC-11 knockdown abolished the repressing effects of polySia avDP20 on A β ₁₋₄₂ induced superoxide production (1.24 +/- 0.06 fold; p<0.000; Fig 3-13).

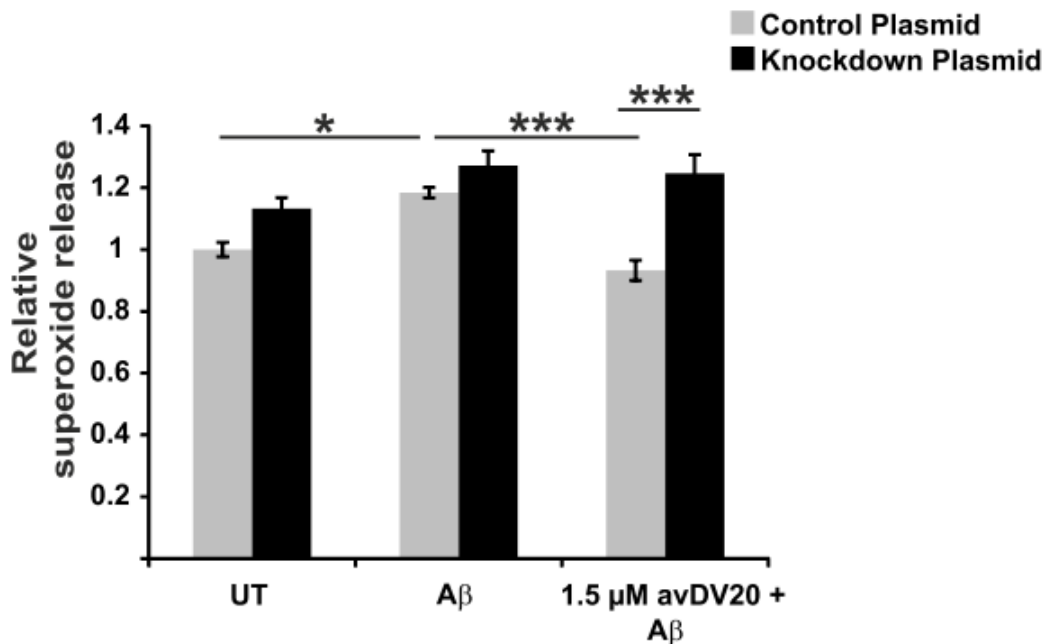


Figure 3-13: SIGLEC-11 knockdown eliminated the repressing effects of polySia avDP20.

In cells which received a control plasmid, A β ₁₋₄₂ increased ROS production significantly compared to untreated cells and polySia avDP20 pre-incubation prevented this rise. Superoxide production in SIGLEC-11 knockdown cells compared to control cells increased and polySia avDP20 pre-incubation did not prevent this rise. Data are presented as mean +/- SEM of at least three independent experiments and were analyzed using one-way ANOVA. *, p<0.05; and ***, p<0.001.

Results

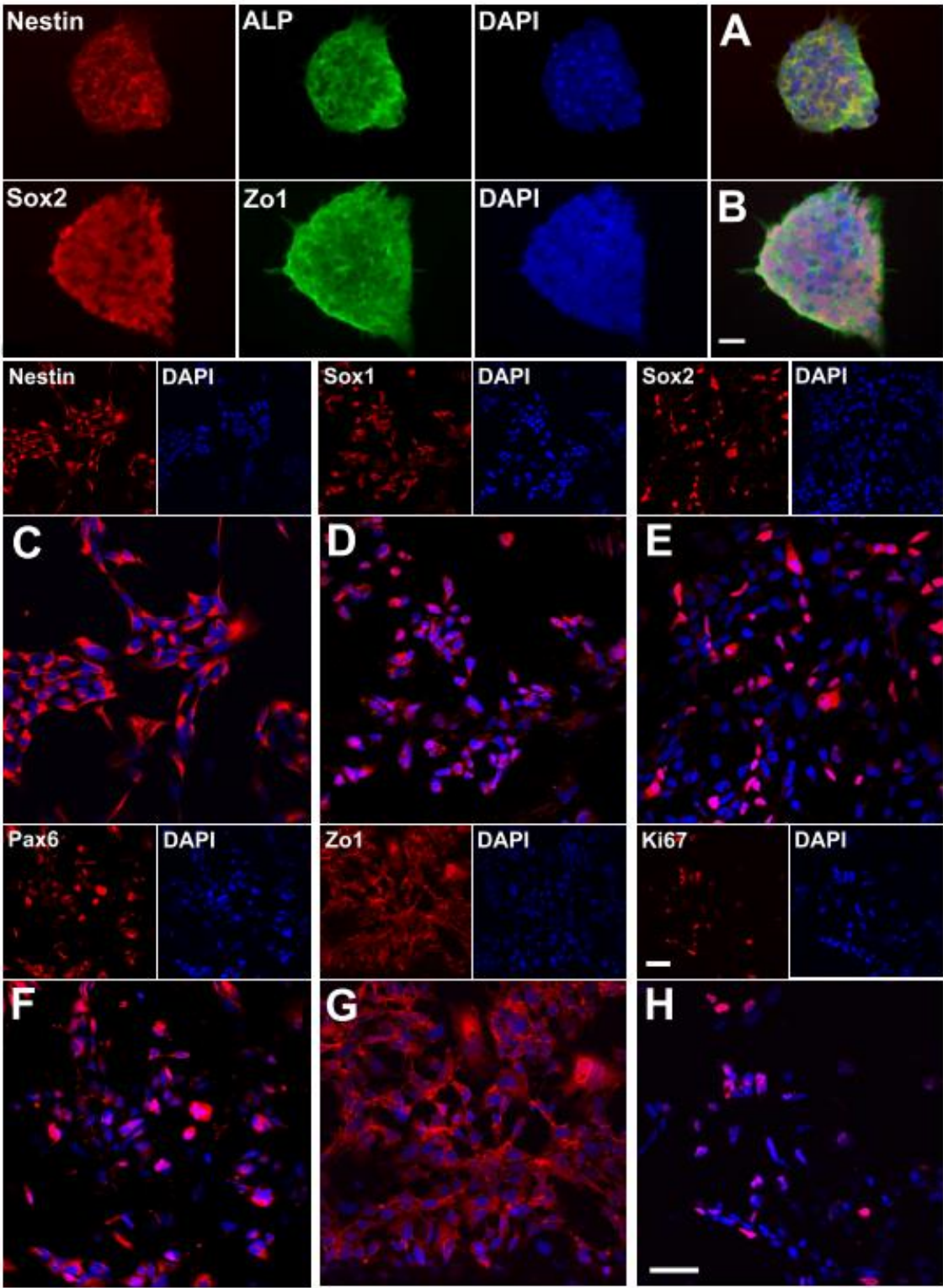
3.3 PolySia avDP20 Modulates iPsdM/Macrophage Function in Co-culture with Neurons

Neher and colleagues showed that microglia actively uptake neurons if A β is present in the culture [39]. To investigate whether polySia avDP20 can hamper this phenomenon, first iPsdM-neuron and macrophage-neuron co-cultures were established. Then, the effect of adding polySia avDP20 to the co-culture systems was explored.

3.3.1 Primitive Neural Stem Cells (pNSCs)

To set up the co-culture system, it was necessary to obtain human neuronal cells. In 2011, a relatively short and fast protocol was published, which used small inhibitory molecules to produce a homogenous culture of pNSCs from human embryonic stem cells [70]. In this study, the same protocol with small modifications was used to produce pNSCs from iPS cells as mentioned in section 2.1.1. pNSCs formation was confirmed by immunocytochemistry at passage 1 (Fig 3-14, A and B) and passage 10 (Fig 3-14, C-H). At passage 1, cells formed small colonies and strongly expressed NSC markers Nestin and ALP (Fig 3-14 A). Furthermore, the pluripotent stem cell marker Sox2 and ZO1 were also robustly expressed in these cells (Fig 3-14 B). By reaching a higher passage number (here 10), cells formed epithelial morphology and still expressed the NSC markers Nestin, Sox1, Sox2 and Pax6. Nestin (Fig 3-14 C) is a type VI intermediate filament protein, which is mainly expressed in dividing NSCs and is involved in the radial growth of the axons. Sox1 (Fig 3-14 D), Sox2 (Fig 3-14 E), and Pax6 (Fig 3-14 F) are transcription factors, which are necessary for maintaining self-renewal and pluripotency of NSC. In addition, these cells were positive for the tight junction protein Zo1 (Fig 3-14, G) and cell proliferation marker Ki67 (Fig 3-14, H). pNSCs in our culture system were able to long-term self-renew over serial passages up to passage 30 on PLO + Fn coated dishes in the presence of hLIF, CHIR99021, and SB431542 inhibitory factors.

Results



Results

Figure 3-14: Characterization of pNSCs derived from iPS cells. pNSCs at passage 1 were positive for NSC markers such as nestin and ALP (**A**). Moreover, these cells expressed pluripotency marker Sox2 and rosette-type NSC marker ZO1 (**B**). Immunocytochemistry data showed that when pNSCs reached a higher passage number (here 10), they kept the expression of NSC markers Nestin, Sox1, Sox2 and Pax6 (**C-F**). In addition, they were positive for Zo1 and Ki67 (**G-H**). Scale bar: 50 μ m.

3.3.2 pNSCs Differentiation towards Mature Neurons

To induce neuronal differentiation, pNSCs were cultured on PLO + Ln coated dishes with appropriate growth factors as mentioned in section 2.1.2. For neuronal characterization, immunocytochemistry with neuronal and non-neuronal markers was performed (Fig 3-15 and 3-16). Cultures were stained for glial markers olig2 (for oligodendrocyte; Fig 3-15 A), Iba1 (for microglial cells; Fig 3-15 B) and GFAP (for astrocyte; Fig 3-15 C) to investigate the neuronal culture's purity. Immunocytochemistry data showed that the produced neuronal cultures did not contain any oligodendrocyte and microglial cells; however, they had GFAP positive cells (Fig 3-15).

Neuronal cultures were stained for specific neuronal markers. Immunocytochemistry data showed that the neurons were positive for microtubule element of tubulin family (β -tubulin-III), neurons intermediate filament (Neurofilament), microtubule-associated protein 2 (MAP2) and hexaribonucleotide binding protein-3 (NeuN), which is a neural nucleus marker (Fig 3-16, **A-C**). Developed neuronal cultures contained mostly catecholaminergic neurons (ChAT), GABAergic neurons (GABA) and a small population of tyrosine hydroxylase (TH) positive neurons (Fig 3-16, **D-F**). Staining with Ki67 showed that even after two weeks of differentiation, the neuronal cultures still contained proliferating cells (Fig 3-16 **G**).

Results

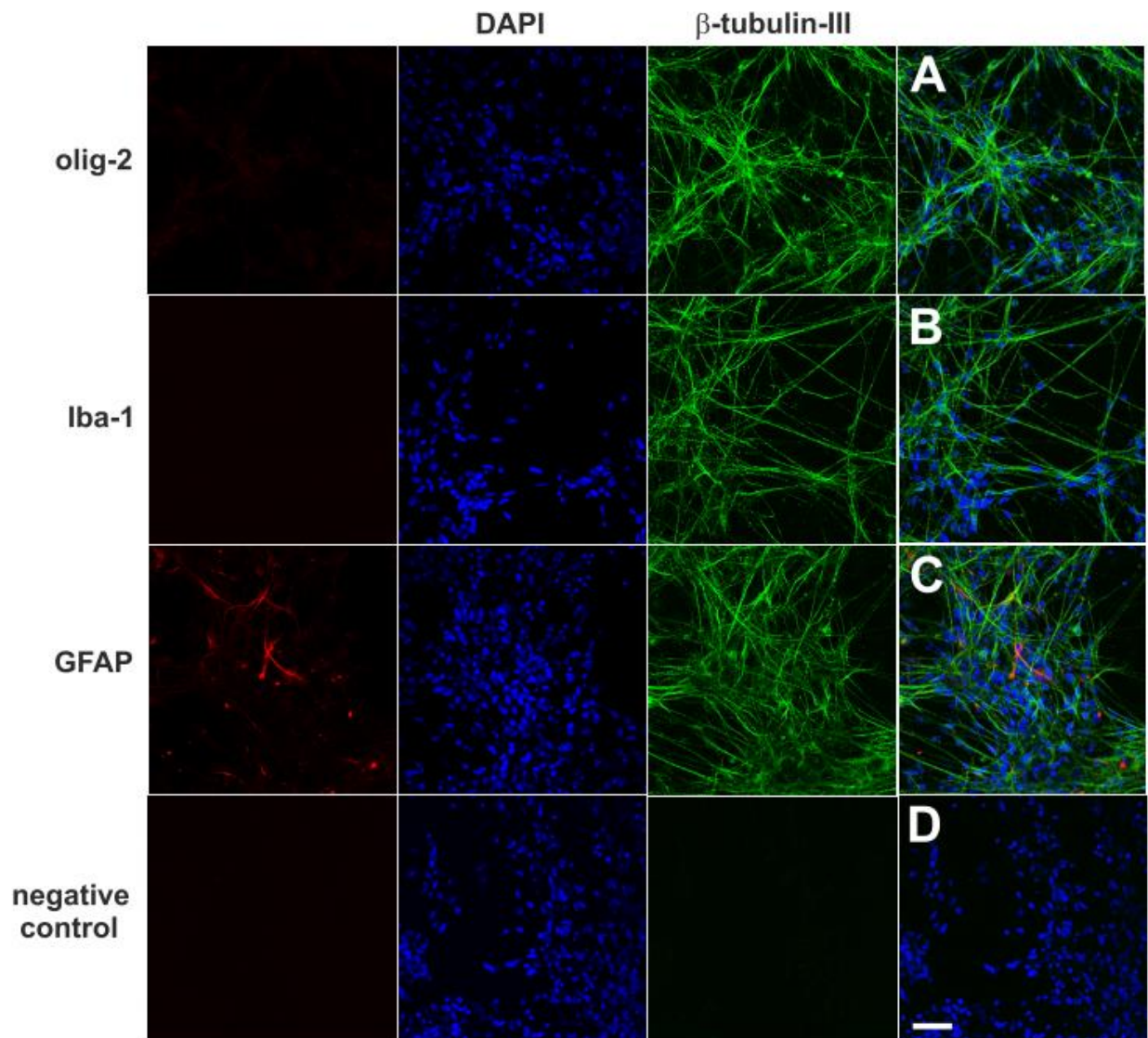
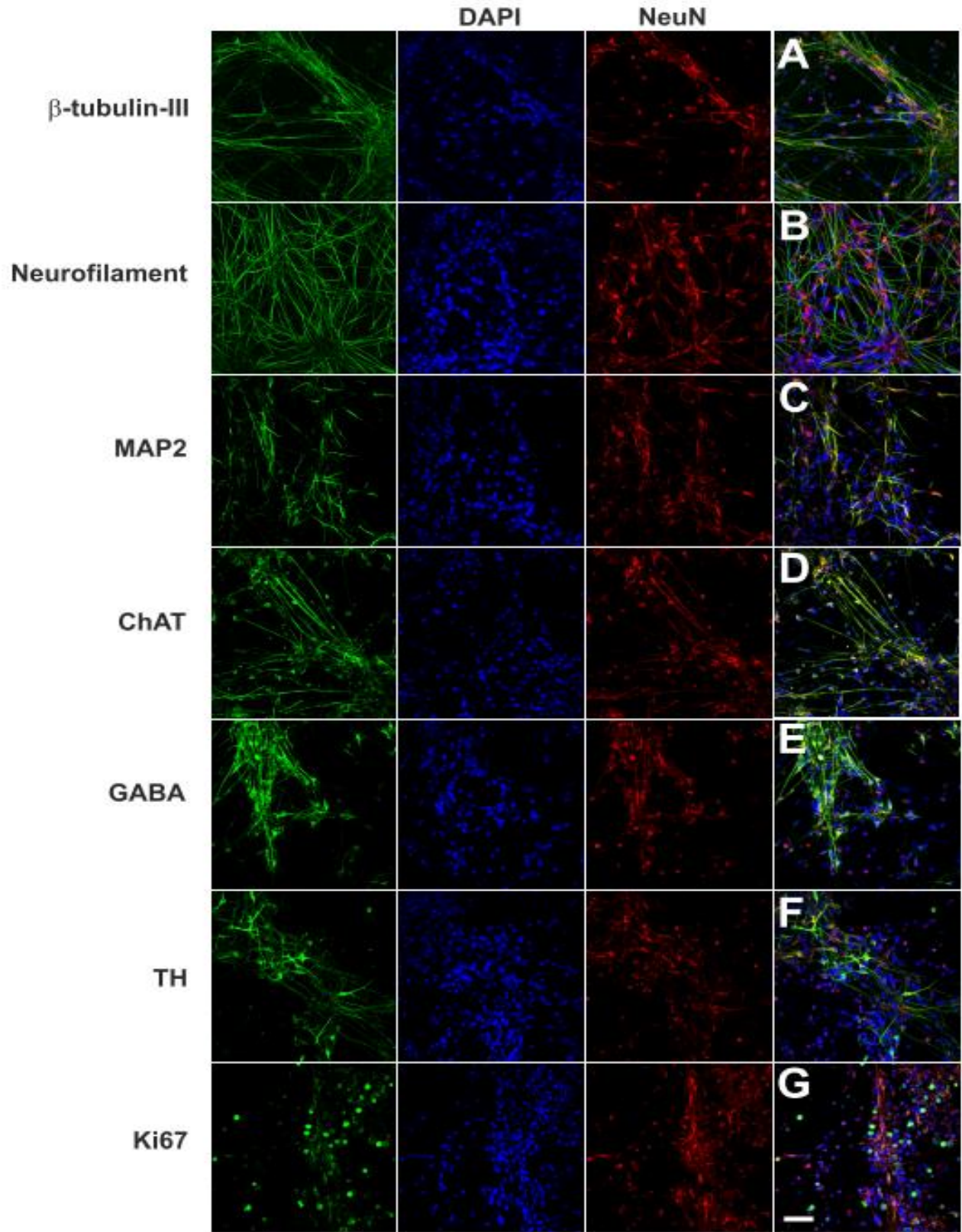


Fig 3-15: Purity of neuronal cell cultures. The developed neuronal cultures were stained for glial cells markers. The cultures were vacant of oligodendrocytes (olig-2, **A**) and microglial cells (Iba-1, **B**). There were always small populations of astrocytes in the neuronal cultures (GFAP, **C**). Negative controls contain no first antibodies (**D**). Scale bar: 50 μ m.

Results



Results

Figure 3-16: Neuron specific markers expression. pNSCs differentiated into neurons with high efficiency. Immunocytochemistry data showed that neuronal cells were positive for β -tubulin-III, Neurofilament, MAP2 and NeuN (**A-C**). The cultures contained different types of neurons such as ChAT, GABA, and TH-positive neurons (**D-F**). In addition, differentiated neuronal cultures had populations of proliferating cells (**G**). Scale bar: 50 μ m.

3.3.3 PolySia avDP20 Has no Effect on Metabolic Activity of Neurons

To measure the metabolic activity of neurons, pNSC were seeded on PLO + Ln coated 96-well plates. They were differentiated to neurons as mentioned in section 2.1.2. Neuronal cultures were treated for 24 hours with different concentrations (0.15 μ M, 0.5 μ M, and 1.5 μ M) of monoSia, triSia, hexaSia, and polySias (avDP20, avDP60, and avDP180). Afterwards, an MTT assay was performed as mentioned in section 2.5.4. MTT results showed that the metabolic activity of neurons did not change after treatment with different forms of Sias compared to the untreated control (Figure 3-17 A).

Next, metabolic activities of neuronal cultures were checked with a wider concentration range of polySia avDP20 (from 5 nM to 5 mM). Once more, pNSC were seeded on PLO + Ln coated 96-well plates as mentioned in section 2.1.2. After differentiation, neurons were treated for 24 hours with different concentrations of polySia avDP20. Then, an MTT assay was done as mentioned in section 2.5.4. MTT outcome showed that PolySia avDP20 did not reduce the metabolic activity of human neurons up to a concentration of 5 mM. However, increased metabolic activity was observed at concentrations of 1.5 mM and 5 mM compared to the untreated group and all lower concentrations ($p < 0.001$; Fig 3-17 B). In detail, 1.5 mM and 5 mM polySia avDP20 increased the metabolic activity of neurons from 1 ± 0.03 to 2.5 ± 0.05 fold and 2.8 ± 0.05 fold, respectively (Fig 3-17 B).

Results

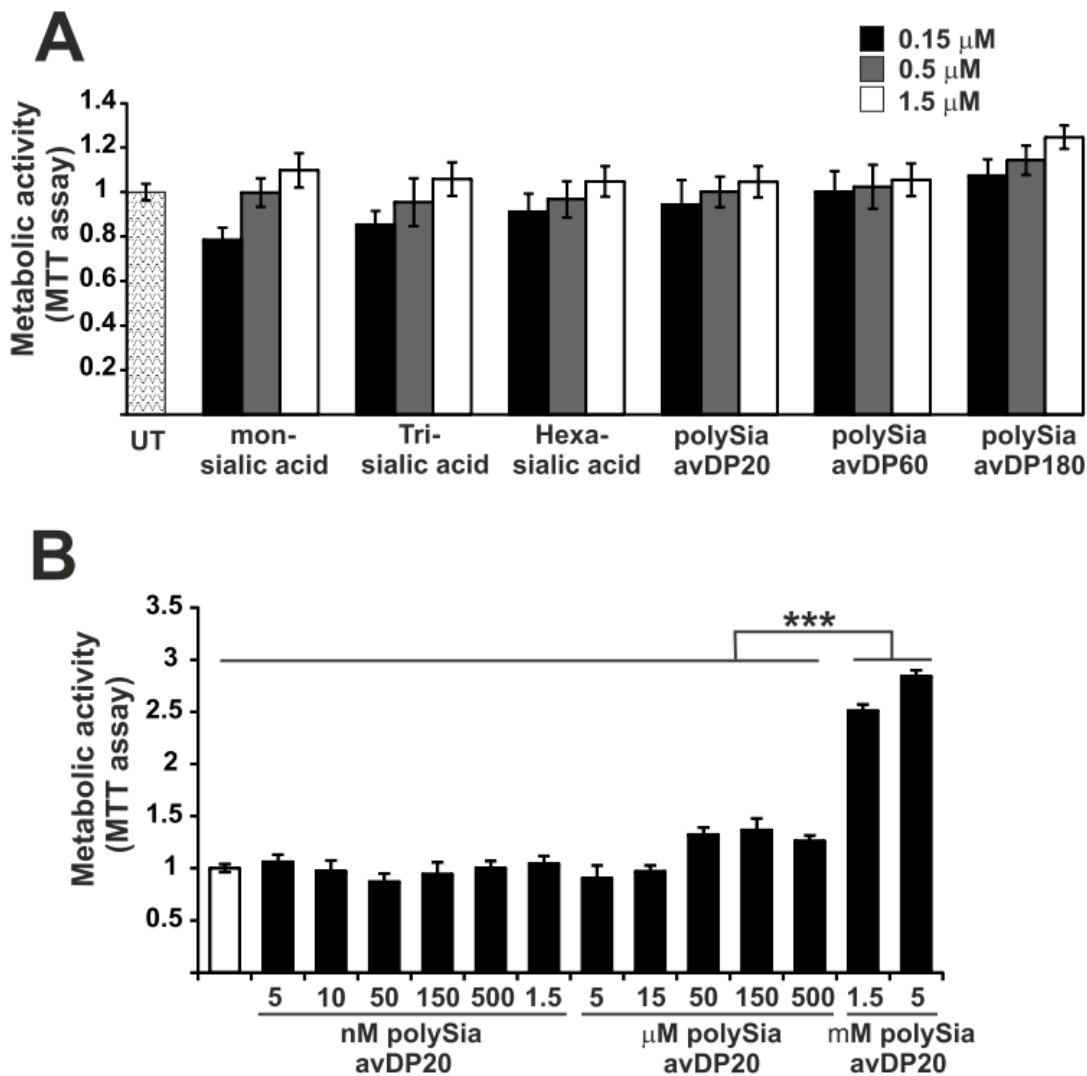


Figure 3-17: Metabolic activity of neurons treated by Sias. Metabolic activity measurements of neuronal cultures treated with different concentrations of monoSia, triSia, hexaSia, and polySias (avDP20, avDP60, and avDP180) after 24 hours showed no effect on cell viability of neurons (A). PolySia avDP20 treatment with different concentrations had no negative effect on neuronal cell viability. Even at 1.5 mM and 5 mM concentrations the cell viability was increased (B). Data are presented as mean \pm SEM of at least three independent experiments and were analyzed using one-way ANOVA (Bonferroni). ***, $p < 0.001$

Results

3.3.4 PolySia avDP20 Is Neuroprotective in iPScM/Macrophage-Neuron Co-culture Systems against A β ₁₋₄₂ Mediated Toxicity

It is known that fibrillar A β ₁₋₄₂ increases microglial phagocytosis function [82]. In addition, it induces uptake of living neurons by microglial cells through exposure of “eat me” signals on the neuronal cell surface [83]. To investigate whether polySia avDP20 co-treatment is able to prevent the toxic effect of fibrillar A β ₁₋₄₂ co-incubation in co-culture systems, two separate iPScM-neuron and macrophage-neuron co-culture systems were established.

For iPScM-neuron co-culture system, pNSCs were seeded in 4-chamber slides and differentiated to mature neurons as mentioned in section 2.1.2. iPScM-neuron co-culture treatments were done as mentioned in section 2.1.6. Co-cultures were double immunostained with antibodies against β -tubulin III (neurons) and Iba1 (iPScM; Fig 3-18 A). Using neurite length as a neurotoxicity marker revealed that solely adding fibrillar A β ₁₋₄₂ to the culture system has no effect on relative neurite length (Fig 3-18 B). Alternatively, addition of the iPScM in the presence of fibrillar A β ₁₋₄₂ significantly reduced relative neurite branch length (Fig 3-18 B). In detail, A β incubation with neurons slightly reduced branch length from 1 +/- 0.02 to 0.9 +/- 0.03 fold ($p=0.104$). However, incubation of A β with iPScM-neuron co-culture further reduced the relative branch length to 0.64 +/- 0.03 fold ($p<0.001$ vs neurons and neurons plus A β ; Fig 3-18 B). This reduction supports the idea of toxic fibrillar A β effect mediated by microglial cells. Incubation with 1.5 μ M PolySia avDP20 protected branches from the toxic effect of fibrillar A β ₁₋₄₂ activated iPScM cells (0.82 +/- 0.03 fold; $p=0.002$; Fig 3-18 A and C). Furthermore, incubation with Trolox protected branches from the toxic effect of fibrillar A β ₁₋₄₂ activated iPScM in co-culture system, too (1.02 +/- 0.03 fold; $p<0.001$; Fig 3-18 C).

Results

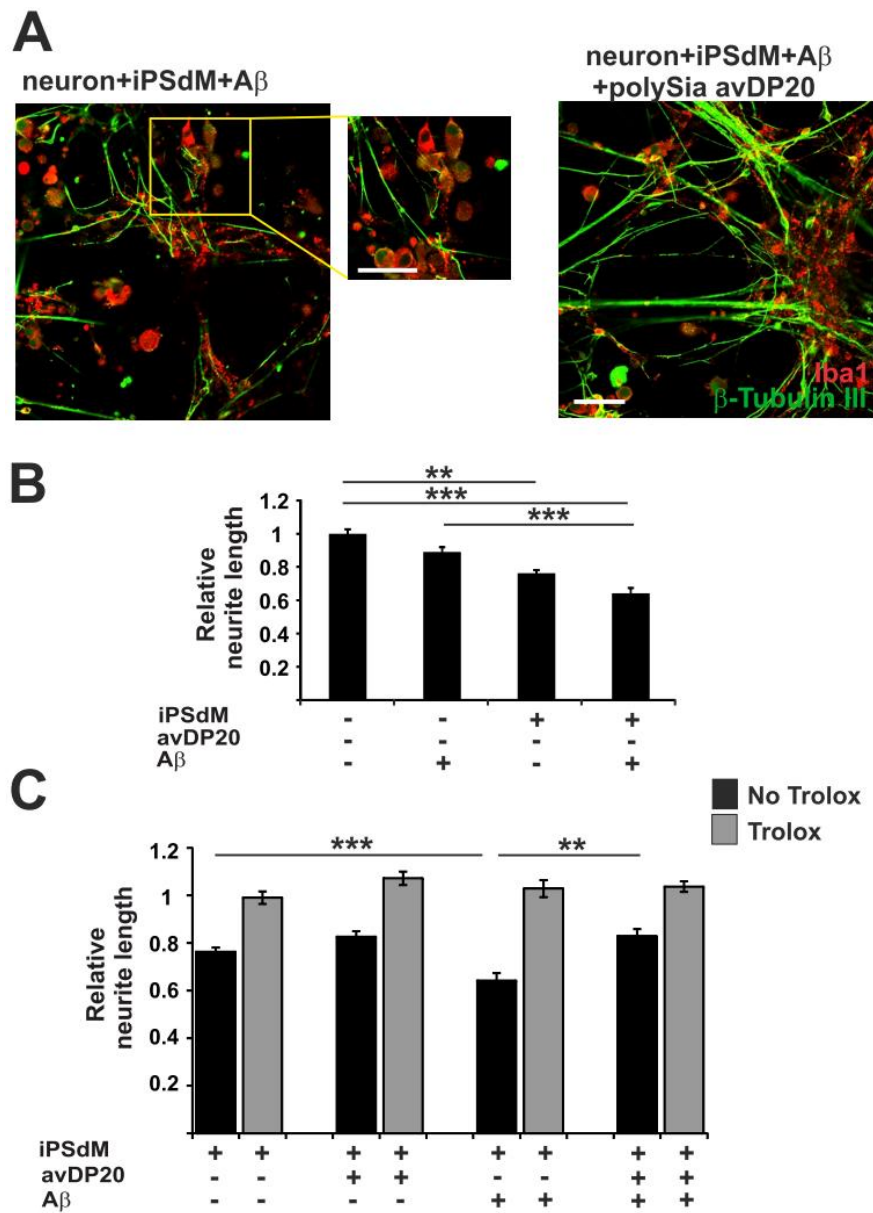


Figure 3-18: Neuroprotective effect of polySia avDP20 in A β -activated iPSdM-neuron co-cultures. Representative immunocytochemistry images of neuron-iPSdM co-culture in the presence of A β with (right picture) or without (left picture) polySia avDP20 (**A**). Relative neurite length was shorter in the presence of A β in neuron-iPSdM co-culture (**B**). Relative neurite length was protected against A β if polySia avDP20 was present in the culture system. Trolox prevented neurotoxic effect in all different co-culture conditions (**C**). Data are presented as mean \pm SEM of at least three independent experiments and were analyzed using one-way ANOVA. **, $p < 0.01$; and ***, $p < 0.001$. Scale bar: 50 μ m.

Results

In neuron-macrophage co-culture system, pNSCs were differentiated to mature neurons as mentioned in section 2.1.2. Macrophage-neuron experiments were done as mentioned in section 2.1.6. Analysis of the neurite length showed the same effect as in the iPSdM-neuron co-culture. Co-cultures were double immunostained with antibodies against Neurofilament (neurons) and CD11b (macrophages ;Fig 3-19 A). Addition of fibrillar A β_{1-42} to the macrophage-neuron co-culture system had no effect on relative neurite length (Fig 3-19 B). Although, inclusion of macrophages in the presence of fibrillar A β_{1-42} significantly reduced the relative neurite branch length (Fig 3-19 B). In detail, A β incubation with neurons reduced the branch length from 1 +/- 0.02 to 0.82 +/- 0.14 fold (p=0.233). Incubation of A β with macrophage-neuron co-culture further decreased relative length of branches to 0.57 +/- 0.05 fold (p=0.012; Fig 3-19 B). As expected, polySia avDP20 and Trolox incubation protected neuronal branches from the toxic effects of fibrillar A β_{1-42} activated macrophages in co-culture systems (0.9 +/- 0.05 fold, p=0.020; 0.9 +/- 0.09 fold, p=0.025, respectively; Fig 3-19 A and C).

Results

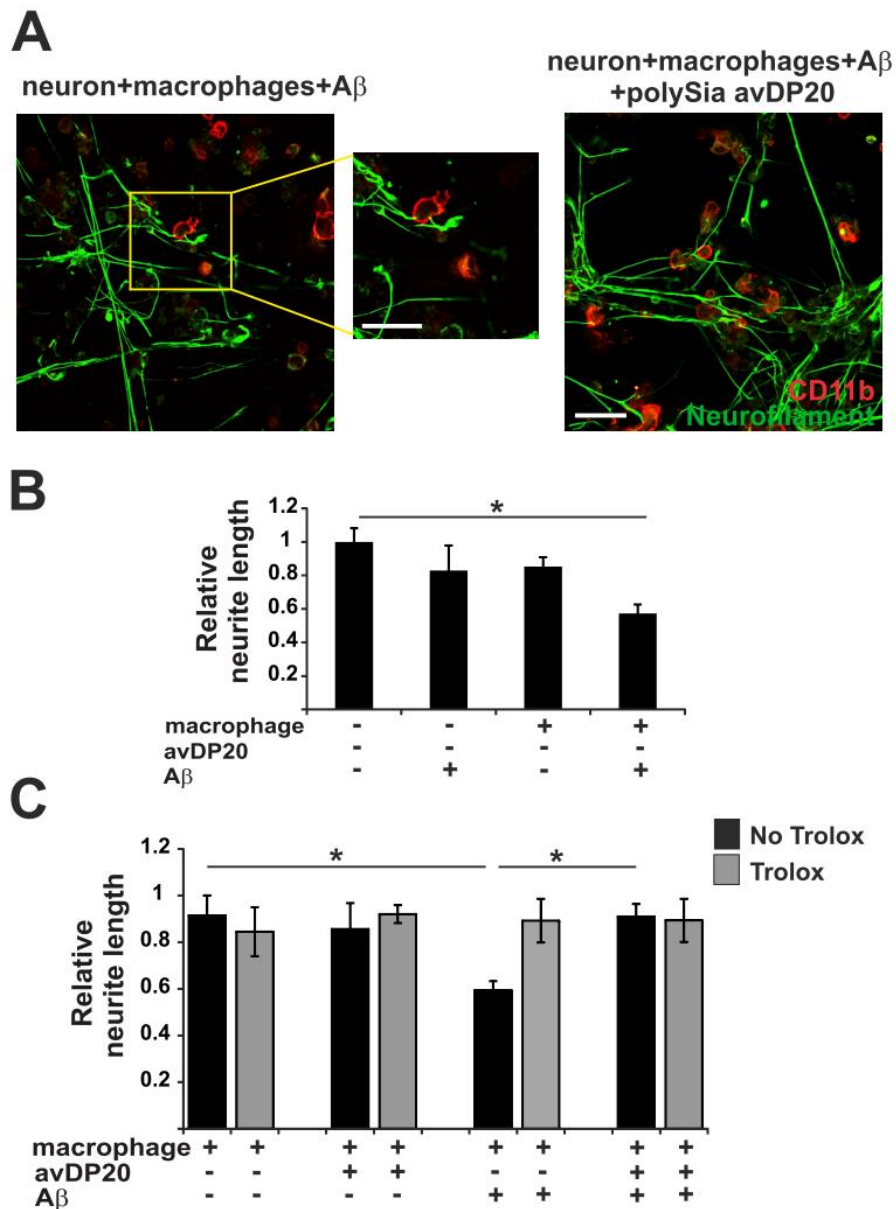


Figure 3-19: Neuroprotective effect of polySia avDP20 in A β -activated macrophage-neuron co-culture. Representative immunocytochemistry images of neuron-macrophages co-culture in the presence of A β with (right picture) or without (left picture) polySia avDP20 (A). Relative neurite length was shorter in the presence of A β in neuron-macrophage co-culture system (B). Addition of polySia avDP20 protected relative neurite length against reducing effects of A β in culture system. Furthermore, Trolox prevented the neurotoxic effect in all different co-culture conditions (C). Data are presented as mean \pm SEM of at least three independent experiments and were analyzed using one-way ANOVA. *, $p < 0.05$. Scale bar: 50 μ m.

Results

3.3.5 PolySia avDP20 Is Neuroprotective in iPScM/Macrophage-Neuron Co-culture Systems against LPS Mediated Toxicity

LPS activates the phagocytosis function of microglia/macrophages indirectly and increases release of ROS, which is directly toxic to neurons [84]. Activation of SIGLEC-11 in transduced murine microglial cells, decreased the gene transcription of LPS-stimulated pro-inflammatory mediators [69]. To investigate whether polySia avDP20 co-treatment has any effect on LPS-activated iPScM/macrophages in co-culture systems, iPScM-neuron and macrophage-neuron co-culture systems were established.

Neuron-iPScM co-culture systems were prepared as mentioned in section 2.1.2 and experiments were done as mentioned in section 2.1.6. Co-cultures were double immunostained with antibodies against β -tubulin III (neurons) and Iba1 (iPScM; Fig 3-20 A). Analysis of neurite lengths revealed that addition of both normal iPScM and LPS-activated iPScM to the neural culture system decreased relative neurite length. However, LPS-activated iPScM cells significantly reduced relative neurite branches length compared to normal iPScM cells ($p=0.04$; Fig 3-20 B). In detail, normal iPScM incubation with neurons reduced branch length from 1 ± 0.03 to 0.76 ± 0.01 fold ($p=0.003$; Fig 3-20 B), and LPS-activated iPScM incubation further reduced relative branch length to 0.64 ± 0.02 fold ($p<0.001$; Fig 3-20 B). To explore the effect of polySia avDP20 in this system, $1.5 \mu\text{M}$ polySia avDP20 was incubated with LPS-activated iPScM cells. Data show that addition of polySia avDP20 protected neurite branches from the toxic effect of LPS-activated iPScM cells in co-culture systems (0.91 ± 0.02 fold; $p=0.001$; Fig 3-20 A and B).

Results

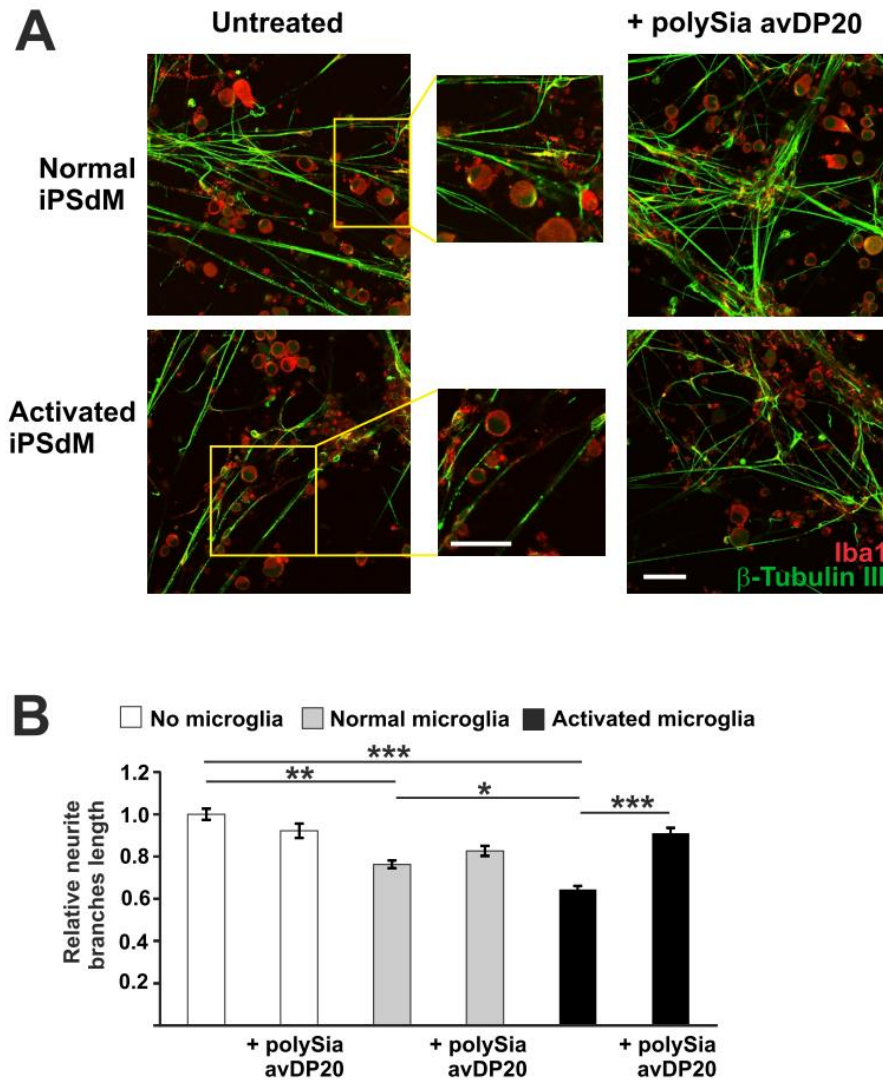
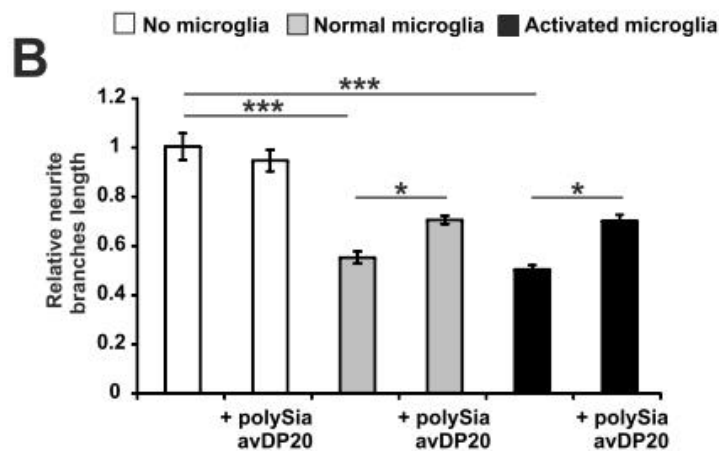
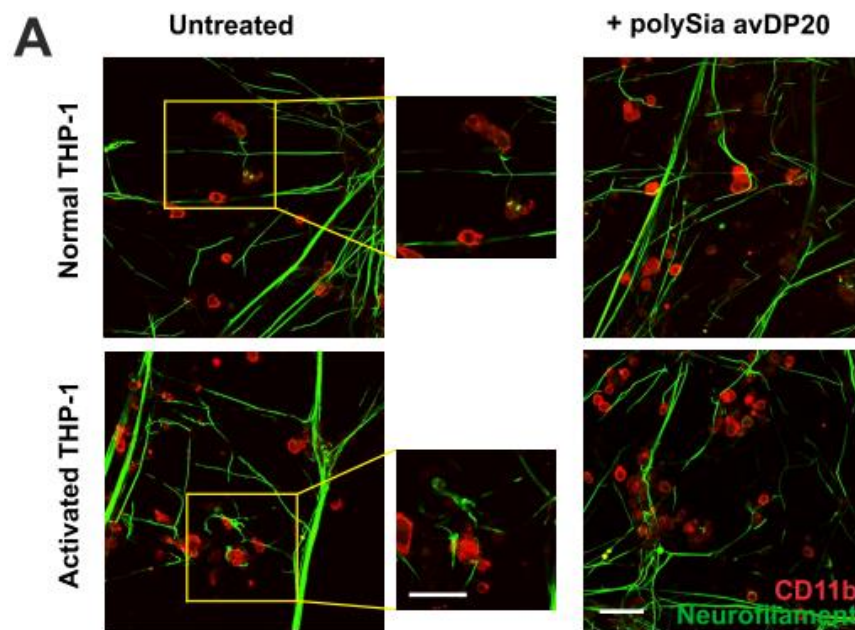


Figure 3-20: Neuroprotective effect of polySia avDP20 in LPS-activated iPSdM-neuron co-cultures. Representative immunocytochemistry images of neuron-iPSdM co-culture in presence of normal iPSdM (upper picture) or LPS-activated iPSdMs (lower picture) with (right pictures) or without (left pictures) polySia avDP20 (**A**). Relative neurite lengths were shorter in presence of both normal iPSdM and LPS-activated iPSdM cells. However, this reduction was more severe in the presence of LPS-activated iPSdM cells. PolySia avDP20 incubation protected neurons from LPS-activated iPSdM cells (**B**). Data are presented as mean \pm SEM of at least three independent experiments and were analyzed using one-way ANOVA. *, $p < 0.05$; **, $p < 0.01$; and ***, $p < 0.001$. Scale bar: 50 μ m.

As mentioned before, neuron-macrophage co-culture systems were prepared. Co-cultures were double immunostained with antibodies against Neurofilament (neurons)

Results

and CD11b (macrophages; Fig 3-21 A). Analysis of neurite length demonstrated that inclusion of both normal macrophages and LPS-activated macrophages to the neural culture system reduced relative neurite lengths. In detail, THP-1 macrophage incubation with neurons reduced branch length from 1 +/- 0.05 to 0.55 +/- 0.02 fold ($p < 0.001$; Fig 3-21 B), and LPS-activated THP-1 macrophages incubation further reduced relative branch length to 0.05 +/- 0.01 fold ($p < 0.001$; Fig 3-21 B). PolySia avDP20 incubation in this system, protected neurite branches from the toxic effects of LPS-activated macrophages in co-culture systems (0.69 +/- 0.02 fold; $p = 0.03$; Fig 3-21 A and B).



Results

Figure 3-21: Neuroprotective effect of polySia avDP20 in LPS-activated macrophage-neuron co-culture. Representative immunocytochemistry images of neuron-macrophage co-culture in presence of normal macrophages (upper pictures) or LPS-activated macrophages (lower pictures) with (right pictures) or without (left pictures) polySia avDP20 (**A**). Relative neurite length was shorter in the presence of both normal macrophages and LPS-activated macrophages. PolySia avDP20 incubation partly protected neurons from LPS-activated macrophages (**B**). Data are presented as mean \pm SEM of at least three independent experiments and were analyzed using one-way ANOVA. *, $p < 0.05$ and ***, $p < 0.001$. Scale bar: 50 μ m.

4 Discussion

A contribution of activated microglial cells and an altered neuronal glycoCalyx on progression of AD has been reported by many studies [68], [69]. Sia molecules are abundant on the outermost surface of intact glycoCalyx. These molecules are recognized by SIGLEC receptors [80]. SIGLEC-11 is specifically expressed in resident tissue macrophages including brain microglial cells [85]. To determine the optimal length of Sia as a SIGLEC-11 ligand, this study used different lengths of oligoSia and polySia in *in vitro* systems and found polySia avDP20 to be a potential ligand for SIGLEC-11. Accumulation of extracellular A β plaques and appearance of inflammatory activated microglial cells are hallmarks of AD [86]. One of the mechanisms by which A β can activate microglial cells is through several scavenger receptors that could also signal through the ITAM-carrying adaptor molecule TYROBP/DAP12. This leads to activation of downstream signaling pathways and results in the increased phagocytosis function of microglia and/or release of ROS that is directly toxic to neurons [66], [74]. Within this study, the role and involvement of microglial SIGLEC-11, an ITIM-carrying receptor, in counter-regulation of A β activatory effects was investigated. This study reveals new evidence concerning the role of polySia molecules in modulating microglial functions in brain and toward neurons. In addition, the results shed light on the potential capacity of polySia avDP20 to be further investigated as a drug for neurodegenerative diseases.

4.1 PolySia avDP20 Is the Potential Ligand for SIGLEC-11

SIGLEC-11 was first identified as a human microglial specific receptor in 2005 and from that time investigations tried to detect the possible ligand for it in the brain [56]. In the first part of this thesis, SIGLEC-11 expression on cell lines was explored and the effect of different lengths of Sias was investigated. Results showed that monoSia and oligoSias did not prevent ROS production from A β activated cells. However, polySia

Discussions

avDP20 and avDP60 were able to prevent ROS production. Measuring metabolic activity of cells showed that polySia avDP60 had negative effect on cell viability. No change in cell survival was observed in polySia avDP20 treated cells. In addition, ELISA data showed that there was a direct binding between polySia avDP20 and rhSIGLEC-11/Fc protein.

4.1.1 SIGLEC-11 Expression

As mentioned before, SIGLEC-11 is a member of CD33-related SIGLECs. SIGLECs in innate immune cells can recognize both self-endogenous and invading pathogen sialylations. According to recent data, there are variations in expression of SIGLECs on circulatory blood immune cells (monocytes, leukocytes, and lymphocytes) compared to tissue macrophages and neutrophils [87], [88]. SIGLEC-3, -5 and -9 are highly expressing on monocytes. SIGLEC-3 is also highly expressed in tissue macrophages, while SIGLEC-5 is not expressed and SIGLEC-9 is only expressed on a subset population [87]. In this study, data show that SIGLEC-11 is expressed on iPSdM cells, THP-1 monocytes, and macrophages both on mRNA and protein levels. This expression makes these cells proper models to find out the potential ligand for SIGLEC-11 receptor. In addition, as it was expected, expression level of SIGLEC-11 is higher in THP-1 macrophages compared to monocytes.

4.1.2 OligoSia and PolySia as a Ligand

The glycocalyx is a dense complex array of sugar units which are attached to the lipids and proteins on the cell surface [89]. The outermost ends of these sugar units are decorated with Sias, which can have diverse conformations due to their length [90]. Commonly, Sia units are able to form oligo/poly structures and accordingly are classified as diSia (DP=2), oligoSia (DP=3-7) and polySia (DP>8) [46]. Comparably, to determine structure's effect on function, distinct lengths of Sia were used in this study: monoSia, oligoSia (with DP3 and DP6), and polySia (with DP20, DP60, and DP180).

Discussions

In mammals, a wide number of gangliosides and glycoproteins are modified by oligoSias (mainly with DP=3-7). This change enables them to be recognized by SIGLEC-7 or SIGLEC-11 which prefer α 2→8 linked Sias [46], [91]. Both SIGLEC-7 and SIGLEC-11 are ITIM bearing/inhibitory receptors and are involved in regulation of innate immune responses. SIGLEC-7 is expressed on natural killer (NK) cells, monocytes, basophils, and mast cells and shows a preference for α 2→8 linked diSias on gangliosides [92], [93]. SIGLEC-11 is expressed in a broad range of tissue macrophages such as Kupffer cells in liver, microglial cells in brain, perfollicular cells in spleen, and lamina propria macrophages in intestine and shows binding specificity to α 2→8 linked Sias [94]. However, unlike SIGLEC-7, SIGLEC-11 does not show clear binding to gangliosides carrying α 2→8 linked Sias. According to the literature, it was clear that SIGLEC-11 prefers α 2→8 linked structures to bind, but the length of Sia which has a great effect on conformation of the molecule was not clear. In this thesis, diverse lengths of small Sia molecules were used (monoSia, oligoSia DP3, oligoSia DP6) and their influence on iPSdM cell response was explored. As expected, cell treatment by monoSia and oligoSias were not adequate to prevent the stimulatory effect of A β on ROS production.

PolySia is a homopolymer of α 2→8 linked Sias which is added to the membrane proteins as a posttranslational modification [91]. In contrast to oligoSias, polySias are added only to some specific proteins which are mainly expressed in the CNS or immune cell network. These proteins consist of neural cell adhesion molecule (NCAM/CD56), synaptic cell adhesion molecule (SynCAM1), CD36, neuropilin2 (NRP-2), α -subunit of the voltage-gated sodium channel and autopolysialylation of sialyltransferases that polymerize polySia (ST8 SialII, ST8 SialIV) [95]–[97]. PolySias play an important role in cell adhesion, migration, and cytokine response of immune cells. Studies showed that polySias are expressed on mice bone marrow (BM) neutrophils and monocytes, but these cells gradually lose the polySia expression while they migrate toward inflammation sites [98]. In human system, monocyte-derived DC and NK cells also regulate polySia expression according to the activation state. In this context, cells

Discussions

express less polySia as they mature [97], [99]. In total, it seems that upon arrival of blood immune cells to the target tissue, the self polySia expression reduces but the expression of self SIGLECs increases. PolySia are recognized by SIGLEC receptors and, as mentioned before, SIGLEC-11 is specifically expressed on microglial cells. This expression makes SIGLEC-11 a potential receptor for polySia, which is highly expressed on neuronal cells. In this thesis, to explore this possibility, iPSdM cells were treated with different lengths of polySia (polySia avDP20, avDP60, and avDP180). Results indeed confirmed that polySia avDP20 and avDP60 treatment prevented ROS release from A β -stimulated iPSdM cells. However, polySia avDP60 showed a negative effect on metabolic activity of iPSdM cells.

4.1.3 PolySia avDP20 Binds to SIGLEC-11

SIGLEC-11-modulated microglial cell behavior in an *in vitro* co-culture system was dependent on neuronal polySia residues, but independent of microglial polySia itself [69]. This thesis shows that polySia avDP20 can modify the response of iPSdM cells and THP-1 macrophages towards A β . ELISA data showed that there is a direct binding between polySia avDP20 and rhSIGLEC-11-Fc protein, but dextran (a branched glucan with different lengths but same molecular weight) did not attach. In addition, SIGLEC-11 knockdown was enough to abolish the averting effect of polySia avDP20 treatment both in iPSdM cells and THP-1 macrophages.

4.2 PolySia avDP20 Changes iPSdM Cell and THP-1 Macrophage Function

Microglia, the brain inspectors, like other immune cells have a specific role to survey brain environment. A β deposition is one of the main signs in AD progression and its total amount is equal to its production minus its removal. This indicates the crucial role of clearance mechanisms and reveals the importance of microglial cells [100]. Accumulation of A β damaged neurons and induced apoptosis cause debris production, which should be cleared by microglial cells. In this situation, microglial cells remove A β

Discussions

and debris by inflammation associated phagocytosis, which is linked with the release of ROS in pathological conditions like AD [74]. In the second part of this thesis, the role of SIGLEC-11 activation by polySia avDP20 in face of A β and apoptotic material was investigated. Results demonstrated that polySia avDP20 incubation reduced uptake of both A β and debris by iPScDM cells and THP-1 macrophages. Moreover, polySia avDP20 prevented the ROS production towards stimulants. This prevention was similar to Trolox and SOD1 effects in blocking ROS production upon phagocytes stimulations.

4.2.1 PolySia avDP20 Reduces Phagocytosis Function

Phagocytosis is one of the normal functions of microglial cells as phagocytes. Phagocytosis occurs either by homeostatic phagocytosis or by inflammation-associated phagocytosis. Fibrillar A β_{1-42} and debris are recognized by danger-associated molecular pattern (DAMPs), which increase microglial inflammation-triggered phagocytosis activity and leads to release of TNF- α , IL- β or ROS and directly harm neurons [82], [101], [102]. Simultaneously, as fast as plaques or apoptotic materials are recognized, several anti-inflammatory responses are activated to maintain homeostasis. Therefore, negative signals are important to balance phagocytic activity [103].

Microglial function is controlled via diverse sets of receptors on the cell surface, and A β can be recognized by some of these surface receptors. Part of these receptors are activatory receptors such as TREM2 or SIRP β 1, which signal via TYROBP/DAP12 (bearing ITAM motif in intracellular part) [104]. Upon activation, these receptors phosphorylate downstream proteins and activate signaling pathways [66], [67], [77]. SIRP β 1 knockdown reduced uptake of A β and apoptotic neural material in mice primary microglial cells [66]. Siglec-h is another example which is expressed on mouse microglial cells and signals via TYROBP/DAP12. Induction of this receptor by Siglec-h specific antibody-coated beads increased phagocytosis function in the microglia line, while knockdown of this receptor neutralized bead uptake [105].

Discussions

On the other side, the function of ITAM carrying receptors is counter-regulated by inhibitory receptors such as SIGLEC receptors. Most SIGLECs carry an ITIM motif in their intracellular part and, by ligand attachment, antagonize the kinase activation signal and hamper signaling pathways [58]. ITIM carrying receptors are negative regulators of immune response and have an important role to prevent the harmful consequences of inflammation [106]. Aggregated A β covered by sialylated glycolipids and glycoproteins are identified by microglial SIGLECs and are not removed by these cells [60]. SIGLEC-3 (an ITIM carrying receptor) positive microglial cells increase in AD patients and there is an association between A β aggregation and the number of SIGLEC-3 positive cells [107]. Moreover, in mice microglial culture systems, elevated SIGLEC-3 levels inhibited A β uptake; while reduced SIGLEC-3 was enough to increase A β phagocytosis and Sia was necessary to modulate this function [107]. Thus, it seems that ITAM and ITIM receptors are counter-regulating A β clearance mechanisms. In this thesis, polySia avDP20 incubation reduced A β uptake in SIGLEC-11 expressing iPScDM cells and THP-1 macrophages, which is in line with current literatures.

In most neurodegenerative diseases the presence of debris in the brain parenchyma is increased [108]. Removal of debris is essential for effective regeneration, while their uptake may lead to inflammation. This could result in neuronal antigen presentation, which activates autoimmune responses [108], [109]. Several studies show that activation of ITIM-carrying receptors lead to reduced debris phagocytosis. In mice system, siglec-e (an ITIM carrying receptor) overexpression reduced uptake of neural debris into microglial cells, while siglec-e knockdown increased debris uptake [68]. In another study, murine microglial cells transduced with SIGLEC-11 exhibited less uptake of apoptotic neural material, while microglial cells that received a control vector had more capacity for apoptotic material uptake [69]. Accordingly, in this thesis polySia avDP20 incubation reduced debris uptake in SIGLEC-11 expressing iPScDM cells and THP-1 macrophages.

Discussions

In total, SIGLEC receptors do not change the homeostatic phagocytosis but they efficiently reduce inflammatory-mediated phagocytosis of fibrillar A β ₁₋₄₂ or debris.

4.2.2 PolySia avDP20 Reduces ROS Production

The direct consequence of microglial activation by debris and A β is the respiratory burst and release of ROS, which contributed to neuronal damage [110]. The source of ROS is mainly microglial NADPH oxidase activity. NADPH oxidase consists of two membrane components (p22^{phox} and gp91^{phox}) and four cytosolic components (p47^{phox}, p67^{phox}, p40^{phox}, and small G-protein Rac). Upon stimulus activation of a microglia/macrophage cell, the cytosolic subunits assemble with membrane components and initiate superoxide (O₂⁻) production [78]. In detail, A β is recognized by surface receptors, which are able to recruit Src-family of Tyr kinase. Then, phosphorylation and activation of Vav guanine nucleotide exchange factor (GEF) activity results in GDP to GTP exchange on Rac GTPase. This exchange leads to assembly of subunits of NADPH oxidase and release of ROS [111][78]. Engagement of tyrosine kinase Syk and membrane NADPH oxidase in response to microglial stimulation is necessary since pretreatment with piceatannol (inhibitor of Syk) significantly reduce A β stimulated tyrosine phosphorylation [73], [112]. In addition, using gp91ds-tat (NADPH oxidase inhibitory peptide) and gp91^{phox} ^{-/-} mice showed that A β stimulated ROS release was revoked [73], [112]. Primary culture of rat microglia and THP-1 monocyte incubation with A β initiated superoxide production, which was inhibited by SOD treatment [73]. In addition, BV2 microglial cell exposure to fibrillary A β ₁₋₄₂ significantly increased ROS production via NADPH oxidase activity [74]. Equally, in this thesis treatment with fibrillary A β increased ROS production in iPSdM cells and THP-1 macrophages, while polySia avDP20 incubation prevented ROS release upon A β inclusion.

If apoptotic material is not removed properly by phagocytosis, then the membrane integrity in apoptotic compartment vanishes over time and they will become necrotic substances [113]. In neonatal cerebellum sections, superoxide produced by microglial cells was the main source of Purkinje cell death [114]. In another model of neonatal

Discussions

stroke, removal of apoptotic neurons by activated microglial cells were limited. However, even this slight removal was protective since depletion of microglial cells before stroke increased accumulation of inflammatory mediators like superoxide [115]. In an *in vitro* study, Siglec-e overexpression in microglial cells reduced ROS production upon debris stimulation, while knockdown of Siglec-e led to increased ROS release [68]. In the same manner, in this thesis debris treatment leads to increase ROS production in iPScM cells and THP-1 macrophages, albeit polySia avDP20 incubation prevented this rise.

4.2.3 PolySia avDP20 Inhibits ROS Production as Effectively as Antioxidants

As mentioned, oxidative stress is one of the main sources of neuronal damage. ROS such as superoxide (O_2^-) and hydrogen peroxide (H_2O_2) are mainly produced by dysfunction of mitochondrial respiratory chain; however, membrane NADPH oxidase also produce ROS [116]. O_2^- can quickly react with nitric oxide (NO) and produce peroxynitrite; as well H_2O_2 can produce hydroxyl radicals ($\bullet HO$). Both peroxynitrite and hydroxyl radicals are highly toxic and damage biological molecules' functions [117]. The brain is responsible for about 20% of basal body O_2 consumption and any interference in the oxygen respiratory chain cause huge damage to neurons (reviewed in Halliwell 2006). Therefore, substances that are able to reduce these highly reactive oxygen radicals can be considered as a potential therapeutic agent in neurodegenerative processes. Trolox is a water-soluble analog of vitamin E, which inhibits lipid peroxidation by scavenging peroxy radicals and is used commonly as an antioxidant in biological experiments to scavenge ROS [118]. SOD1 is one of the three human superoxide dismutases enzymes. SOD1 catalyzes O_2^- to H_2O_2 , which is then later broken down by catalase [119]. Siglec-e is a negative regulator of ROS released by mouse microglial cells [68]. Trolox kept neurite length in the normal range when neurons were co-cultured with Siglec-e knockdown microglial cells [68]. In this thesis, both Trolox and SOD1 treatments prevented the phagocytosis associated ROS release from iPScM cells and THP-1 macrophages. In the same way, treatment with polySia avDP20 prevented release of ROS upon A β and debris challenge via SIGLEC-11 ITIM

Discussions

signaling, since knockdown of this receptor was enough to abolish polySia avDP20 effect. Thus, in total polySia avDP20 like Trolox and SOD1 is able to keep ROS release at the basic level in *in vitro* cultures.

4.3 PolySia avDP20 Has Neuroprotective Function

Neurons, as the central components of the CNS, are in close relation with microglial cells. Presence of A β or LPS in brain parenchyma induces immune responses by microglial cells. Microglia, by recognition of these stimuli, become active and produce neurotoxic pro-inflammatory factors. They may become overactive by damaged neurons, harming adjacent neurons [110]. In the third part of this thesis, neurons differentiated from iPS cells to establish a co-culture system and the effects of diverse polySia avDP20 concentrations were explored. Afterwards, the role of polySia avDP20 treatment in face of A β and LPS stimulation in neuron-iPSdM or neuron-macrophage co-culture systems were investigated. Results show that polySia avDP20 incubation reduced neurotoxicity effects of both A β and LPS mediated by iPSdM cells or THP-1 macrophages. Moreover, this protective effect towards stimulants was similar to Trolox incubation, however, it was not as strong.

4.3.1 Human Neuron Culture from iPS Cells

To establish a human co-culture system, a stable NSC line was necessary to constantly have neurons in culture. pNSCs were obtained from iPS cells according to a short protocol which initially used small inhibitory molecules to get pNSCs from human ES cells [70]. As mentioned before, four small inhibitory molecules (hLIF, CHIR99021, SB431542 and Compound E) were used to differentiate pNSCs from iPS cells. HLIF already has been shown to be essential for maintaining pluripotency [120]. CHIR99021 inhibits GSK-3 β , which is a main component in the canonical Wnt pathway with a negative role in neuronal induction. Thus, inhibition of GSK-3 β activates the canonical Wnt pathway and increases neural induction [121]. SB431542 inhibits mesodermal

Discussions

induction and helps the cell culture to go towards ectodermal fate [122]. Compound E aids to stop cell differentiation [70]. All these factors help to differentiate pNSCs from iPS cells. pNSCs express NSC markers nestin, Pax6, Sox1 and Sox2. Nestin is a type VI intermediate filament protein which is expressed by uncommitted neural progenitor cells and is extensively expressed by our pNSCs [123]. Pax6 has been shown to increase neurogenesis from human fetal striatal NSCs. In addition, Pax6 and Sox2 are required for maintaining progenitor proliferative capacity of NSCs [124], [125]. pNSCs were also positive for Ki67, so they kept their proliferative phenotype.

pNSCs easily differentiate into neurons in the presence of BDNF and GDNF in 2 weeks. The resulting neurons were highly positive for neuronal markers NeuN, β -tubulin-III, neurofilament and MAP2. They have been positive for the neurotransmitters ChAT and GABA, but only few cells have been positive for the dopaminergic marker TH [126].

4.3.2 PolySia avDP20 Is Neurotrophic

Between different candidate molecules who have roles in neuronal plasticity, neural cell adhesion molecule (NCAM) and its attached polySia chains have received most attention. NCAM according to its molecular weight is present in four main isoforms (NCAM-180, NCAM-140, NCAM-120 and soluble NCAM) with one of the main post-translational modifications, which is the addition of a linear homopolymer of α 2 \rightarrow 8 linked Sias [127]. The expression of polySia-NCAM is highly regulated. Peak expression occurs during the early stages of brain development, followed by a continuous reduction, which leads to its regional expression in three types of neurons in adult brains. The first population is located in layer II of the paleocortex, which mostly lacks NeuN expression (immature neurons) [48]. To the second population belong mature NeuN positive inhibitory interneurons located in cortical areas such as prefrontal cortex, hippocampus, and amygdala [48]. The third population includes differentiated neurons with polySia negative soma but polySia positive neuritis, like hippocampus mossy fibers or pyramidal cells of CA1 region [48]. The most defining character of polySia is related to its polyanionic nature, which gives this molecule the anti-adhesive feature. This

Discussions

feature enables it to have an important role in cell-cell and cell-matrix interactions [46]. Polysialyltransferases (PSTs) are key regulators of polySia synthesis in mammalian cells [128]. Due to this fact, many experiments have been done in recent years to examine polySia's function on neuronal cell behavior by changing the expression of PSTs. Motor neurons derived from mouse ES cells when transduced to express more PST (results in more polySia expression) showed increased survival and neurite outgrowth towards denervated muscles [129]. ES cell-derived dopaminergic neurons transduced with a lentiviral-expressing PST and grafted into a hemiparkinsonian mouse model showed increased survival without phenotypic change and neurite outgrowth [130]. Furthermore, increased PST expression resulted in complete recovery in mice with correction of behavioral impairment [130]. In this thesis, treatment of iPS-derived neuronal cells with different lengths and concentrations of Sia, oligoSia and polySia had no negative effect on metabolic activity of neurons. Moreover, treatment with polySia avDP20 improved neuronal metabolic activity in a concentration dependent manner.

4.3.3 PolySia avDP20 Effect in A β Stimulated iPSdM/macrophage-neuron Co-culture Systems

Phagocytosis and polySia: In a healthy situation, microglial cells are in resting state. This means that their soma stay stable, but their processes are motile and continuously survey their microenvironment [103]. Any alteration in normal conditions, which is sensed by microglia, impairs microglial homeostasis and damages neurons [103]. Uptake of neurons occurs by two mechanisms: phagocytosis, which is removal of apoptotic or necrotic neurons that express eat me signals, and phagoptosis, which is removal of live neurons that transiently express eat me signals [84]. One of the important eat me signals on the neuronal surface is the appearance of PS, which is normally located in the inner leaflet of the cell membrane. Its exposure on the outside of the neuron can be increased by A β ₁₋₄₂ incubation [131]. PS is recognized by opsonins like milk fat globule EGF factor 8 (MFG-E8) and then bound to the vitronectin receptor on the microglial surface or directly to another microglial receptor called brain-specific

Discussions

angiogenesis inhibitor1 (BAL1) [84]. In a rat neuron-microglia co-culture system, low concentration of A β induced neuronal loss without increasing apoptosis or necrosis, further investigation showed that neuronal loss was mediated by the microglial phagocytosis function, which was boosted by A β [83]. Blocking PS or inhibiting microglial phagocytosis was enough to save neurons [83]. Later on, the same group showed that A β induced peroxynitrite release from microglia forced neurons to show PS eat me signal. Then, this neurons were taken up by phagoptosis through the PS-MFG-E8-vitronectin pathway [39]. Besides, treatment with peroxynitrite scavenger or vitronectin receptor antagonist was enough to inhibit neuronal loss [39]. In line with this literature, in the thesis at hand treatment of neuronal cultures with A β alone showed no difference in neurite length. However, co-incubation of iPSdM-neuron or macrophage-neuron co-culture systems with A β showed reduced neurite branches length. Another eat me signal is the removal of the Sia cap from surface neuronal glycoproteins [126]. The altered glycocalyx followed by C1q opsonization, which recognizes by mouse microglial CR3 or human macrophage CR3; although, in both situations intact neurites with sialylated glycoproteins remain undamaged [126], [132]. Thus, it seems that neurite sialylation is an inhibitory signal for microglial cells and macrophages. Indeed, there are some don't eat me signals on neuronal surface like CD47 and sialylated glycoproteins that are recognized by microglial receptors SIRP1 α and SIGLEC-11 to prevent phagocytosis [84]. In a mouse neuron-microglia co-culture system, intact polySia expressing neuronal cultures were incubated with SIGLEC-11 vector transduced microglial cells [69]. This culture showed higher neurite density compare to incubation with control vector transduced microglia. However, in polySia removed neuronal culture this outcome was not observed [69]. In line with this observations, here the toxic effect of A β incubation in iPSdM-neuron and macrophage-neuron co-cultures was eliminated by co-treatment with polySia avDP20.

ROS and polySia: Another consequence of microglial cell activation by A β is ROS release, which is directly toxic to neurons in co-culture experiments [79]. APP overexpression alone was not toxic for APP-expressing-neuroblastoma cells; despite

Discussions

the fact that co-culture of these neurons with microglial cells leads to enormous cell death via ROS release by microglial cells [133]. A β incubation can induce NADPH-oxidase assembly in rat primary microglial cells and release of ROS in a dose dependent manner [134]. Nevertheless, melatonin as an antioxidant inhibited superoxide release by impairing the assembly of NADPH oxidase in these microglial cells [134]. In this thesis, incubation of co-cultures with Trolox was able to keep neurite length in A β treated iPSdM/macrophage-neuron neuronal cultures as in untreated neuronal cultures. Incubation of the co-cultures with polySia avDP20 led to the same protective effect as seen with Trolox. In total, polySia avDP20 seems to be working through reducing the phagocytosis function of iPSdM and macrophages, besides inhibiting the release of ROS by phagocytes when they encounter A β .

4.3.4 PolySia avDP20 Effect in LPS Stimulated iPSdM/macrophage-neuron Co-culture Systems

LPS is the major immunostimulatory element in cell walls of Gram-negative bacterias, which has been studied for a long time to uncover the underlying mechanisms of microglia activation. Upon microglial stimulation with LPS, which mainly is recognized by Toll-like 4 receptor (TLR-4), these cells become activated and release diverse cytotoxic mediators such as NO, IL1- β , TNF- α , various ROS, and other neurotoxic factors [40], [135]. Rat neuron treatment with LPS alone was not neurotoxic. However, when neurons were cultured under filter inserts containing LPS-activated microglial cells, neuronal cell death observed [40]. Further investigation showed that LPS increased NO and superoxide secretion from microglial cells, which then reacted, formed peroxynitrite and directly damaged neurons. Thus, they concluded that LPS neurotoxicity is indirect and via microglial cell activation, but they did not investigate phagocytosis function of microglial cells [40]. Afterward, additional studies with lipoteichoic acid (LTA) and muramyl dipeptide (MDP), the major immunostimulatory elements in cell walls of Gram-positive bacterias, showed that there is a LTA concentration dependent reduced neuronal cell number in a rat neuron-microglial cell

Discussions

culture [136]. This reduction was mediated by release of NO by microglial cells and the later on production of peroxynitrite, since blocking of either substances significantly inhibited neuronal loss [136]. They have not seen an increase in apoptotic cells. They concluded that neurons either go through necrotic cell death or that they are rapidly removed by activated microglial cells. Later on, it was shown that death of neurons was simply prevented by phagocytosis inhibition even without disrupting inflammation [39]. The authors of this study declared that in a direct contact neuron-microglia co-culture system, LTA and LPS promoted neuronal loss, since microglial separation via transwell co-culture was enough to prevent neuronal loss. They assume that LTA or LPS microglial cell stimulation leads to more peroxynitrite production and more PS eat me signal exposure on neuronal cells, that is recognized by microglial cell receptors and leads to phagoptosis of neurites by microglial cells [39]. In this thesis, LPS activated iPSdM cells significantly reduced neurite length compare to normal iPSdM cells incubation. Furthermore, polySia avDP20 prevented this neurotoxicity. Activated macrophages did not show a higher toxicity compared to normal macrophages perhaps by non-identical responses of different THP-macrophages batches to LPS. However, polySia avDP20 reduced this toxicity. PolySia avDP20 showed this neurotrophic effects directly by starting inhibitory signaling, which reduced either neurons phagoptosis or prevented ROS production. It is also possible to improve polySia avDP20 effectiveness by increasing its concentration, since polySia avDP20 did not change neurons metabolic activity till 5 mM concentration.

Discussions

4.4 Summary

SIGLEC-11 is an inhibitory receptor expressed on microglial cells and macrophages and can recognize α 2→8 linked Sias structures. The surface of neuron is decorated by different lengths of polySias. PolySia-SIGLEC-11 interaction is important to keep normal physiological conditions in neuron-microglia co-culture systems. However, till now it was not clear which length of polySia is recognized by SIGLEC-11.

In this study the low molecular weight polySia with average degree of polymerization 20 (polySia avDP20), among different polySia lengths, introduced as the best length which was recognized by SIGLEC-11. PolySia avDP20 pre-treatment upon A β or debris stimulation kept superoxide release of microglia/macrophages as low as of untreated cells. This effect was not observed when cells were pre-treated with monoSia or oligoSias. Furthermore, compared to other polySia lengths (avDP60 and avDP180), polySia avDP20 had no effect on the metabolic activity of cells. Knockdown of SIGLEC-11 was enough to prevent the inhibitory function of polySia avDP20. Additional experiments showed that the anti-superoxide effect of polySia avDP20 was as potent as Trolox and SOD1. Phagocytosis analysis in iPSdM cells and macrophages revealed that polySia avDP20 pre-treatment did reduce uptake of A β and debris, which are inflammatory phagocytosis stimulants. Neurons were differentiated from pNSCs to investigate the consequence of polySia avDP20 addition to co-cultures with iPSdM/macrophages. Co-culture of A β or LPS stimulated iPSdM/macrophage with neurons led to shorter neurite length. This length could stay like untreated neurons if polySia avDP20 was present.

Thus, this study suggests polySia avDP20 as a ligand for SIGLEC-11 receptor to reduce the inflammatory response of phagocytes towards provoking stimulants.

References

References

- [1] M.-È. Tremblay, B. Stevens, A. Sierra, H. Wake, A. Bessis, and A. Nimmerjahn, "The role of microglia in the healthy brain.," *J. Neurosci.*, vol. 31, no. 45, pp. 16064–9, Nov. 2011.
- [2] M. T. Heneka, M. P. Kummer, and E. Latz, "Innate immune activation in neurodegenerative disease.," *Nat. Rev. Immunol.*, vol. 14, no. 7, pp. 463–77, 2014.
- [3] M. Prinz and J. Priller, "Microglia and brain macrophages in the molecular age: from origin to neuropsychiatric disease.," *Nat. Rev. Neurosci.*, vol. 15, no. 5, pp. 300–12, 2014.
- [4] G. J. Guillemin and B. J. Brew, "Microglia, macrophages, perivascular macrophages, and pericytes: a review of function and identification.," *J. Leukoc. Biol.*, vol. 75, no. 3, pp. 388–397, 2004.
- [5] D. Gate, K. Rezai-Zadeh, D. Jodry, A. Rentsendorj, and T. Town, "Macrophages in Alzheimer's disease: The blood-borne identity," *J. Neural Transm.*, vol. 117, no. 8, pp. 961–970, 2010.
- [6] C. Kaur, a J. Hao, C. H. Wu, and E. a Ling, "Origin of microglia.," *Microsc. Res. Tech.*, vol. 54, no. 1, pp. 2–9, Jul. 2001.
- [7] W. Y. Chan, S. Kohsaka, and P. Rezaie, "The origin and cell lineage of microglia: new concepts.," *Brain Res. Rev.*, vol. 53, no. 2, pp. 344–54, Feb. 2007.
- [8] F. Ginhoux, M. Greter, M. Leboeuf, S. Nandi, P. See, S. Gokhan, M. F. Mehler, S. J. Conway, L. G. Ng, E. R. Stanley, I. M. Samokhvalov, and M. Merad, "Fate mapping analysis reveals that adult microglia derive from primitive macrophages.," *Science*, vol. 330, no. 6005, pp. 841–5, Nov. 2010.
- [9] K. Kierdorf, D. Erny, T. Goldmann, V. Sander, C. Schulz, E. G. Perdiguero, P. Wieghofer, A. Heinrich, P. Riemke, C. Hölscher, D. N. Müller, B. Luckow, T. Brouwer, K. Debus, G. Fritz, G. Opdenakker, A. Diefenbach, K. Biber, M.

References

- Heikenwalder, F. Geissmann, F. Rosenbauer, and M. Prinz, "Microglia emerge from erythromyeloid precursors via Pu.1- and Irf8-dependent pathways.," *Nat. Neurosci.*, vol. 16, no. 3, pp. 273–280, 2013.
- [10] F. Ginhoux, S. Lim, G. Hoeffel, D. Low, and T. Huber, "Origin and differentiation of microglia.," *Front. Cell. Neurosci.*, vol. 7, no. April, p. 45, Jan. 2013.
- [11] A. R. Simard and S. Rivest, "Bone marrow stem cells have the ability to populate the entire central nervous system into fully differentiated parenchymal microglia.," *FASEB J.*, vol. 18, no. 9, pp. 998–1000, 2004.
- [12] J. Priller, a Flügel, T. Wehner, M. Boentert, C. a Haas, M. Prinz, F. Fernández-Klett, K. Prass, I. Bechmann, B. a de Boer, M. Frotscher, G. W. Kreutzberg, D. a Persons, and U. Dirnagl, "Targeting gene-modified hematopoietic cells to the central nervous system: use of green fluorescent protein uncovers microglial engraftment.," *Nat. Med.*, vol. 7, no. 12, pp. 1356–1361, 2001.
- [13] H. Nittby, A. Brun, J. Eberhardt, L. Malmgren, B. R. R. Persson, and L. G. Salford, "Increased blood-brain barrier permeability in mammalian brain 7 days after exposure to the radiation from a GSM-900 mobile phone," *Pathophysiology*, vol. 16, no. 2–3, pp. 103–112, 2009.
- [14] B. Ajami, J. L. Bennett, C. Krieger, W. Tetzlaff, and F. M. V Rossi, "Local self-renewal can sustain CNS microglia maintenance and function throughout adult life.," *Nat. Neurosci.*, vol. 10, no. 12, pp. 1538–1543, 2007.
- [15] B. Ajami, J. L. Bennett, C. Krieger, K. M. McNagny, and F. M. V Rossi, "Infiltrating monocytes trigger EAE progression, but do not contribute to the resident microglia pool.," *Nat. Neurosci.*, vol. 14, no. 9, pp. 1142–9, Sep. 2011.
- [16] M. Prinz and A. Mildner, "Microglia in the CNS: immigrants from another world.," *Glia*, vol. 59, no. 2, pp. 177–87, Feb. 2011.
- [17] T. Jonsson, J. K. Atwal, S. Steinberg, J. Snaedal, P. V. Jonsson, S. Bjornsson, H. Stefansson, P. Sulem, D. Gudbjartsson, J. Maloney, K. Hoyte, A. Gustafson, Y. Liu, Y. Lu, T. Bhangale, R. R. Graham, J. Huttenlocher, G. Bjornsdottir, O. a. Andreassen, E. G. Jönsson, A. Palotie, T. W. Behrens, O. T. Magnusson, A. Kong, U. Thorsteinsdottir, R. J. Watts, and K. Stefansson, "A mutation in APP

References

- protects against Alzheimer's disease and age-related cognitive decline," *Nature*, vol. 488, no. 7409, pp. 96–99, 2012.
- [18] J. a Miller, R. L. Woltjer, J. M. Goodenbour, S. Horvath, and D. H. Geschwind, "Genes and pathways underlying regional and cell type changes in Alzheimer's disease.," *Genome Med.*, vol. 5, no. 5, p. 48, 2013.
- [19] F. L. Heppner, R. M. Ransohoff, and B. Becher, "Immune attack: the role of inflammation in Alzheimer disease," *Nat. Rev. Neurosci.*, vol. 16, no. 6, pp. 358–372, 2015.
- [20] Y. Zhang, R. Thompson, H. Zhang, and H. Xu, "APP processing in Alzheimer's disease.," *Mol. Brain*, vol. 4, no. 1, p. 3, 2011.
- [21] S. Moore, L. D. B. Evans, T. Andersson, E. Portelius, J. Smith, T. B. Dias, N. Saurat, A. McGlade, P. Kirwan, K. Blennow, J. Hardy, H. Zetterberg, and F. J. Livesey, "APP Metabolism Regulates Tau Proteostasis in Human Cerebral Cortex Neurons," *Cell Rep.*, vol. 11, no. 5, pp. 689–696, 2015.
- [22] I. Benilova, E. Karran, and B. De Strooper, "The toxic A β oligomer and Alzheimer's disease: an emperor in need of clothes.," *Nat. Neurosci.*, vol. 15, no. 3, pp. 349–57, Mar. 2012.
- [23] J. El Khoury and A. D. Luster, "Mechanisms of microglia accumulation in Alzheimer's disease: therapeutic implications.," *Trends Pharmacol. Sci.*, vol. 29, no. 12, pp. 626–32, Dec. 2008.
- [24] D. H. Small and C. A. Mclean, "Alzheimer ' s Disease and the Amyloid β Protein : What Is the Role of Amyloid ?," 1999.
- [25] A. Sandebring, H. Welander, B. Winblad, C. Graff, and L. O. Tjernberg, "The Pathogenic A β 43 Is Enriched in Familial and Sporadic Alzheimer Disease," *PLoS One*, vol. 8, no. 2, 2013.
- [26] A. J. Hanson, S. Craft, and W. A. Banks, "The APOE Genotype : Modification of Therapeutic Responses in Alzheimer ' s Disease," pp. 114–120, 2015.

References

- [27] M. Malik, J. F. Simpson, I. Parikh, B. R. Wilfred, D. W. Fardo, P. T. Nelson, and S. Estus, "CD33 Alzheimer's Risk-Altering Polymorphism, CD33 Expression, and Exon 2 Splicing," *J. Neurosci.*, vol. 33, no. 33, pp. 13320–13325, Aug. 2013.
- [28] M. M. Carrasquillo, J. E. Crook, O. Pedraza, C. S. Thomas, V. S. Pankratz, M. Allen, T. Nguyen, K. G. Malphrus, L. Ma, G. D. Bisceglia, R. O. Roberts, J. a. Lucas, G. E. Smith, R. J. Ivnik, M. M. Machulda, N. R. Graff-Radford, R. C. Petersen, S. G. Younkin, and N. Ertekin-Taner, "Late-onset Alzheimer's risk variants in memory decline, incident mild cognitive impairment, and Alzheimer's disease," *Neurobiol. Aging*, vol. 36, no. 1, pp. 60–67, 2015.
- [29] J. Avila, J. J. Lucas, M. Perez, and F. Hernandez, "Role of tau protein in both physiological and pathological conditions.," *Physiol. Rev.*, vol. 84, no. 2, pp. 361–384, 2004.
- [30] M. Kolarova, F. García-Sierra, A. Bartos, J. Ricny, and D. Ripova, "Structure and pathology of tau protein in Alzheimer disease," *Int. J. Alzheimers. Dis.*, vol. 2012, 2012.
- [31] D. E. Hurtado, L. Molina-Porcel, M. Iba, A. K. Aboagye, S. M. Paul, J. Q. Trojanowski, and V. M.-Y. Lee, "A β accelerates the spatiotemporal progression of tau pathology and augments tau amyloidosis in an Alzheimer mouse model.," *Am. J. Pathol.*, vol. 177, no. 4, pp. 1977–1988, 2010.
- [32] G. S. Bloom, "Amyloid- β and Tau: The Trigger and Bullet in Alzheimer Disease Pathogenesis.," *JAMA Neurol.*, pp. 1–4, Feb. 2014.
- [33] P. L. McGeer, S. Itagaki, H. Tago, and E. G. McGeer, "Reactive microglia in patients with senile dementia of the Alzheimer type are positive for the histocompatibility glycoprotein HLA-DR.," *Neurosci. Lett.*, vol. 79, no. 1–2, pp. 195–200, Aug. 1987.
- [34] M. Noda, H. Nakanishi, and N. Akaike, "Glutamate release from microglia via glutamate transporter is enhanced by amyloid-beta peptide.," *Neuroscience*, vol. 92, no. 4, pp. 1465–74, Jan. 1999.
- [35] S. W. Barger, M. E. Goodwin, M. M. Porter, and M. L. Beggs, "Glutamate release from activated microglia requires the oxidative burst and lipid peroxidation," *J.*

References

- Neurochem.*, vol. 101, no. 5, pp. 1205–1213, 2007.
- [36] T. M. Weitz and T. Town, “Microglia in Alzheimer’s Disease: It’s All About Context.,” *Int. J. Alzheimers. Dis.*, vol. 2012, p. 314185, Jan. 2012.
- [37] K. Bhaskar, N. Maphis, G. Xu, N. H. Varvel, O. N. Kokiko-Cochran, J. P. Weick, S. M. Staugaitis, A. Cardona, R. M. Ransohoff, K. Herrup, and B. T. Lamb, “Microglial derived tumor necrosis factor- α drives Alzheimer’s disease-related neuronal cell cycle events,” *Neurobiol. Dis.*, vol. 62, pp. 273–285, 2014.
- [38] C. K. Combs, J. C. Karlo, S. C. Kao, and G. E. Landreth, “beta-Amyloid stimulation of microglia and monocytes results in TNF α -dependent expression of inducible nitric oxide synthase and neuronal apoptosis.,” *J. Neurosci.*, vol. 21, no. 4, pp. 1179–88, Feb. 2001.
- [39] J. J. Neher, U. Neniskyte, J.-W. Zhao, A. Bal-Price, A. M. Tolkovsky, and G. C. Brown, “Inhibition of microglial phagocytosis is sufficient to prevent inflammatory neuronal death.,” *J. Immunol.*, vol. 186, no. 8, pp. 4973–83, Apr. 2011.
- [40] Z. Xie, M. Wei, T. E. Morgan, P. Fabrizio, D. Han, C. E. Finch, and V. D. Longo, “Peroxynitrite mediates neurotoxicity of amyloid beta-peptide1-42- and lipopolysaccharide-activated microglia.,” *J. Neurosci.*, vol. 22, no. 9, pp. 3484–3492, 2002.
- [41] Y. Doi, T. Mizuno, Y. Maki, S. Jin, H. Mizoguchi, M. Ikeyama, M. Doi, M. Michikawa, H. Takeuchi, and A. Suzumura, “Microglia activated with the toll-like receptor 9 ligand CpG attenuate oligomeric amyloid β neurotoxicity in in vitro and in vivo models of Alzheimer’s disease.,” *Am. J. Pathol.*, vol. 175, no. 5, pp. 2121–2132, 2009.
- [42] T. Mizuno, Y. Doi, H. Mizoguchi, S. Jin, M. Noda, Y. Sonobe, H. Takeuchi, and A. Suzumura, “Interleukin-34 selectively enhances the neuroprotective effects of microglia to attenuate oligomeric amyloid- β neurotoxicity.,” *Am. J. Pathol.*, vol. 179, no. 4, pp. 2016–27, Oct. 2011.
- [43] T. Mizuno, “The biphasic role of microglia in Alzheimer’s disease.,” *Int. J. Alzheimers. Dis.*, vol. 2012, p. 737846, Jan. 2012.

References

- [44] a Varki, "Diversity in the sialic acids.," *Glycobiology*, vol. 2, no. 1, pp. 25–40, Feb. 1992.
- [45] B. Wang and J. Brand-Miller, "The role and potential of sialic acid in human nutrition.," *Eur. J. Clin. Nutr.*, vol. 57, no. 11, pp. 1351–1369, 2003.
- [46] C. Sato and K. Kitajima, "Disialic, oligosialic and polysialic acids: distribution, functions and related disease.," *J. Biochem.*, vol. 154, no. 2, pp. 115–36, Aug. 2013.
- [47] T. Yamamoto, "Marine bacterial sialyltransferases," *Mar. Drugs*, vol. 8, no. 11, pp. 2781–2794, 2010.
- [48] R. L. Schnaar, R. Gerardy-Schahn, and H. Hildebrandt, "Sialic acids in the brain: gangliosides and polysialic acid in nervous system development, stability, disease, and regeneration.," *Physiol. Rev.*, vol. 94, no. 2, pp. 461–518, 2014.
- [49] A. Varki and P. Gagneux, "Multifarious roles of sialic acids in immunity.," *Ann. N. Y. Acad. Sci.*, vol. 1253, pp. 16–36, Apr. 2012.
- [50] R. Schauer, "Sialic acids as regulators of molecular and cellular interactions.," *Curr. Opin. Struct. Biol.*, vol. 19, no. 5, pp. 507–14, Oct. 2009.
- [51] H. Cao and P. R. Crocker, "Evolution of CD33-related siglecs: regulating host immune functions and escaping pathogen exploitation," *Immunology*, vol. 132, no. 1, pp. 18–26, Jan. 2011.
- [52] C. Jandus, H.-U. Simon, and S. von Gunten, "Targeting siglecs--a novel pharmacological strategy for immuno- and glycotherapy.," *Biochem. Pharmacol.*, vol. 82, no. 4, pp. 323–32, Aug. 2011.
- [53] S. Pillai, I. A. Netravali, A. Cariappa, and H. Mattoo, "Siglecs and immune regulation.," *Annu. Rev. Immunol.*, vol. 30, pp. 357–92, Jan. 2012.
- [54] F. Schwarz, O. M. Pearce, X. Wang, A. N. Samraj, H. Läubli, J. O. Garcia, H. Lin, X. Fu, A. Garcia-Bingman, P. Secret, C. E. Romanoski, C. Heyser, C. K. Glass,

References

- S. L. Hazen, N. Varki, A. Varki, and P. Gagneux, "Siglec receptors impact mammalian lifespan by modulating oxidative stress.," *Elife*, vol. 4, pp. 1–19, Jan. 2015.
- [55] H. Cao, U. Lakner, B. de Bono, J. Traherne, J. Trowsdale, and A. D. Barrow, "SIGLEC16 encodes a DAP12-associated receptor expressed in macrophages that evolved from its inhibitory counterpart SIGLEC11 and has functional and non-functional alleles in humans.," *Eur. J. Immunol.*, vol. 38, no. 8, pp. 2303–15, Aug. 2008.
- [56] A. H. Gene, T. Hayakawa, T. Angata, A. L. Lewis, T. S. Mikkelsen, N. M. Varki, and A. Varki, "B RE VIA," vol. 309, no. September, p. 2005, 2005.
- [57] B. E. Tourdot, M. K. Brenner, K. C. Keough, T. Holyst, P. J. Newman, and D. K. Newman, "Immunoreceptor tyrosine-based inhibitory motif (ITIM)-mediated inhibitory signaling is regulated by sequential phosphorylation mediated by distinct nonreceptor tyrosine kinases: a case study involving PECAM-1.," *Biochemistry*, vol. 52, no. 15, pp. 2597–608, Apr. 2013.
- [58] B. Linnartz and H. Neumann, "Microglial activatory (immunoreceptor tyrosine-based activation motif)- and inhibitory (immunoreceptor tyrosine-based inhibition motif)-signaling receptors for recognition of the neuronal glycoalyx.," *Glia*, vol. 61, no. 1, pp. 37–46, Jan. 2013.
- [59] N. Yamamoto, Y. Fukata, M. Fukata, and K. Yanagisawa, "GM1-ganglioside-induced A β assembly on synaptic membranes of cultured neurons," *Biochim. Biophys. Acta - Biomembr.*, vol. 1768, no. 5, pp. 1128–1137, 2007.
- [60] A. Salminen and K. Kaarniranta, "Siglec receptors and hiding plaques in Alzheimer's disease.," *J. Mol. Med. (Berl)*, vol. 87, no. 7, pp. 697–701, Jul. 2009.
- [61] a Kakio, S. I. Nishimoto, K. Yanagisawa, Y. Kozutsumi, and K. Matsuzaki, "Cholesterol-dependent formation of GM1 ganglioside-bound amyloid beta-protein, an endogenous seed for Alzheimer amyloid.," *J. Biol. Chem.*, vol. 276, no. 27, pp. 24985–90, Jul. 2001.
- [62] T. Ariga, K. Kobayashi, a Hasegawa, M. Kiso, H. Ishida, and T. Miyatake, "Characterization of high-affinity binding between gangliosides and amyloid beta-

References

- protein.," *Arch. Biochem. Biophys.*, vol. 388, no. 2, pp. 225–230, 2001.
- [63] T. Ariga, M. P. McDonald, and R. K. Yu, "Role of ganglioside metabolism in the pathogenesis of Alzheimer's disease--a review.," *J. Lipid Res.*, vol. 49, no. 6, pp. 1157–75, Jun. 2008.
- [64] D. Patel, J. Henry, and T. Good, "Attenuation of β -amyloid induced toxicity by sialic acid-conjugated dendrimeric polymers," *Biochim. Biophys. Acta - Gen. Subj.*, vol. 1760, no. 12, pp. 1802–1809, 2006.
- [65] A. Griciuc, A. Serrano-Pozo, A. R. Parrado, A. N. Lesinski, C. N. Asselin, K. Mullin, B. Hooli, S. H. Choi, B. T. Hyman, and R. E. Tanzi, "Alzheimer's disease risk gene CD33 inhibits microglial uptake of amyloid beta.," *Neuron*, vol. 78, no. 4, pp. 631–43, May 2013.
- [66] S. Gaikwad, S. Larionov, Y. Wang, H. Dannenberg, T. Matozaki, A. Monsonego, D. R. Thal, and H. Neumann, "Signal regulatory protein-beta1: a microglial modulator of phagocytosis in Alzheimer's disease.," *Am. J. Pathol.*, vol. 175, no. 6, pp. 2528–39, Dec. 2009.
- [67] S. Rivest, "TREM2 enables amyloid β clearance by microglia," *Cell Res.*, vol. 25, no. 5, pp. 535–536, 2015.
- [68] J. Claude, B. Linnartz-Gerlach, A. P. Kudin, W. S. Kunz, and H. Neumann, "Microglial CD33-related Siglec-E inhibits neurotoxicity by preventing the phagocytosis-associated oxidative burst.," *J. Neurosci.*, vol. 33, no. 46, pp. 18270–6, Nov. 2013.
- [69] Y. Wang and H. Neumann, "Alleviation of neurotoxicity by microglial human Siglec-11.," *J. Neurosci.*, vol. 30, no. 9, pp. 3482–8, Mar. 2010.
- [70] W. Li, W. Sun, Y. Zhang, W. Wei, R. Ambasudhan, P. Xia, M. Talantova, T. Lin, J. Kim, X. Wang, W. R. Kim, S. a Lipton, K. Zhang, and S. Ding, "Rapid induction and long-term self-renewal of primitive neural precursors from human embryonic stem cells by small molecule inhibitors.," *Proc. Natl. Acad. Sci. U. S. A.*, vol. 108, no. 20, pp. 8299–304, May 2011.

References

- [71] K. Roy, "Establishment of microglial precursors derived from human induced pluripotent stem cells to model SOD1-mediated amyotrophic lateral sclerosis PhD thesis In fulfillment of the requirements for the degree," no. August, 2012.
- [72] Y. Liu, S. Walter, M. Stagi, D. Cherny, M. Letiembre, W. Schulz-Schaeffer, H. Heine, B. Penke, H. Neumann, and K. Fassbender, "LPS receptor (CD14): a receptor for phagocytosis of Alzheimer's amyloid peptide.," *Brain*, vol. 128, no. Pt 8, pp. 1778–89, Aug. 2005.
- [73] D. R. McDonald, K. R. Brunden, and G. E. Landreth, "Amyloid fibrils activate tyrosine kinase-dependent signaling and superoxide production in microglia.," *J. Neurosci.*, vol. 17, no. 7, pp. 2284–94, Apr. 1997.
- [74] T. Schilling and C. Eder, "Amyloid- β -induced reactive oxygen species production and priming are differentially regulated by ion channels in microglia.," *J. Cell. Physiol.*, vol. 226, no. 12, pp. 3295–302, Dec. 2011.
- [75] J. Kopatz, "Microglial sialic-acid-binding and Siglec-11 in neuroinflammation," pp. 1–92, 2014.
- [76] E. a Bordt and B. M. Polster, "NADPH Oxidase- and Mitochondria-derived Reactive Oxygen Species in Proinflammatory Microglial Activation: A Bipartisan Affair" *Free Radic. Biol. Med.*, vol. 76, pp. 34–46, 2014.
- [77] R. S. Flannagan, V. Jaumouillé, and S. Grinstein, "The cell biology of phagocytosis.," *Annu. Rev. Pathol.*, vol. 7, pp. 61–98, Jan. 2012.
- [78] B. L. Wilkinson and G. E. Landreth, "The microglial NADPH oxidase complex as a source of oxidative stress in Alzheimer's disease.," *J. Neuroinflammation*, vol. 3, p. 30, Jan. 2006.
- [79] M. L. Block, "NADPH oxidase as a therapeutic target in Alzheimer's disease.," *BMC Neurosci.*, vol. 9 Suppl 2, p. S8, 2008.
- [80] B. Linnartz-Gerlach, J. Kopatz, and H. Neumann, "Siglec functions of microglia," *Glycobiology*, vol. 24, no. 9, pp. 794–799, 2014.

References

- [81] H. Rivera, M. Shibayama, V. Tsutsumi, V. Perez-Alvarez, and P. Muriel, "Resveratrol and trimethylated resveratrol protect from acute liver damage induced by CCl₄ in the rat.," *J. Appl. Toxicol.*, vol. 28, no. 2, pp. 147–155, 2008.
- [82] X.-D. Pan, Y.-G. Zhu, N. Lin, J. Zhang, Q.-Y. Ye, H.-P. Huang, and X.-C. Chen, "Microglial phagocytosis induced by fibrillar β -amyloid is attenuated by oligomeric β -amyloid: implications for Alzheimer's disease.," *Mol. Neurodegener.*, vol. 6, no. 1, p. 45, Jan. 2011.
- [83] U. Neniskyte, J. J. Neher, and G. C. Brown, "Neuronal death induced by nanomolar amyloid β is mediated by primary phagocytosis of neurons by microglia.," *J. Biol. Chem.*, vol. 286, no. 46, pp. 39904–13, Nov. 2011.
- [84] G. C. Brown and J. J. Neher, "Microglial phagocytosis of live neurons.," *Nat. Rev. Neurosci.*, vol. 15, no. 4, pp. 209–16, 2014.
- [85] X. Wang, N. Mitra, P. Cruz, L. Deng, N. Varki, T. Angata, E. D. Green, J. Mullikin, T. Hayakawa, and a. Varki, "Evolution of Siglec-11 and Siglec-16 Genes in Hominins," *Mol. Biol. Evol.*, vol. 29, no. 8, pp. 2073–2086, Mar. 2012.
- [86] J. M. Rubio-Perez and J. M. Morillas-Ruiz, "A review: inflammatory process in Alzheimer's disease, role of cytokines.," *ScientificWorldJournal.*, vol. 2012, p. 756357, Jan. 2012.
- [87] V. Padler-Karavani, N. Hurtado-Ziola, Y. C. Chang, J. L. Sonnenburg, A. Ronaghy, H. Yu, A. Verhagen, V. Nizet, X. Chen, N. Varki, A. Varki, and T. Angata, "Rapid evolution of binding specificities and expression patterns of inhibitory CD33-related Siglecs in primates," *FASEB J.*, vol. 28, no. 3, pp. 1280–1293, 2014.
- [88] S. M. Lehmann, C. Krüger, B. Park, K. Derkow, K. Rosenberger, J. Baumgart, T. Trimbuch, G. Eom, M. Hinz, D. Kaul, P. Habbel, R. Kälin, E. Franzoni, A. Rybak, D. Nguyen, R. Veh, O. Ninnemann, O. Peters, R. Nitsch, F. L. Heppner, D. Golenbock, E. Schott, H. L. Ploegh, F. G. Wulczyn, and S. Lehnardt, "An unconventional role for miRNA: let-7 activates Toll-like receptor 7 and causes neurodegeneration.," *Nat. Neurosci.*, vol. 15, no. 6, pp. 827–35, Jun. 2012.
- [89] A. Varki, "Sialic acids in human health and disease.," *Trends Mol. Med.*, vol. 14,

References

- no. 8, pp. 351–60, Aug. 2008.
- [90] S. Hanashima, C. Sato, H. Tanaka, T. Takahashi, K. Kitajima, and Y. Yamaguchi, “NMR study into the mechanism of recognition of the degree of polymerization by oligo/polysialic acid antibodies.,” *Bioorg. Med. Chem.*, vol. 21, no. 19, pp. 6069–76, Oct. 2013.
- [91] T. Janas and T. Janas, “Membrane oligo- and polysialic acids,” *Biochim. Biophys. Acta - Biomembr.*, vol. 1808, no. 12, pp. 2923–2932, 2011.
- [92] H. Attrill, A. Imamura, R. S. Sharma, M. Kiso, P. R. Crocker, and D. M. F. Van Aalten, “Siglec-7 undergoes a major conformational change when complexed with the $\alpha(2,8)$ -disialylganglioside GT1b,” *J. Biol. Chem.*, vol. 281, no. 43, pp. 32774–32783, 2006.
- [93] S. Mizrahi, B. F. Gibbs, L. Karra, M. Ben-Zimra, and F. Levi-Schaffer, “Siglec-7 is an inhibitory receptor on human mast cells and basophils.,” *J. Allergy Clin. Immunol.*, vol. 10, no. July, pp. 1–7, 2014.
- [94] T. Angata, S. C. Kerr, D. R. Greaves, N. M. Varki, P. R. Crocker, and A. Varki, “Cloning and characterization of human Siglec-11. A recently evolved signaling molecule that can interact with SHP-1 and SHP-2 and is expressed by tissue macrophages, including brain microglia.,” *J. Biol. Chem.*, vol. 277, no. 27, pp. 24466–74, Jul. 2002.
- [95] S. Kitazume-Kawaguchi, S. Kabata, and M. Arita, “Differential Biosynthesis of Polysialic or Disialic Acid Structure by ST8Sia II and ST8Sia IV,” *J. Biol. Chem.*, vol. 276, no. 19, pp. 15696–15703, 2001.
- [96] U. Yabe, C. Sato, T. Matsuda, and K. Kitajima, “Polysialic acid in human milk: CD36 is a new member of mammalian polysialic acid-containing glycoprotein,” *J. Biol. Chem.*, vol. 278, no. 16, pp. 13875–13880, 2003.
- [97] S. Curreli, Z. Arany, R. Gerardy-Schahn, D. Mann, and N. M. Stamatou, “Polysialylated neuropilin-2 is expressed on the surface of human dendritic cells and modulates dendritic cell-T lymphocyte interactions,” *J. Biol. Chem.*, vol. 282, no. 42, pp. 30346–30356, 2007.

References

- [98] N. M. Stamatos, L. Zhang, a. Jokilammi, J. Finne, W. H. Chen, a. El-Maarouf, a. S. Cross, and K. G. Hankey, “Changes in polysialic acid expression on myeloid cells during differentiation and recruitment to sites of inflammation: Role in phagocytosis,” *Glycobiology*, vol. 24, no. 9, pp. 864–879, 2014.
- [99] P. M. Drake, J. K. Nathan, C. M. Stock, P. V. Chang, M. O. Muench, D. Nakata, J. R. Reader, P. Gip, K. P. K. Golden, B. Weinhold, R. Gerardy-Schahn, F. a. Troy, and C. R. Bertozzi, “Polysialic Acid, a Glycan with Highly Restricted Expression, Is Found on Human and Murine Leukocytes and Modulates Immune Responses,” *J. Immunol.*, vol. 181, no. 10, pp. 6850–6858, 2008.
- [100] A. Aguzzi, B. a Barres, and M. L. Bennett, “Microglia: scapegoat, saboteur, or something else” *Science*, vol. 339, no. 6116, pp. 156–61, Jan. 2013.
- [101] L. C. Davies, S. J. Jenkins, J. E. Allen, and P. R. Taylor, “Tissue-resident macrophages.,” *Nat. Immunol.*, vol. 14, no. 10, pp. 986–95, 2013.
- [102] I. a Clark and B. Vissel, “Alzheimer’s disease: Amyloid beta not a primary initiator, but one of the secondary DAMPs,” *Br. J. Pharmacol.*, p. n/a–n/a, 2015.
- [103] K. Kierdorf and M. Prinz, “Factors regulating microglia activation.,” *Front. Cell. Neurosci.*, vol. 7, no. April, p. 44, 2013.
- [104] Y. Wang, M. Cella, K. Mallinson, J. D. Ulrich, K. L. Young, M. L. Robinette, S. Gilfillan, G. M. Krishnan, S. Sudhakar, B. H. Zinselmeyer, D. M. Holtzman, J. R. Cirrito, and M. Colonna, “TREM2 Lipid Sensing Sustains the Microglial Response in an Alzheimer’s Disease Model,” *Cell*, vol. 160, no. 6, pp. 1061–1071, 2015.
- [105] J. Kopatz, C. Beutner, K. Welle, L. G. Bodea, J. Reinhardt, J. Claude, B. Linnartz-Gerlach, and H. Neumann, “Siglec-h on activated microglia for recognition and engulfment of glioma cells,” *Glia*, vol. 61, no. 7, pp. 1122–1133, 2013.
- [106] T. a M. Steevens and L. Meyaard, “Immune inhibitory receptors: essential regulators of phagocyte function.,” *Eur. J. Immunol.*, vol. 41, no. 3, pp. 575–87, Mar. 2011.
- [107] A. Griciuc, A. Serrano-Pozo, A. R. Parrado, A. N. Lesinski, C. N. Asselin, K.

References

- Mullin, B. Hooli, S. Choi, B. T. Hyman, and R. E. Tanzi, "Alzheimer's disease risk gene *cd33* inhibits microglial uptake of amyloid beta," *Neuron*, vol. 78, no. 4, pp. 631–643, 2013.
- [108] H. Neumann, M. R. Kotter, and R. J. M. Franklin, "Debris clearance by microglia: An essential link between degeneration and regeneration," *Brain*, vol. 132, no. 2, pp. 288–295, 2009.
- [109] R. Huizinga, B. J. van der Star, M. Kipp, R. Jong, W. Gerritsen, T. Clarner, F. Puentes, C. D. Dijkstra, P. van der Valk, and S. Amor, "Phagocytosis of neuronal debris by microglia is associated with neuronal damage in multiple sclerosis," *Glia*, vol. 60, no. 3, pp. 422–431, 2012.
- [110] M. L. Block, L. Zecca, and J.-S. Hong, "Microglia-mediated neurotoxicity: uncovering the molecular mechanisms.," *Nat. Rev. Neurosci.*, vol. 8, no. 1, pp. 57–69, Jan. 2007.
- [111] M. E. Bamberger, M. E. Harris, D. R. McDonald, J. Husemann, and G. E. Landreth, "A cell surface receptor complex for fibrillar beta-amyloid mediates microglial activation.," *J. Neurosci.*, vol. 23, no. 7, pp. 2665–2674, 2003.
- [112] L. Park, J. Anrather, P. Zhou, K. Frys, R. Pitstick, S. Younkin, G. a Carlson, and C. Iadecola, "NADPH-oxidase-derived reactive oxygen species mediate the cerebrovascular dysfunction induced by the amyloid beta peptide.," *J. Neurosci.*, vol. 25, no. 7, pp. 1769–1777, 2005.
- [113] M. R. Elliott and K. S. Ravichandran, "Clearance of apoptotic cells: Implications in health and disease," *J. Cell Biol.*, vol. 189, no. 7, pp. 1059–1070, 2010.
- [114] J. L. Marín-Teva, I. Dusart, C. Colin, A. Gervais, N. Van Rooijen, and M. Mallat, "Microglia Promote the Death of Developing Purkinje Cells," *Neuron*, vol. 41, no. 4, pp. 535–547, 2004.
- [115] J. V Faustino, X. Wang, C. E. Johnson, A. Klibanov, N. Derugin, M. F. Wendland, and Z. S. Vexler, "Microglial cells contribute to endogenous brain defenses after acute neonatal focal stroke.," *J. Neurosci.*, vol. 31, no. 36, pp. 12992–13001, 2011.

References

- [116] B. Halliwell, "Free radicals and antioxidants: a personal view.," *Nutr. Rev.*, vol. 52, no. 8 Pt 1, pp. 253–265, 1994.
- [117] P. Milani, G. Ambrosi, O. Gammoh, F. Blandini, and C. Cereda, "SOD1 and DJ-1 converge at Nrf2 pathway: A clue for antioxidant therapeutic potential in neurodegeneration," *Oxid. Med. Cell. Longev.*, vol. 2013, 2013.
- [118] B. Halliwell, "Oxidative stress and neurodegeneration: Where are we now?," *J. Neurochem.*, vol. 97, no. 6, pp. 1634–1658, 2006.
- [119] M. S. Rotunno and D. a Bosco, "An emerging role for misfolded wild-type SOD1 in sporadic ALS pathogenesis.," *Front. Cell. Neurosci.*, vol. 7, no. December, p. 253, 2013.
- [120] R. L. Williams, D. J. Hilton, S. Pease, T. a Willson, C. L. Stewart, D. P. Gearing, E. F. Wagner, D. Metcalf, N. a Nicola, and N. M. Gough, "Myeloid leukaemia inhibitory factor maintains the developmental potential of embryonic stem cells.," *Nature*, vol. 336, no. 6200, pp. 684–687, 1988.
- [121] J. Gaulden and J. F. Reiter, "Neur-ons and neur-offs: regulators of neural induction in vertebrate embryos and embryonic stem cells.," *Hum. Mol. Genet.*, vol. 17, no. R1, pp. R60–6, Apr. 2008.
- [122] a Rodaway, H. Takeda, S. Koshida, J. Broadbent, B. Price, J. C. Smith, R. Patient, and N. Holder, "Induction of the mesendoderm in the zebrafish germ ring by yolk cell-derived TGF-beta family signals and discrimination of mesoderm and endoderm by FGF.," *Development*, vol. 126, no. 14, pp. 3067–78, Jun. 1999.
- [123] M. L. Hendrickson, A. J. Rao, O. N. a Demerdash, and R. E. Kalil, "Expression of nestin by neural cells in the adult rat and human brain.," *PLoS One*, vol. 6, no. 4, p. e18535, Jan. 2011.
- [124] S. Gómez-López, O. Wiskow, R. Favaro, S. K. Nicolis, D. J. Price, S. M. Pollard, and A. Smith, "Sox2 and Pax6 maintain the proliferative and developmental potential of gliogenic neural stem cells In vitro.," *Glia*, vol. 59, no. 11, pp. 1588–99, Nov. 2011.

References

- [125] T. Kallur, R. Gisler, O. Lindvall, and Z. Kokaia, "Pax6 promotes neurogenesis in human neural stem cells.," *Mol. Cell. Neurosci.*, vol. 38, no. 4, pp. 616–28, Aug. 2008.
- [126] B. Linnartz-Gerlach, C. Schuy, A. Shahraz, A. J. Tenner, and H. Neumann, "Sialylation of neurites inhibits complement-mediated macrophage removal in a human macrophage-neuron Co-Culture System," *Glia*, p. n/a–n/a, 2015.
- [127] E. Gascon, L. Vutskits, and J. Z. Kiss, "Polysialic acid-neural cell adhesion molecule in brain plasticity: from synapses to integration of new neurons.," *Brain Res. Rev.*, vol. 56, no. 1, pp. 101–18, Nov. 2007.
- [128] K. Angata and M. Fukuda, "Polysialyltransferases: Major players in polysialic acid synthesis on the neural cell adhesion molecule," *Biochimie*, vol. 85, no. 1–2, pp. 195–206, 2003.
- [129] A. El Maarouf, D. M. Yaw, and U. Rutishauser, "Improved Stem Cell-Derived Motoneuron Survival , Migration , Sprouting , and Innervation With Enhanced Expression of Polysialic Acid," vol. 24, pp. 797–809, 2015.
- [130] V. Goncharova, S. Das, W. Niles, I. Schraufstatter, A. K. Wong, T. Povaly, D. Wakeman, L. Miller, E. Y. Snyder, and S. K. Khaldoyanidi, "Homing of neural stem cells from the venous compartment into a brain infarct does not involve conventional interactions with vascular endothelium.," *Stem Cells Transl. Med.*, vol. 3, no. 2, pp. 229–40, Feb. 2014.
- [131] H. M. Abdul and D. A. Butterfield, "Protection against amyloid beta-peptide (1-42)-induced loss of phospholipid asymmetry in synaptosomal membranes by tricyclodecan-9-xanthogenate (D609) and ferulic acid ethyl ester: Implications for Alzheimer's disease," *Biochim. Biophys. Acta - Mol. Basis Dis.*, vol. 1741, no. 1–2, pp. 140–148, 2005.
- [132] B. Linnartz, J. Kopatz, A. J. Tenner, and H. Neumann, "Sialic acid on the neuronal glycocalyx prevents complement C1 binding and complement receptor-3-mediated removal by microglia.," *J. Neurosci.*, vol. 32, no. 3, pp. 946–52, Jan. 2012.
- [133] B. Qin, L. Cartier, M. Dubois-Dauphin, B. Li, L. Serrander, and K. H. Krause, "A

References

- key role for the microglial NADPH oxidase in APP-dependent killing of neurons,” *Neurobiol. Aging*, vol. 27, no. 11, pp. 1577–1587, 2006.
- [134] J. Zhou, S. Zhang, X. Zhao, and T. Wei, “Melatonin impairs NADPH oxidase assembly and decreases superoxide anion production in microglia exposed to amyloid- β 1-42,” *J. Pineal Res.*, vol. 45, no. 2, pp. 157–165, 2008.
- [135] O. a. Olajide, H. S. Bhatia, A. C. P. De Oliveira, C. W. Wright, and B. L. Fiebich, “Inhibition of neuroinflammation in LPS-activated microglia by cryptolepine,” *Evidence-based Complement. Altern. Med.*, vol. 2013, 2013.
- [136] A. Kinsner, V. Pilotto, S. Deininger, G. C. Brown, S. Coecke, T. Hartung, and A. Bal-Price, “Inflammatory neurodegeneration induced by lipoteichoic acid from *Staphylococcus aureus* is mediated by glia activation, nitrosative and oxidative stress, and caspase activation.,” *J. Neurochem.*, vol. 95, no. 4, pp. 1132–43, Nov. 2005.

Acknowledgements

Acknowledgements

I would like to express my deepest gratitude to Prof. Dr. Harald Neumann for providing me the opportunity to work in his group. I am thankful for his trust, ideas, discussions, and guidance all these years through this work. I would like to thank Prof. Dr. Sven Burgdorf who kindly accepted to participate as the second referee to the thesis dissertation. I am also grateful to Prof. Dr. Waldemar Kolanus and Prof. Dr. Maximilian Weigend for agreeing to participate as referees.

I wholeheartedly thank all my colleagues in AG Neumann's lab: Bettina, Christine, Janine, Jens, Jessica, Johannes, Liviu, Megan, Mona, Moritz, Omar, Oskan, Renè, Rita, Shoba, Vanessa, Viola, and Vlad. I am deeply grateful for all your help, advice and discussions. I am thankful to everyone involved in creating such a great research environment, which was not possible without the entire Reconstructive Neurobiology Institute members.

Many thanks to Dr. Jens Kopatz for his help in purification of polySia avDP20 and all fruitful discussions during this work. I thank Prof. Dr. Gieselmann and his lab for their help in the initial steps of establishing polySia purifications. Also I thank Prof. Dr. Hornung and his lab for providing THP-1 monocytes.

I thank Dr. Bettina Linnartz-Gerlach, Dr. Jens Kopatz, Mona-Ann Mathews, and Megan Rothstein for taking the time to proofread this thesis. Many thanks to you for all your suggestions and comments, which helped me a lot to improve this thesis.

Last but absolutely not the least, I profoundly grateful to my family maman Elahe, baba Behzad, and Mitra who are far from me but their support were countless. I would never reach to this stage without them.

Declaration

Declaration

I, hereby confirm that this work submitted is my own. This thesis has been written independently and with no other sources and aids than stated. The presented thesis has not been submitted to another university and I have not applied for a doctorate procedure so far.

Hiermit versichere ich, dass die vorgelegte Arbeit – abgesehen von den ausdrücklich bezeichneten Hilfsmitteln – persönlich, selbständig und ohne Benutzung anderer als der angegebenen Hilfsmittel angefertigt wurde. Aus anderen Quellen direkt oder indirekt übernommene Daten und Konzepte sind unter Angabe der Quelle kenntlich gemacht worden.

Die vorliegende Arbeit wurde an keiner anderen Hochschule als Dissertation eingereicht. Ich habe früher noch keinen Promotionsversuch unternommen.

Bonn, November 2015

Anahita Shahraz

Curriculum Vitae

Curriculum Vitae

Anahita Shahraz

PhD Student Molecular Biomedicine

Address Neural Regeneration Group, Institute of Reconstructive Neurobiology
Life & Brain Center, University of Bonn,
Sigmund-Freud-Str. 25, 53127 Bonn, Germany
Tel. +49-228-6885-543; e-mail: shahraz@uni-bonn.de

Education and Professional Experience

- 2011 – Present **PhD in Molecular Biomedicine**
Thesis title: “*Neuroprotective Effects of Polysialic Acid and SIGLEC-11 in Activated Phagocytic Cells*”
Coordinator: Prof. Dr. Harald Neumann, Neural Regeneration Group, Institute of Reconstructive Neurobiology, LIFE & BRAIN Center, University of Bonn, Bonn, Germany
Member of the International Immunology Training Program Bonn (IITB), University of Bonn, Germany
Member of the International Graduate School of Theoretical and Experimental Medicine (THEME), University of Bonn, Germany
- 2008 – 2011 **MSc in Cellular Development**
Thesis title “*The effects of Wnt3a on Unrestricted Somatic Stem Cells (USSCs) differentiation to Dopaminergic Neurons*”
Coordinators: Dr. Bahman Zeynali, Department of Biology Science, University of Tehran, Tehran, Iran
GPA: A⁺ (18.73)
- 2004 – 2008 **BSc in Zoology**
Thesis title: “*An Overview on Angiogenesis, Stimulators and Inhibitors*”
Coordinator: Dr. Hori Sepehri, Department of Biology Science, University of Tehran, Tehran, Iran
GPA: A (16.77)
- 2003 **High School Diploma**
Etrat High School, Tehran, Iran
GPA: A⁺ (18.81)

Publications

- **Shahraz A**, Kopatz J, Mathy R, Kappler J, Winter D, Kapoor S, Schütza V, Scheper T, Gieselmann V and Neumann H (2015), “*Anti-inflammatory activity of low molecular weight polysialic acid on human macrophages*”. Nat. Sci. Rep. doi: 10.1038/srep16800
- Linnartz-Gerlach B, Schuy C, **Shahraz A**, Tenner A J and Neumann H (2015), “*Sialylation of neurites inhibits complement-mediated macrophage removal in a human macrophage-neuron Co-Culture System*”. Glia. doi: 10.1002/glia.22901
- Sierra A, Abiega O, **Shahraz A** and Neumann H (2013), “*Janus-faced microglia: beneficial and detrimental consequences of microglial phagocytosis*”. Front. Cell. Neurosci. 7:6. doi: 10.3389/fncel.2013.00006
- Dastjerdi F V, Zeynali B, Tafreshi A P, **Shahraz A**, Chavoshi M S, Najafabadi I K, Vardanjani M M, Atashi A and Soleimani M (2012), “*Inhibition of GSK-3 β enhances neural differentiation in unrestricted somatic stem cells*”. Cell Biology International. 36: 967–972. doi: 10.1042/CBI20110541

Submitted Patent

- Neumann H., Kopatz J., **Shahraz A.**, Karlstetter M., Langmann T. “Polysialic acid use for treatment of neurodegenerative and neuroinflammatory disease”. PCT/EP2014/055445, 2014

Oral Presentations

- **Shahraz A.**, Kopatz J., Neumann H. “*Scavenging effect of low molecular weight polysialic acid on activated human microglia*”. ImmunoSensation cluster science day, Bonn, Germany, November 3-4, 2014.
- **Shahraz A.**, Mathews M., Neumann H. “*Anti-inflammatory polarization of microglia by ITIM-SHP1 signaling*”. DFG-Research unit 1336 internal meeting, Göttingen, Germany, September 12-13, 2014.
- **Shahraz A.** Neumann H. “*Role of polysialic acid and siglec11 in microglia-neuron interaction*”. PhD-students Fourth THEME Symposium, Bad Honnef, Germany, October 1-2, 2013.

Poster Presentations

- **Shahraz A.**, Kopatz J., Neumann H. “*Low molecular weight polysialic acid suppresses inflammatory, but not homeostatic phagocytosis in THP1 macrophages*”. ImmunoSensation cluster science day, Bonn, Germany, November 2-3, 2015.
- **Shahraz A.**, Kopatz J., Neumann H. “*Low molecular weight polysialic acid shows anti-inflammatory effects on human THP1 macrophages*”. XII Meeting on Glial Cells in Health and Disease, Bilbao, Spain, July 15-18, 2015.

Curriculum Vitae

- **Shahraz A.**, Kopatz J., Neumann H. “*Polysialic acids prevent amyloid- β plaques mediated neurotoxicity*”. Saxon Biotechnology Symposium, Dresden, Germany. March 19, 2014.
- **Shahraz A.**, Kopatz J., Neumann H. “*Function of human-specific sialic acid binding receptor Siglec-11 in amyloid- β mediated neurotoxicity*”. XI Meeting on Glial Cells in Health and Disease, Berlin, Germany, July 3-6, 2013.
- **Shahraz A.**, Kopatz J., Kummer M., Brüstle O., Neumann H. “*Human pluripotent stem cell derived microglia/neurons and Siglec-11 transgenic mice to study the function of the Siglec-11 in amyloid- β mediated neurotoxicity*”. PhD-students Third THEME Symposium, Bad Honnef, Germany. October 1-2, 2012.
- **Shahraz A.**, Tafreshi A., Zeynali B. “*Wnt3a induces differentiation of unrestricted somatic stem cells (USSCs) towards dopaminergic neural precursor*”. Stem cells in development and disease, Berlin, Germany. September 11-14, 2011.
- Zeynali B., **Shahraz A.**, Chavoshi M., Khaki I., Molavi M, Tafreshi A. “*Expression of canonical Wnt signaling components in Unrestricted somatic stem cells(USSCs)*”. Stem cells and tissue formation congress. Dresden, Germany. July 11-14, 2010.